T-box Genes in Limb Development and Disease

Thesis

T-box Genes in Limb Development and Disease

Charalampos Rallis

Thesis submitted for the degree of Doctor of Philosophy

October 2004

Division of Developmental Biology
National Institute for Medical Research
Mill Hill
London

Open University

Submission date: 5 October 2004
Award date: 17 November 2004

Acknowledgements

I would like to thank my supervisor Malcolm Logan for giving me the great opportunity to work with him, for his great ideas, support, guidance and patience all these years and for being a great teacher.

I also want to thank all the people in the lab for making it a great place to work in. Carolina, Steve, Jeff and April thank you.

I especially want to thank Jo Del Buono our super-technician in the lab. Without her, this work wouldn't be possible.

I would like to thank all the people in the Division of Developmental Biology and Developmental Neurobiology for reagents and advice, the laidlaw green staff, especially Amanda Hewett and Peter Mealyer, for taking care all the mice and Liz Hurst for the generation of scanning EM images.

Finally, I want to thank my parents and all my friends for their support and Despina for always being there for me.

CONTENTS

LIST OF ABBREVIATIONS

A	Anterior
AER	apical ectodermal ridge
BABB	benzyl alcohol benzyl benzoate
Bp	base pair
BSA	bovine serum albumine
C	caudal
D	distal
DIG	Digoxigenin
DII	1,1'-diocatadecyl-3,3,3',3'-tetramethylindocarbonocyanine perchlorate
DMSO	dimethylsulfoxide
dpc	days postcoitum
E	ectoderm
EN	engrailed
f	fibula
FL	forelimb
fm	femur
h	humerus
HOS	Holt-Oram syndrome
IM	intermediate mesoderm
LP	lateral mesoderm
LPM	lateral plate mesoderm
VL	ventral lip of dermomyotome
M	mesoderm
µl	microlitre
ml	millilitre
mM	millimolar
µg	microgram
µm	micrometer
ng	nanogram
HH	Hamburger-Hamilton
HL	hindlimb
ORF	open reading frame
P	posterior
PBS	phosphate buffer saline
PCD	programmed cell death
PCR	polymerase chain reaction

PFA	paraformaldehyde
pH3	phosphorylated histone 3
Pr	proximal
R	rostral
r	radius
RA	retinoic acid
rpm	rounds per minute
S	somite
SM	somitic mesoderm
t	tibia
u	ulna
UMS	ulnar-mammary syndrome
WT	wild-type
ZnF	zinc-finger
ZPA	zone of polirizing activity
°C	degree Celcius

LIST OF FIGURES

LIST OF TABLES

ABSTRACT

T-box genes comprise an ancient family of transcriptional regulators with important functions during development. The aim of this study is to investigate the roles of two closely related T-box genes *Tbx5* and *Tbx3* in limb development using the mouse and chick embryo as model organisms. These genes are physically linked in the genome, and human mutations in *TBX5* and *TBX3* lead to congenital diseases.

Tbx5, is expressed in the forelimb but not in the hindlimb of the developing vertebrate embryo and has been proposed to have a role in limb-type specification. However, *Tbx5* is also required for normal limb development since haploinsufficiency of *TBX5* in human causes Holt-Oram Syndrome (HOS), a dominant disorder characterized by fore(upper) limb deformities and heart defects. I have taken two approaches to investigate the role of *Tbx5* in limb-type specification and outgrowth. The first is a conditional knock-out method in the mouse where I inactivated *Tbx5* specifically in the developing forelimbs. As a complementary strategy I injected dominant-negative and dominant-active forms of *Tbx5* in the developing chicken wing using replication-competent avian retroviruses. My results from the mouse, suggest that *Tbx5* has a vital role during early limb formation. In addition, my data using the chicken retroviral system establish a role for *Tbx5* in later limb patterning events and provide an insight into understanding the genesis of HOS deformities in man.

Tbx3 is expressed in both forelimbs and hindlimbs of the developing embryo. *Tbx3* is required for normal limb development since haploinsufficiency of *TBX3* in human causes Ulnar-Mammary Syndrome (UMS) a disorder characterized by limb defects and in addition, mammary and apocrine gland abnormalities. To examine the role of *Tbx3* in normal limb development I misexpressed

transcriptional activator and repressor forms of *Tbx3* in the developing forelimb using the avian retroviral system. Ectopic expression of repressor forms of *Tbx3* throughout the forelimb results in a rostral shift in the position of the limb along the main body axis. In contrast, a transcriptional activator form of *Tbx3* is able to shift the limb position to more caudal locations.

My data, suggest a new role for *Tbx3* in axial positioning of the limb. Furthermore, my data reveal a genetic interplay between *Tbx3*, *dHand* and *Gli3* during early limb-forming stages. I show that *dHand* and *Gli3*, genes previously implicated in antero-posterior patterning of the presumptive limb-forming region are also involved in positioning the forelimb primordia.

A. INTRODUCTION

A. INTRODUCTION

Vertebrate embryonic development is defined as a process that adds complexity to the initial and relative simple situation of a fertilized egg. The complexity does not refer only to the increase in total cell numbers but also the generation of different cell types and the formation of recognizable organs or structures with distinct functions. Many organs or structures are formed from a primordium: a group of cells that may be derived from different embryonic layers (endoderm, mesoderm or ectoderm). As development proceeds, a spatial and temporal program of cell behaviour and gene expression is initiated. These genetic programs may involve interactions between mesenchymal and ectodermal components required for the coordinated growth and patterning of the structure. Interestingly, an evolutionary conserved set of specific molecular interactions and cellular events operates in the primordia of many structures and organs, including teeth, limbs, lungs and pancreas. Among these systems, the developing limbs are an excellent model to study pattern formation and growth regulation during embryogenesis.

1. Vertebrate Limb Formation

1.1 Positioning the limb primordia

Limbs (forelimbs and hindlimbs in tetrapods) develop as budding outgrowths from either side of the main body axis. The first step in the development of the vertebrate limb is the specification of a group of cells within the lateral plate mesoderm (LPM) that will give rise to the limb primordium. The forelimb and hindlimb fields are located in specific positions along the rostro-caudal axis of the embryo and this location is fixed in tetrapod vertebrates (Burke et al., 1995). Forelimbs always develop at the cervical-thoracic junction while hindlimbs

develop at the lumbar-sacral junction (Fig. 1A). Nevertheless, the molecular mechanisms that are responsible for limb positioning have remained elusive. The best candidate genes to be specifying the position of the fields of LPM that will give rise to limb buds remain the *Hox* paralogues. *Hox* genes first identified in *Drosophila melanogaster*, encode homeodomain transcription factors shown to provide spatial cues during the development of many embryonic structures in vertebrates and invertebrates (Deschamps et al., 1999; Krumlauf, 1994). Many of these genes are expressed in nested patterns along the rostro-caudal axis of the embryo including the lateral plate mesoderm (LPM) and may provide positional identity to these cells (Burke, 2000; Burke et al., 1995; Cohn et al., 1995; Cohn et al., 1997). Nevertheless, loss-of-function experiments in the mouse have failed to provide direct evidence for a role for Hox genes in positioning the limb along the rostro-caudal axis of the embryo. The only exception to date, comes from the *Hoxb5* knock-out (Rancourt et al., 1995). Mice in which *Hoxb5* is inactivated exhibit a bilateral or unilateral shift in forelimb position. The shift can extent from half to one somite. The clavicle retains its medial articulation with its normal target, the sternum, resulting in a V-shaped shoulder girdle. As a result of the limb displacement, the brachial plexus nerves enter the limb not in the medial limb mesenchyme but instead in the posterior. However, the defects are not restricted only to the limb. Anterior homeotic transformations of the cervico-thoracic vertebrae from C6 through T1 are also evident. Identical vertebrae homeotic transformations are also evident in *Hoxb6*$^{-/-}$ mice. It is generally believed that the *Hox* code contributes to position the limb fields in a variety of vertebrates. Further mechanisms, downstream of the *Hox* code, are believed to act in refining the positional information provided by *Hox* genes. Retinoic acid (RA) is involved in controlling

Hox gene expression in the LPM at the time at which the fields are determined (Marshall et al., 1996). *Ralhd2*, the enzyme important in RA synthesis, is shown to be crucial for limb positioning, initiation and patterning (Mic et al., 2004; Niederreither et al., 2002; Stratford et al., 1996; Stratford et al., 1999).

Other evidence of genetic cues controlling limb position come from the characterization of mouse mutants. *Luxate* (*lx*) is a spontaneous mutation in the mouse that has been mapped to chromosome 5. *lx* mutants show polydactyly that is restricted to the hindlimbs. More importantly, the hindlimbs are shifted in their axial position. It has been suggested that *lx* mutation affects the positioning of signaling centers such as the zone of polirizing activity (ZPA) along the rostro-caudal axis of the developing mouse embryo (Yada et al., 2002).

1.2 Limb bud initiation

The exact mechanism of limb initiation is still unclear. Experiments in chicken embryos have suggested that axial cues secreted from the intermediate mesoderm (IM, the precursor of the kidney that lies between the somites and the LPM) may be responsible for initiating limb outgrowth (Martin, 1998). The molecular nature of these signals has remained elucive. *Fgf8* was considered as a candidate signal for limb induction. *Fgf8* is transiently expressed in the IM at the forelimb and hindlimb levels during limb initiation. Moreover, Fgf8 protein (and other proteins of the Fibroblast growth factor family), is capable of directing initiation and normal development, of an ectopic limb bud from the embryonic flank (Cohn et al., 1995; Crossley et al., 1996; Vogel et al., 1996; Yonei-Tamura et al., 1999). However, recent experiments in the mouse have shown that deletion of *Fgf8* in the intermediate mesoderm and before limb initiation, had no effect on initial limb bud outgrowth (Boulet et al., 2004). Members of another

family of secreted proteins, *Wnts*, are recently implicated as key factors for limb initiation (Kawakami et al., 2001). *Wnt2b*, is expressed in IM and later in the LPM at the level of the forelimb and *Wnt8c*, which is present in the IM and later in the LPM at the level of the hindlimb are capable of inducing ectopic limbs when misexpressed in the interlimb flank. These Wnts are signaling through the β-catenin/canonical pathway and are thought to be necessary and sufficient for the induction of *Fgf10* expression in the LPM of the presumptive limb region which is required for limb initiation and outgrowth (Fig. 1B).

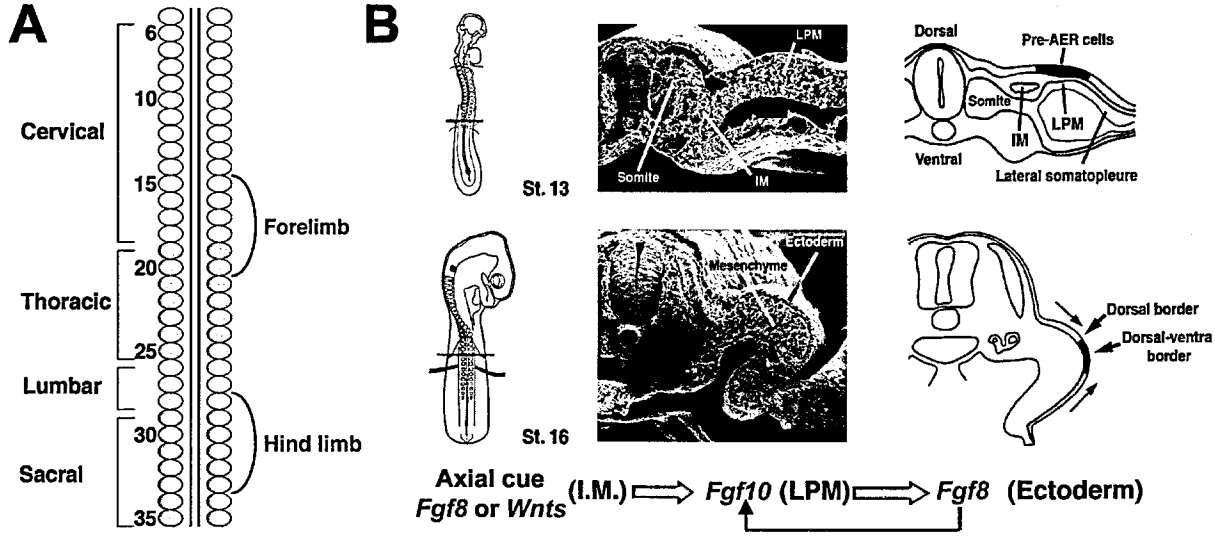

Figure 1. Limb positioning along the rostrocaudal axis of the developing vertebrate embryo and the limb initiation pathway. **A.** Schematic of the axial structures of a chicken embryo. Somites are numbered and axial level is designated. In all tetrapods, forelimbs develop at the cervical-thoracic junction while hindlimbs develop at the lumbar-sacral junction. **B.** The limb initiation pathway. At stage 13 of chicken development an axial cue (Wnt family members) expressed in the lateral plate mesoderm (LPM) induce Fgf10. At later stages (stage 16) Fgf10 signals to the overlying ectoderm and induces Fgf8 in the AER cells. A positive feedback loop between Fgf10 and Fgf8, mediated by Wnt3a, is established that promotes limb ougrowth.

Fgf10 is a crucial component of the limb initiation pathway. Experiments in chick and mouse have shown that the apical ectodermal ridge (AER), a specialized epithelium that runs along the distal tip of the limb, is important during limb outgrowth and patterning. Experiments in chick and mouse have demonstrated that *Fgf10* is required for the induction of *Fgf8* expression in the AER (Fig. 1B) (Min et al., 1998; Ohuchi et al., 1997; Sekine et al., 1999; Yonei-Tamura et al., 1999). *Fgf10* knock-out mice, exhibit severe limb truncations. In the forelimb region the scapula and clavicle are present but all other limb elements are absent. In the hindlimb, a rudimentary pelvis is observed but hindlimb components such as digits, tibia, fibula and femur are completely absent (Min et al., 1998; Sekine et al., 1999). The importance of *Fgfs* has also been demonstrated by targeted inactivation of Fgf receptors. Lack of *Fgfr2* in mouse embryos disrupts limb initiation (Xu et al., 1998). The induction of *Fgf8* in the AER by the mesodermally expressed *Fgf10* is shown to be mediated by *Wnt3* (or *Wnt3a* in the chick) (Barrow et al., 2003; Kawakami et al., 2001). *Wnt3* is expressed throughout the limb ectoderm while *Wnt3a* is expressed in the AER. Conditional knock-out of *Wnt3* produces phenotypes, from a normal hindlimb to the complete absence of all hindlimb elements. However a pelvis is visible. The phenotypes are explained as a failure of the induction or maintenance of *Fgf8* expression in the AER. Finally, the effects of *Wnt3/Wnt3a* have been shown to be mediated through the β-catenin/canonical Wnt-pathway (Barrow et al., 2003; Kawakami et al., 2001). In conclusion, limb initiation is triggered through an inductive cascade of signals from intermediate mesoderm to lateral plate mesoderm to ectoderm and involve members of the Wnt and Fgf families of secreted signaling molecules.

1.3 Limb Outgrowth and Patterning

The developing limbs are patterned in three axes: Proximal-distal (from shoulder- to tip of digits), anterior-posterior (from thumb-to little finger) and dorsal-ventral (from back to palm of the hand). For normal limb development to proceed, the establishment of key signaling centers within the nascent bud is essential (Fig.2A). Two important signaling centers of the limb are the apical ectodermal ridge (AER) which is essential for proximal-distal patterning of the limb, and the zone of polarizing activity (ZPA), an area of mesenchymal cells in the posterior limb which is required for antero-posterior patterning.

1.3.1 Proximo-distal patterning of the limbs

The AER is a specialized ectodermal structure located at the distal tip of the limb (Fig.2A). Surgical ablation of the AER, leads to failure of the limb to form distal structures, suggesting that patterning of the distal limb is dependent on the AER (Saunders et al., 1957). The observation that less severe truncations result when the AER is removed at progressively later stages contributed to the development of the so-called progress zone (PZ) model (Summerbell, 1974). According to this model, undifferentiated cells in a zone at the distal-most limb mesenchyme (the progress zone), undergo a progressive change in positional information such that their specification is altered from more proximal to more distal fates. This positional change is kept active as long as the cells remain in the progress zone. As cells proliferate and cell numbers within the limb bud increase, cells leave the zone. As they leave, cells become fixed with the positional value last attained while within the zone. Nevertheless, some reports have shown that following AER removal, some distal mesenchyme cells are eliminated by cell death (Dudley et al., 2002). In addition, in conditional knock-

out of *Fgf8* digits are present (Lewandoski et al., 2000). These results are not consistent with the progress zone model. Embryological experiments in the chick and genetic experiments in the mouse (in which *Fgf4* and *Fgf8* are deleted from the developing limbs at different time points in the developing forelimb and hindlimb) were performed (Dudley et al., 2002; Sun et al., 2002). An alternative model has been suggested in which the P-D axis is specified early in limb development as distinct domains and during subsequent development these progenitor populations are expanded before final differentiation. The distal mesenchyme becomes progressively 'determined' that is, irreversibly fixed, to a progressively limited range of potential proximo-distal fates (Dudley et al., 2002; Sun et al., 2002).

Removal of the AER, the source of the Fgfs, results in limb truncations. A positive-feedback loop between AER and limb mesoderm was discovered that is essential for continued outgrowth and cell survival. Mesodermally-expressed *Fgf10* signals to the overlying ectoderm and induces *Fgf8* expression. *Fgf8* in turn, signals back to the mesenchyme and maintains *Fgf10* expression in the mesenchyme. The positive feedback loop that is established between *Fgf8* and *Fgf10* promotes limb growth (Fig.1B) (Ohuchi et al., 1997; Sun et al., 2002). Fgf receptors that mediate the reciprocal regulation loop are Fgfr1 and Fgfr2. Fgfr1 has two splice variants that are both present in the mesenchyme. Fgfr2 has two splice variants Fgfr2-IIIb and Fgfr2-IIIc. *Fgfr2-IIIb* is expressed in the ectoderm while *Fgfr2-IIIc* is present in the mesenchyme. Inactivation of *Fgfr2* or only the *Fgfr2-IIIb* isoform results in absence of the forelimbs (Arman et al., 1999; De Moerlooze et al., 2000; Revest et al., 2001; Xu et al., 1998) Mice with inactivation of the mesodermally-expressed *IIIc* isoform of *Fgfr2* do have limbs

(but the animals have growth and ossification problems) (Eswarakumar et al., 2002) possibly due to redundancy with *Fgfr1* present in the mesenchyme.

Retinoic acid (RA) and genes such as *Meis1*, *Meis2, Pbx1* and *Hox* genes have been implicated in proximo-distal specification of limb elements. *Hoxa11* and *Hoxa13* are expressed in distinct domains along the proximo-distal axis. *Hoxa13* is expressed in the autopod area (most distal, handplate), while *Hoxa11* in the zeugopod region (encompassing the radius/ulna or tibia/fibula) (Nelson et al., 1996). RA has been shown to proximalize regenerating urodele limbs, leading to tandem PD duplication of limb structures (Maden, 1982) and, in the chick, grafts of limb tissue exposed to RA develop structures of a more proximal identity (Tamura et al., 1997). Therefore, RA has been shown to be required and sufficient for the proximalization of limb cells (Niederreither et al., 2002; Stratford et al., 1996; Stratford et al., 1999). The action of RA is mediated through the maintainance of the normal proximal domain of *Meis1/Meis2* genes in the limb. In the limb bud, RA signaling is restricted to the proximal limb by FGF activity (Mercader et al., 2000) that emanates from the AER. Studies in *Drosophila* have shown that the gene *extradenticle* (*exd*) is required for proximo-distal specification of the wing. Gene deletion studies in the mouse have shown that inactivation of *Pbx1*, the homologue of *Exd*, results in loss of proximal limb structures while distal structures are unaffected. *Exd/Pbx1* are homeobox transcription factors that are important co-factors for Hox proteins. Exd and Pbx1 are able to dimerise with Hox proteins and modulate their DNA binding affinity. Transcripts of *Exd* or *Pbx1* are present in the whole wing or limb mesenchyme respectively. However, the function of *Exd/Pbx1* is regulated post-translationally through a mechanism that involves translocation into the nucleus. Only nuclear *Exd/Pbx1* protein is functional. *Homothorax* (*Hth*) and its

vertebrate homologues *Meis1* and *Meis2* physically interact with Exd/Pbx1 and regulate their nuclear import. *Meis1* in the chicken is expressed in proximal limb regions up to the stylopod/zeugopod boundary. Ectopic expression of *Meis1* results in nuclear translocation of Pbx1 throughout the limb mesenchyme. Distal limb development is disrupted and distal-to-proximal transformations are induced. In conclusion restriction of functional Meis1/Pbx1 heterodimers to proximal regions of the limb is essential to specify cell fates and differentiation patterns along the P–D axis of the limb (Mercader et al., 1999).

1.3.2 Antero-posterior patterning of the limbs

The ZPA has a central role in the patterning of the antero-posterior axis of the limb. The ZPA is a group of cells in the posterior limb mesenchyme that produce the secreted morphogen Shh and serves as a signaling centre for the anterior-posterior axis of the limb (Fig. 2A and 2C). A ZPA graft or ectopic expression of Shh in the anterior limb mesenchyme causes cell respecification and produces mirror image digit duplications. This activity has been modeled as a concentration-dependent response to a diffusible morphogen. Ablation of Shh expression using knock-out strategies in mouse causes severe disruption to antero-posterior patterning of the limb. For example, *Shh*$^{-/-}$ mouse embryos have only one digit (the anterior-most) and a single zeugopodal bone (Litingtung et al., 2002; Riddle et al., 1993; Tabin, 1991; Tickle and Eichele, 1994). These results show that *Shh* plays a critical role in establishing distinct fates for correct antero-posterior patterning of the limbs. Recent experiments in the mouse demonstrated the ultimate fate of Shh-producing cells. A *gfpcre* fusion cassette containing a nuclear localization signal was inserted at the ATG of *Shh* gene. Mice heterozygous for the *Shhgfpcre* allele do not exhibit noticeable

phenotypes. GFP expression was observed to co-localize with *Shh* mRNA in the limb. In this way, fate mapping of the cells that have expressed *Shh* in the limb is possible. The descendants of the Shh-producing cells encompass a broad posterior domain includind digits IV and V and contributing to the posterior of digit III as well as the posterior zeugopod. In addition, a tamoxifen inducible *ShhcreER^{T2}* allele was generated. Mouse carrying the allele were crossed with the *Rosa26* (*R26R*) reporter mice for the generation of *ShhcreER^{T2}/+;R26R/+* mice. Mothers were injected with tamoxifen at different time-points during pregnancy. Populations of *Shh*-expressing cells at discrete developmental time-points are revealed by the expression of *LacZ*. These experiments suggested that, while anterior digits depend on different concentrations of Shh, cells that form posterior digits express *Shh* longer. The length of time of exposure to Shh may be critical in the specification of the differences between the most posterior digits suggesting that Shh morphogen is dictated by a temporal as well as a spatial gradient (Harfe et al., 2004).

Genetic studies in *Drosophila* have led to better understanding of gene function required for fly wing development. In *Drosophila* embryos, all known functions of Hh signaling are mediated by the zinc-finger transcriptional effector Cubitus interruptus (Ci). In vertebrates the *Ci* homolog, *Gli3,* is essential for antero-posterior limb patterning both prior to and during *Shh* signaling. In the absence of *Shh* signaling, *Gli3* is proteolytically cleaved and the truncated protein (Gli3^{R}) acts as a repressor of *Shh* targets. Gli3^{R}, present in the anterior limb mesenchyme, acts by causing restriction of *dHand* (also known as *Hand2*), a bHLH transcriptional activator (Dai and Cserjesi, 2002; Dai et al., 2002), in the posterior limb mesenchyme. In addition, Gli3 restricts the Shh-independent early expression of *5'HoxD* genes (essential for normal digit formation) and the

BMP antagonist *Gremlin* to the posterior mesenchyme. In turn, *dHand* prevents *Gli3* expression from spreading posteriorly. The genetic interaction between *Gli3* and *dHand*, pre-patterns the limb and positions the ZPA in the posterior limb mesenchyme (te Welscher et al., 2002a; Zuniga and Zeller, 1999). Studies in the mouse have demonstrated the requirement of *dHand* for *Shh* expression in the ZPA. In mouse embryos homozygous for a *dHand* null allele, limb buds are severely under-developed and *Shh* is never expressed (Charite et al., 2000). Conversely, misexpression of *dHand* in the anterior limb mesenchyme in transgenic mice and in chicken using avian retroviruses, results in formation of an additional ZPA, revealed by ectopic expression of *Shh*, giving rise to limb abnormalities that include polydactyly with duplication of posterior skeletal elements (Charite et al., 2000; Fernandez-Teran et al., 2000). Analysis of $Shh^{-/-}$ mice revealed a feedback mechanism in which *Shh* signaling is required to maintain the full *dHand* expression domain in the developing limb (Charite et al., 2000).

In the presence of Shh, proteolysis of Gli3 is inhibited generating an anterior-to-posterior gradient of $Gli3^{R}$ in the limb mesenchyme (Litingtung et al., 2002; Wang et al., 2000). While data suggest that the full-length Gli3 ($Gli3^{FL}$) is able to act as a mild transcriptional activator (Bai et al., 2004; Lei et al., 2004; Wang et al., 2000) other reports suggest that, depending on the context, it also has the ability to act as a repressor (Sasaki et al., 1997).

The mouse mutation *Extra toes* (Xt^{J}) generates a Gli3 null allele resulting in preaxial (anterior) digit I iterations in heterozygotes. The limbs of Xt^{J}/Xt^{J} homozygotes ($Gli3^{-/-}$) are normal to the level of the wrist/ankle, but exhibit severe polydactyly, which has been causally attributed to ectopic *Shh* expression in the anterior limb mesenchyme (Buscher et al., 1997; Buscher et

al., 1998; Litingtung et al., 2002). *Shh*$^{-/-}$/*Gli3*$^{-/-}$ mice develop polydactylous limbs. Although *Shh*$^{-/-}$/*Gli3*$^{-/-}$ digits exhibit loss of wild-type identities, some A/P

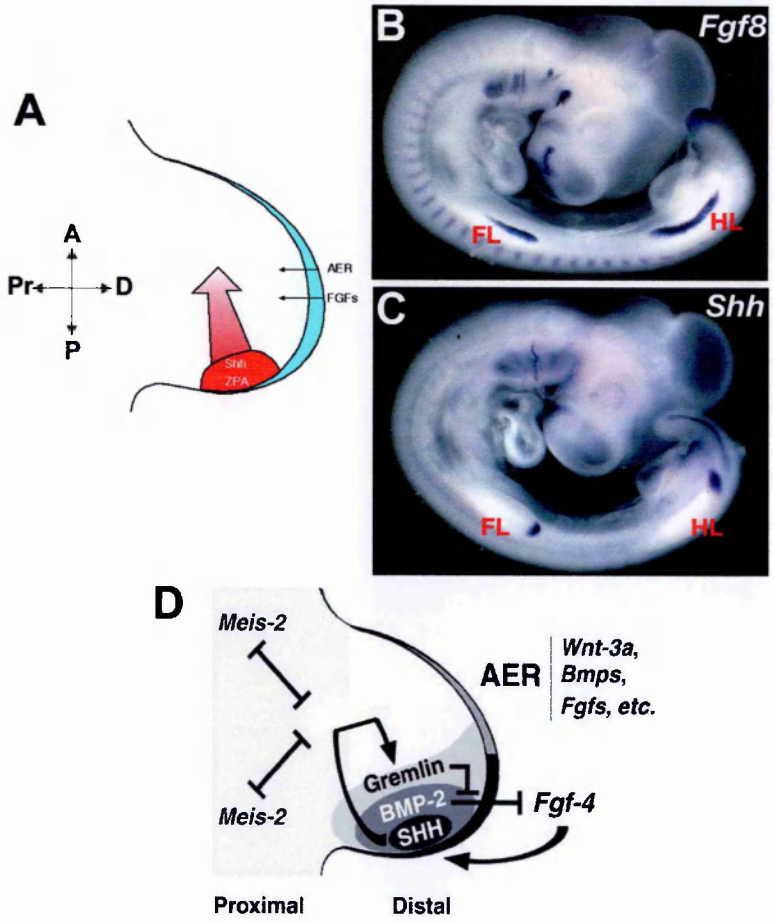

Figure 2. Normal patterning of the vertebrate limb requires the establishment of signaling centres within the developing bud and interactions between them. **A.** Schematic representation of the signaling centres of the limb. The apical ectodermal ridge (AER), is located at the distal tip of the limb bud and the zone of polarizing activity (ZPA) at the posterior limb mesenchyme. *In situ* hybridization on chicken embryos for *Fgf8* (**B**) and *Shh* (**C**), molecular markers of the AER and ZPA, respectively. **D.** Schematic representation of the key molecules that participate in the Shh/Fgf4 positive feedback loop. These interactions provide a functional link between the anterior-posterior and proximal-distal patterning mechanisms important for coordinated development of the limb bud. A:anterior; P: posterior; Pr:proximal; D:distal; FL:forelimb; HL:hindlimb.

polarity is still observed. Interestingly, *Shh*$^{-/-}$/*Gli3*$^{-/-}$ and *Gli3*$^{-/-}$ limbs are indistinguishable despite the endogenous and ectopic Shh expression in *Gli3*$^{-/-}$ limb buds (Litingtung et al., 2002; te Welscher et al., 2002b). *Shh* therefore has no effect on skeletal patterning in the absence of *Gli3*. *Gli3*$^{-/-}$ polydactyly must be a direct effect of losing Gli3 function, and is not due to ectopic expression of Shh or dHand. This observation explains why *Gli3*$^{-/-}$ limbs clearly lack the mirror-image digit duplications expected from an ectopic anterior ZPA (Litingtung et al., 2002; te Welscher et al., 2002b). The development of *Shh*$^{-/-}$/*Gli3*$^{+/-}$ mice revealed that, in the absence of *Shh*, removing *Gli3* restores limb skeletal elements in a dose-dependent manner. *Shh*$^{-/-}$/*Gli3*$^{+/-}$ limbs develop two identifiable zeugopod elements with clear A/P asymmetry. *Shh*$^{-/-}$/*Gli3*$^{+/-}$ limbs typically form three or four digits. The direct correlation between *Gli3* levels and digit number supports the hypothesis that *Gli3*, rather than Shh, directly regulates digit number. The balance between Gli3^{R} and Gli3^{FL} is also critical. Mice that express only the truncated form of Gli3 (*Gli3*$^{\Delta 699}$ allele) exhibit iterations of central digits (central polydactyly) as a result of excessive Gli3^{R} (Bose et al., 2002). The effects of *Shh* signalling require *Gli3*, and are mediated by regulating the relative balance of Gli3^{R} and Gli3^{FL} activities.

1.3.3 The *Fgf/Shh* positive feedback loop. A link between proximo-distal and antero-posterior patterning

Limb bud morphogenesis is controlled by reciprocal interactions of the AER and ZPA. *Shh* signaling by the polarizing region is responsible for patterning the antero-posterior axis of the limb but also for the maintenance of *Fgf* expression in the AER. *Fgfs* serve to maintain *Shh* expression (Laufer et al., 1994; Niswander et al., 1994). *Shh* maintains *Fgf4* by up-regulating *Gremlin* in the

adjacent mesenchyme (Fig.2D) (Capdevila et al., 1999; Zuniga et al., 1999). *Gremlin* is a bone morphogenetic protein (Bmp) antagonist (Hsu et al., 1998) that prevents *Bmp2* expressed in response to *Shh*, from down-regulating *Fgf4* (Ganan et al., 1998; Pizette and Niswander, 1999). *Fgf8*, is not directly dependent on *Shh* for its transcription (Chiang et al., 2001). However, in the absence of *Gremlin*, the AER becomes disorganized and *Fgf8* expression is down-regulated (Khokha et al., 2003). Thus, the signaling centers in the posterior and distal tip of the limb bud are interdependent for their activity, and this positive feedback loop is required for producing a normal limb structure. The signaling loop between *Shh* and Fgfs operates throughout limb development until embryonic day 6 (E6) in the mouse or st.27 (HH) in the chick (Sanz-Ezquerro and Tickle, 2000), when *Fgf4* and *Gremlin* are no longer expressed and *Shh* is down-regulated (Riddle et al., 1993). Concomitantly, the rate of cell proliferation in the limb decreases.

2. The T-box family of transcriptional regulators

2.1 Evolution and genomics

T-box genes comprise an ancient family of transcriptional regulators found from sponges to humans. The family is characterized by the presence of a highly conserved motif, the T-box, that encodes a 180 amino acid DNA-binding /dimerisation domain, the T-domain. A mouse mutation in a T-box gene was first described more than 80 years ago but the cloning of the founding member of this family, the mouse *T* or *Brachyury* gene was only achieved more than 60 years later (Dobrovolskaia-Zavadskaia, 1927; Kispert and Hermann, 1993; Kispert et al., 1995; Smith et al., 1991; Wilkinson et al., 1990).

With identification of T-box genes in the genomes of a range of model organisms it has been possible to group T-box genes in five subfamilies: the *Brachyury*, *T-brain1*, *Tbx1*, *Tbx2* and *Tbx6* subfamilies (Fig.3). Genes in the same subfamily are predicted to have arisen from the duplication of a single ancestral gene and may exhibit overlapping sites of expression that in some cases may indicate functional redundancy. However, these T-box genes can also have acquired unique expression patterns and/or functions by divergence after the initial duplication event.

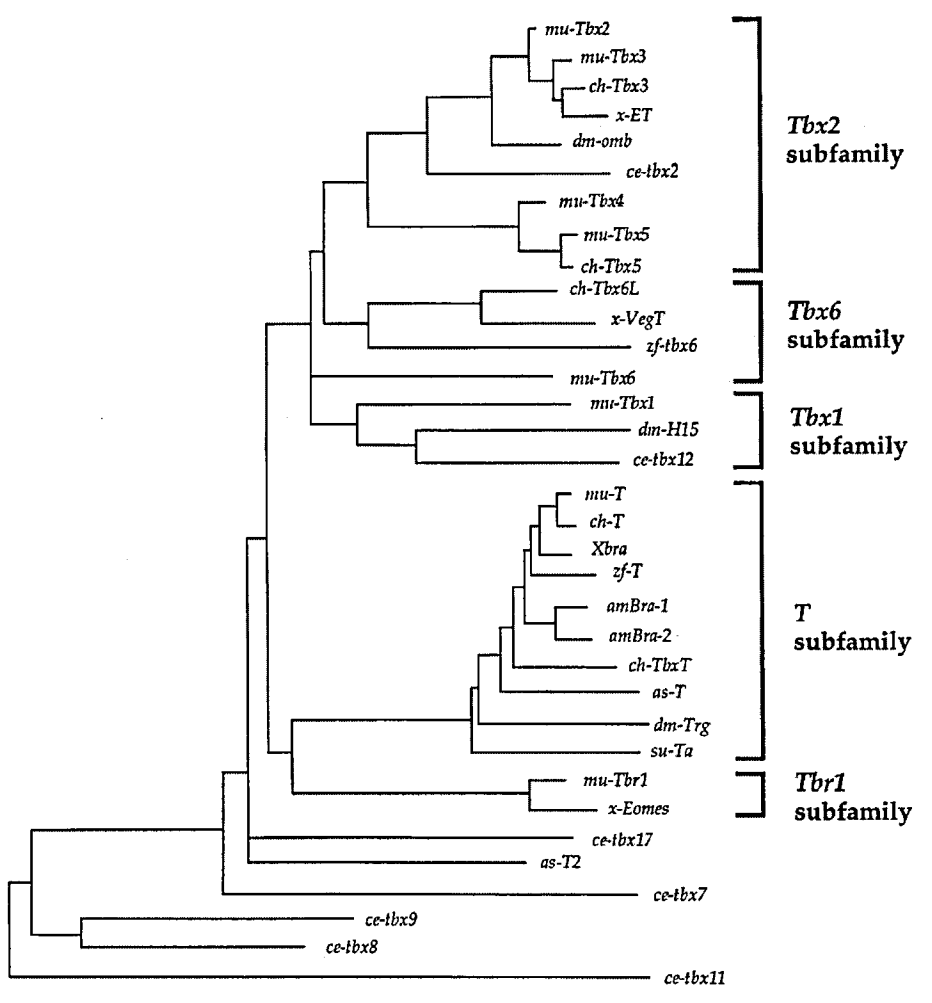

Figure 3. Phylogenetic tree of the T-box gene family (acquired from Papaioannou and Silver, 1998). T-box subfamilies are grouped and indicated by brackets. Five *c.elegans* and one Ascidian gene at the bottom of the tree have yet to be classified into particular subfamilies.

Abbreviations: mu: murine, ch: chick, x: *Xenopus*, dm: *D. melanogaster*, ce: *C.elegans*, zf: zebrafish, as: ascidian, am: amphioxus, su: sea urchin.

In vertebrates, the *Tbx2/3/4/5* subfamily of T-box genes consists of four members *Tbx2, Tbx3, Tbx4* and *Tbx5*. These genes are organised in the genome as two pairs of linked genes, *Tbx2-Tbx4* and *Tbx3-Tbx5*, which are thought to be a product of an ancestral gene tandem duplication, followed by duplication and dispersion of the two gene clusters (Fig.4) (Agulnik et al., 1996).

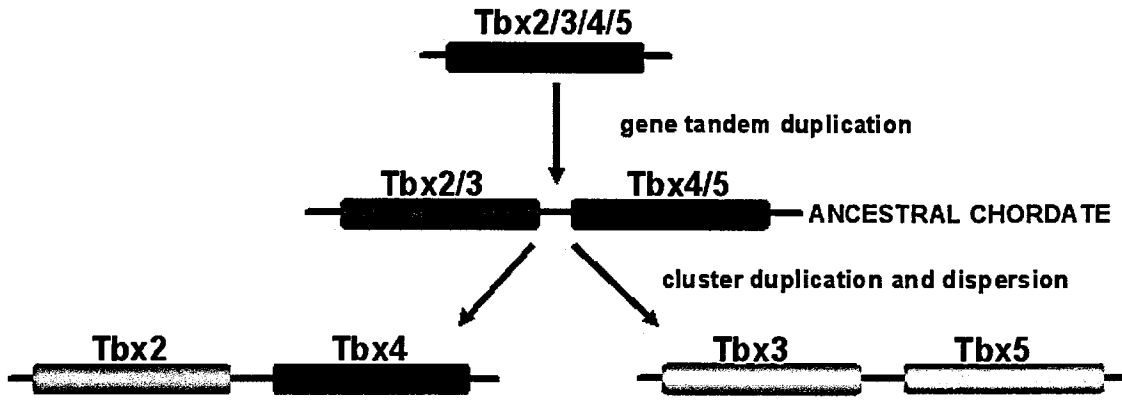

Figure 4. Schematic showing the origin and evolution of Tbx2/3/4/5 subfamily of T-box transcriptional regulators (Modified from Agulnik et al., 1996).

2.2 *Tbx2* and *Tbx3* in development

In vitro data suggest that human and mouse *Tbx2* and *Tbx3* encode for transcriptional repressors and have been implicated in cell cycle and cancer (Brummelkamp et al., 2002; Carlson et al., 2001; Lingbeek et al., 2002). Both *Tbx2* and *Tbx3* can repress $p19^{ARF}$ murine tumor suppressor (Brummelkamp et al., 2002; Lingbeek et al., 2002) and inhibit senescence. *Tbx2* is shown to be repressing p21-cyclin dependent inhibitor (Prince et al., 2004). In melanocytes, *Tbx2* represses melanocyte-specific tyrosinase-related protein 1 (TRP-1) (Carreira et al., 1998) while it is a direct target of Mitf, a factor required for

melanocyte proliferation and maintenance of melanoblast identity (Carreira et al., 2000). Human and mouse *Tbx3* are reported to have two variants (TBX3 and TBX3+2a) originating from alternative splicing of the 60 bp 2a exon. The two splice variants both present in all tissues analysed (where *Tbx3* is expressed) have different DNA binding properties with only TBX3 able to bind T-box consensus binding sites. In addition TBX3 promotes cell cycle progression while TBX3+2a promotes senescence (Fan et al., 2004).

Common gene regulation function has been reported for *Tbx2* and *Tbx3* during heart and retina development (Habets et al., 2002; Hoogaars et al., 2004). *Tbx2* and *Tbx3* are expressed in embryonic myocardium that will not form chamber myocardium. In these sites, Tbx2 and Tbx3 repress genes that are part of the chamber differentiation program (*Tbx2* represses Atrial Nutriuretic Factor,ANF, and *Tbx3* represses natriuretic precursor peptide A and the gap junction protein Connexin40) leading to chamber specific gene expression and myocardial differentiation (Habets et al., 2002; Hoogaars et al., 2004). In the *Xenopus* retina both genes are reported to inhibit Gli-dependent *Shh* signaling (Takabatake et al., 2002). Tbx2 has been shown to repress all *Gli* homologues (*Gli1*, *Gli2* and *Gli3*) while Tbx3 is able to repress only *Gli1* and *Gli2.*

Tbx2 and *Tbx3* are expressed in the two stripes in the anterior and posterior mesenchyme of the developing forelimb and hindlimb (st.20 HH in the chick, E10.5 dpc in the mouse) (Gibson-Brown et al., 1998; Logan et al., 1998; Tumpel et al., 2002). Experiments in the chick have shown that the posterior domain of *Tbx3* expression in the limb is positively regulated by *Shh* signaling while the anterior expression domain is repressed by *Shh.* This has been interpreted to suggest a potential role of *Tbx3* in the antero-posterior patterning of the vertebrate limb (Tumpel et al., 2002).

All mutations described in T-box genes to date have severe effects on normal development. Importantly, a number of human disorders have been linked to mutations in T-box genes, confirming their medical importance (Table 1). Haploinsufficiency of human *TBX3* causes Ulnar-mammary syndrome (UMS, OMIM 181450). UMS, affects the ulnar ray of the limb with phenotypes ranging from hypoplasia of the terminal phalanx of the fifth digit, to the complete absence of forearm and hand. Patients with UMS also have abnormal development of breasts, teeth and genitalia. Male patients typically have delayed onset of puberty (Packham and Brook, 2003). Mice in which *Tbx3* has been deleted, exhibit forelimb abnormalities that resemble the deficiencies observed in human (Davenport et al., 2003). However, there are some important differences between the human disease and the phenotype of *Tbx3*$^{-/-}$ mice. UMS patients are predominantly affected in the upper-limb, but in homozygous *Tbx3* knock-out mice the hindlimbs show the most severe defects and heterozygotes have no limb phenotype (Davenport et al., 2003). *Tbx2* and *Tbx3* have also been reported to control the identity of posterior digits in the developing chick leg through *Bmp* and *Shh* signaling (Suzuki et al., 2004). Misexpression of *Tbx2* and *Tbx3* induced posterior transformation of digit III to digit IV and digit II to digit III, respectively. Conversely, misexpression of activator forms of *Tbx2* and *Tbx3* induced anterior transformation. In both cases, alterations in the expression of *Bmp2, Shh* and *HoxD* genes were observed. In addition, *Tbx2* and *Tbx3* rescued inhibition of interdigital BMP signaling mediated by Noggin. These studies suggested that *Tbx3* specifies digit III, and the combination of *Tbx2* and *Tbx3* specifies digit IV, acting together via *Shh* and *Bmp* signaling pathways.

2.3 *Tbx4* and *Tbx5* in development

Tbx4 is expressed in the developing hindlimb region prior to overt limb outgrowth but not in the forelimb.

Subfamily	Gene	Human Chromosome	Expression	Heterozygous phenotype in human (or null pheno-type of mouse homolog)
Brachyury	BRACHYURY	6	Primitive streak, tail bud, and notochord	Spinal cord defects (anteroposterior axis defects)
	TBX19 (TPIT)	1	Pituitary	Adrenal insufficiency
T-brain1	T-BRAIN1	2	Cerebral cortex	
	EOMESODERMIN/ (?T-BRAIN2)	3	Trophoblast, early primitive streak, and cerebral cortex	(Early postimplantation failure)
	TBX21 (T-BET)	17	Th1 lineage, lung, and spleen (adult)	
Tbx1	TBX1	22	Heart and pharyngeal arges	DiGeorge syndrome
	TBX10	11		
	Tbx13 (MmTbx7)*			
	Tbx14 (MmTbx8)*			
	TBX15	1	Craniofacial region and limbs	Coat development, skeletal development
	TBX18	6	Heart, somites, and limbs	Somite generation defects
	TBX20 (TBX12)	7	Heart, eye, ventral neural tube, and limb	
	TBX22	X	Fetus	Cleft palate-ankyloglossia
Tbx2	TBX2	17	Limbs and heart	X-linked cleft palate
	TBX3 (including an alternative splice form)	12	Limbs and heart	Ulnar-mammary syndrome
	TBX4	17	Allantois, hindlimb	Small Patella Syndrome
	TBX5 (including an alternative splice form)	12	Forelimb	Holt-Oram syndrome (failure of heart development)
Tbx6	TBX6	16	Primitive streak and tail bud	(Respecification of posterior paraxial mesoderm as neurectoderm)

*These sequences have been reported in mouse but not human; the human genes are hypothetical.

Table 1. T-box transcriptional regulators, implicated in developmental processes and in human disorders.

The hindlimb-restricted expression pattern persists at later stages of limb development (Gibson-Brown et al., 1998; Logan et al., 1998). *Tbx4* is required for hindlimb development since Haplo-insufficiency of *TBX4* in human, causes Small Patella Syndrome (SPS, OMIM 147891), an autosomal-dominant skeletal dysplasia characterized by patellar aplasia or hypoplasia and by anomalies of the pelvis and feet (Bongers et al., 2004). Ablation of *Tbx4* function using targeted mutagenesis in the mouse showed that embryos homozygous for the null allele fail to undergo chorioallantoic fusion and die by 10.5 days post coitus. The allantoises of *Tbx4*-mutant embryos are stunted, apoptotic and display abnormal differentiation. Heterozygous embryos show a mild, transient growth defect in the allantois. Induction of a hindlimb occurs normally in *Tbx4* mutants and initial patterning of the hindlimb bud appears normal. However, hindlimb buds from *Tbx4* mutants fail to develop either in vivo or in vitro and *Fgf10* expression is not maintained in the mesenchyme (Naiche and Papaioannou, 2003). These results have been interpreted to suggest that *Tbx4* is not involved in limb initiation. Interestingly, misexpression of a dominant-negative form of *Tbx4* (Tbx4-engrailed fusion) in the developing hindlimb of chicken embryos, leads to a failure of leg formation. In addition, when *Tbx4* is misexpressed in the interlimb flank, an additional limb is induced (Takeuchi et al., 2003). These data suggest that *Tbx4* is necessary and sufficient for hindlimb initiation.

Tbx5 is expressed in the presumptive forelimb region prior to overt limb outgrowth but not in the hindlimb. The forelimb-restricted expression pattern persists at later stages of development (Gibson-Brown et al., 1998; Logan et al., 1998). Direct evidence for a role of *Tbx5* in forelimb development has been

provided by the discovery that mutations in human *TBX5* cause Holt-Oram Syndrome (HOS, OMIM #142900). HOS is an autosomal dominant disorder affecting 1 in 100 000 live births. It is completely penetrant with a highly variable expression and causes both cardiac and skeletal congenital abnormalities. The skeletal abnormalities affect the forelimb, and include loss of anterior structures, or even phocomelia. In other cases elongated phalanges of the thumb are observed. Abnormalities are also bilateral and asymmetrical, affecting the left side more severely than the right. Defects observed in the heart affect the conduction system, atrial and ventricular septation. A high proportion of patients have an ocular defect. Mutations in *TBX5* have been identified in both familial and sporadic cases of HOS. The majority of mutations in *TBX5* are null alleles that cause the HOS phenotype by haploinsufficiency. In some cases missense mutations have been identified to produce phenotypes that affect heart and limbs in different extent. Missense mutations at the amino-terminus of the DNA binding domain cause severe cardiac but milder skeletal abnormalities. In contrast mutations at the C-terminal end of the T-box cause only mild cardiac defects but severe skeletal ones (Basson et al., 1999). Targeted deletion of *Tbx5* in the mouse has demonstrated that this gene is essential for normal heart and limb development (Bruneau et al., 1999; Bruneau et al., 2001). Heterozygote *Tbx5* mutant mice ($Tbx5^{del/+}$) are an excellent model for Holt-Oram syndrome heart deficiencies. All adult $Tbx5^{del/+}$ mice have enlarged hearts with atrial septal defects. $Tbx5^{del/+}$ mice have only subtle defects in the limbs. Elongated phalangeal segments of the first forelimb digit (equivalent to the human thumb) and hypoplastic bones of the wrist are present (Bruneau et al., 2001). *Tbx5* null embryos do not survive beyond embryonic day (E) 10 due to the severity of the heart defects (Bruneau et al., 2001).

3. Limb-type specification

Genes involved in limb initiation and patterning are expressed in identical patterns in both the developing forelimb and hindlimb. Cells in the developing forelimb interpret this signals and form fingers, while cells in the hindlimb interpret the same signaling cascades and develop into toes (Fig.5). The nature of the factors responsible for controlling this differential response is now beginning to be revealed.

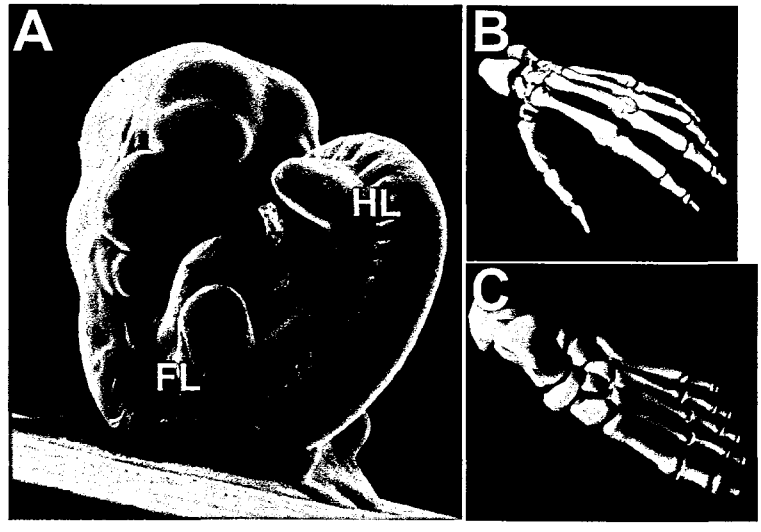

Figure 5. A. Scanning electron micrograph of a mouse embryo at E10.5. The forelimbs (FL) and the hindlimbs (HL) are visible as budding outgrowths. At these early stages forelimbs and hindlimbs are morphologically uniform, and cells in both types of limbs are subject to common signaling cues. However, cells in the forelimbs and hindlimbs respond differently and form morphologically distinct structures such as the hand (**B**) and the foot (**C**).

The acquisition of limb-type identity during embryonic development was first demonstrated by embryological experiments. Transplantations in the newt demonstrated that cells of the limb-forming region were able to give rise to fully developed limbs when transplanted in the flank (Harrison, 1918). Experiments using chick embryos showed that a graft from the wing-forming region generates an ectopic wing and a graft taken from the leg-forming region generates a new leg (Jacobson and Sater, 1988). Limb-type specification

occurs prior to limb initiation. If heterotopic grafts in the chick are performed after a limb bud has formed, a chimaeric limb develops that contains elements of both limb-types (Kieny, 1964; Saunders, 1948). Furthermore, when proximal mesoderm is grafted beneath the AER of the developing chick wing (Saunders et al., 1957; Saunders et al., 1959) its proximodistal fate is re-specified, but its limb-type identity remains fixed. Limb-type identity is determined by the mesodermal, rather than the ectodermal, component of the limb. Experiments in the chick have shown that when leg ectoderm is combined with wing mesoderm, a wing is formed. (Saunders and Gasseling, 1968; Zwilling, 1956a; Zwilling, 1956b). Embryological experiments have established the criteria that candidate genes for limb-type identity need to meet. Candidates are expected to be expressed prior overt limb-outgrowth. Their expression is expected to be maintained during subsequent limb bud stages. Their expression is also expected to be restricted to the limb mesenchyme.

Three candidates genes for limb-type specification have been identified. *Tbx5* and *Tbx4*, as already mentioned, are expressed the forelimb and hindlimb buds, respectively (Gibson-Brown et al., 1998; Ruvinsky et al., 2000; Simon et al., 1997; Takabatake et al., 2002). *Pitx1*, a paired-type homeodomain factor is expressed in the developing hindlimb but not in the forelimb (Lamonerie et al., 1996; Szeto et al., 1999). All three genes are expressed throughout the limb mesenchyme and not in the limb ectoderm (Gibson-Brown et al., 1998; Isaac et al., 1998; Logan et al., 1998; Ohuchi et al., 1998). Ectopic expression of *Tbx5* in the developing chick hindlimb bud can, at least partially, transform the identity of the leg to a more wing-like morphology (Rodriguez-Esteban et al., 1999; Takeuchi et al., 1999). In the converse experiment, hindlimb-specific gene *Tbx4* misexpressed in the forelimb can transform the wing to a more hindlimb

character (Takeuchi et al., 1999). A role for *Pitx1* in the specification of hindlimb identity has been supported by both gene-misexpression experiments in the chick and gene deletion approaches in the mouse. Misexpression of *Pitx1* in the developing wing, induces *Tbx4* expression in the distal wing mesenchyme and partially transforms both muscle and skeletal elements of the forelimb to a hindlimb-like character (Logan and Tabin, 1999). Gene inactivation experiments in the mouse demonstrated that in *Pitx1* null mice, the hindlimb does form, but features of hindlimb identity are lost and the limb has a forelimb-like character (Lanctot et al., 1999; Szeto et al., 1999). Levels of *Tbx4* transcripts are lower in *Pitx1*$^{-/-}$ hindlimbs than in wild type (Lanctot et al., 1999). This is consistent the data obtained from *Pitx1* misexpression in the chick, that Pitx1 contributes to *Tbx4* expression in the hindlimb, but also demonstrates that Pitx1 is not absolutely required for the induction of *Tbx4*.

Although the limb phenotypes obtained in chicks following the ectopic expression of *Tbx5*, *Tbx4* or *Pitx1* are dramatic, the resulting limbs are made up of intermediate limb-type characteristics. This can be explained by the observation that, following the misexpression of *Tbx4* or *Pitx1*, the endogenous expression of *Tbx5* in the forelimb is unchanged (Logan and Tabin, 1999; Rodriguez-Esteban et al., 1999; Takeuchi et al., 1999). This observation indicates that in these misexpression experiments, cells in the limb are presented with two competing programmes (forelimb vs hindlimb).

4. Aims of this study

Tbx5 and *Tbx3* are two closely-related transcription factors that are physically linked in the genome (human chromosome 12, mouse chromosome 5). To examine the role of *Tbx5* in forelimb development and understand the nature of HOS deformities, I have undertaken two strategies to disrupt its function in the developing limb bud. I have used a conditional knock-out strategy to delete *Tbx5* function specifically in the developing limbs. The second approach involves using avian retroviruses to misexpress dominant-negative *Tbx5* constructs to decrease *Tbx5* function in the developing wing bud. As a complementary strategy to misexpression of dominant-negative forms of *Tbx5*, I also misexpressed full length and dominant-active forms of the gene.

Tbx3 has an intriguing, dynamic expression during embryogenesis. In addition, the implication of human *TBX3* in disease, reveals the requirement of this gene during limb and mammary gland development. To examine the role of *Tbx3* in normal limb development I have undertaken the strategy to misexpress full length and dominant-negative constructs of *Tbx3* in the developing forelimb using the avian retroviral system.

B. MATERIALS AND METHODS

B. MATERIALS AND METHODS

1. DNA preparations

All DNA preparation were carried out using the Qiagen miniprep kit. For cell transfections DNA was prepared using the Cesium ultracentrifugation method (Sambrook, 1989).

2. Embryos

Mouse embryos were staged according to Kaufman (Kaufman, 1992). Noon on the day a vaginal plug was observed was taken to be E0.5 days of development. The mouse lines carrying a conditional allele of *Tbx5*$^{lox/lox}$ (Bruneau et al., 2001) and a *Prx1Cre* transgene (Logan et al., 2002) have been described previously.

Fertilised chicken eggs (Needle's farms, Winter's farms, The Poultry Farm) were incubated at 37°C and staged according to Hamburger Hamilton (HH) (Hamburger and Hamilton, 1951).

3. Tail and embryo sac DNA preparation

Tails are digested overnight at 55° C, with 0.5 ml of lysis buffer (0.3% SDS, 50 mM Tris pH7.5, 50 mM EDTA, 100mM NaCl) supplemented with 0.5 mg/ml proteinase K per tail. DNA is precipitated with 0.5 ml isopropanol and the pellet washed with 70% ethanol. The DNA is then resuspended in 100 μl of 10 μM Tris pH 7.5 at room temperature over night or 37° C for 1-2 hours. Embryo sacs were digested in 100 μl of lysis buffer following an identical procedure.

4. Genotyping

PCR analysis to genotype pup tail and embryonic material (E10, 30 somites), was carried out in a single reaction using three primers that identify the endogenous *Tbx5* allele, and both the conditional (floxed) and deleted (floxed-out) *Tbx5* allele as described in Bruneau et al., 2001

5. RNA preparation

Total RNA was isolated from chick and mouse embryos using the Trizol reagent (GibcoBRL). Fresh tissue, was homogenized in 800 μl Trizol in eppendorf tubes. It was then incubated 10 minutes at room temperature and then centrifugated 14000rpm for 3 minutes. The aqueous phase was transferred in a new tube and the RNA was precipitated using isopropanol and diluted in water.

6. Detection of Tbx3 isoforms

For the detection of mouse and chick *Tbx3* isoforms, we performed PCR using as template total RNA from mouse E10.5 dpc, chick st.19 (HH) and st.16 (HH) embryos. Based on published sequences of mouse *Tbx3* (variant 1 Accession no: NM_011535 and variant 2 Accession no: NM_198052) the following primers were designed: forward primer: 5'-TCTGAAGACCATGGAACCCGA-3', reverse primer: 5'-CAGTAACGGCGATGAATTCTG-5'. Based on the published sequence for chick *Tbx3* (Accession no: AF033669) the following primers where designed: forward primer: 5'-GCTGCAGAGACTGCTATCCCC-3', reverse primer: 5'-ATGAATTCAGT CTCCGGGAAC-3'. Mouse variant 1 is represented by a 624 bp PCR product while variant 2 by a 560 bp PCR product. For the chick, possible variants will be represented by a 685 bp PCR product (for variant 1 that contains the 60 bp insertion) and a 625 bp product (for variant 2). The PCR products were separated on a 2% agarose gel.

7. Cloning of expression constructs

For the expression plasmids containing full length, deletion, -engrailed and -VP16 fusion forms of *Tbx3* and *Tbx5* fusion ORFs were cloned in pcDNA3.1(-) (Invitrogen). *Tbx5* and *Tbx3* ORFs were cloned at the NcoI, EcoRI sites of Slax13, Slax13En and Slax13VP16 shuttle vectors. They were then excised from Slax using Cla I and their 5' and 3' ends were modified using T4 DNA polymerase (Biolabs). pcDNA3.1(-) was linearized using EcoRV. The plasmid was then de-phosphorylated for the prevention of self-ligation and was purified using a gel isolation kit (Qiagen). The ORFs were ligated with the linearized vector and putative positive clones were tested using diagnostic digestion with BamHI to produce a unique DNA fragment.

8. Transfections

Transfections for luciferase assays were performed in 12-well tissue culture plate (Nunc) using Superfect transfection reagent (Qiagen) according to the manufacturer's protocol. DNA was diluted in 50 μl DMEM unsupplemented medium and 10 μl of Superfect was added. The mix was incubated 10 minutes, room temperature, 500 μl of supplemented DMEM was added and the mixture was added to the cells. Cells were incubated with the mixture 2.5 hours and then washed and appropriate supplemented medium was added. Cells were left to grow for 24 hours before luciferase assays were performed.

9. Luciferase assays

Luciferase assays were performed in cos1 cells. Two types of reporter plasmids were used. The first contains a glyceraldehyde-3-phosphate dehydrogenase promoter fragment (essentially described in Alexander et al., 1988) upstream of

the *Renilla* Luciferase gene. The second is pGL3-promoter (Promega) that contains a single *Brachyury* binding site (Kispert et al., 1995) together with a basal SV40 promoter upstream of the *Firefly* Luciferase gene. The *Brachyury* palindromic sequence oligo 5'-GGGAATTTCACACCTAGGTGTGAAATTCCC-3' was diluted in water in a concentration of 325 ng/μl, heated to 100° C for 5 minutes and left to cool slowly at room temperature for the formation of dsDNA. A portion of the dsDNA (1.5 μg) was then phosphorylated using T4 polynucleotide kinase treatment (Biolabs) for 30 minutes at 37° C and then the enzyme inactivated at 65° C for 20 minutes. pGL3-promoter plasmid (Promega) was linearised with SmaI and treated with calf intestine alkaline phosphatase (Roche). Linearised plasmid and oligo were ligated and ligation products isolated and sequenced.

Renilla and *Firefly* Luciferase assays were carried out using the appropriate Reporter Assay Systems (Promega) according to the manufacturer's protocol. All combinations were performed in triplicate. Normalisation of the results was carried out using β-Galactosidase Reporter Assay (Promega) according to the manufacturer's protocol. The results were statistically processed using the Excel program.

10. Cloning of retroviral constructs

Cloning of retroviral constructs was carried out as described previously (Logan and Tabin, 1998). All the constructs were cloned in the shuttle vector Slax13 or variations of it (Slax13En for engrailed fusions and Slax13VP16 for fusions with Vp16 activation domain) in restriction sites NcoI and EcoRI. The ORFs or ORFs fused to Engrailed or Vp16 were excised with Cla I and cloned at Cla I site of the retroviral vector RCASBP(A). Putative positive clones were identified by diagnostic digestion with NcoI for the production of unique DNA fragment.

The *Tbx5*$^{\Delta}$ construct contains a.a. 1-274 of the full length chick *Tbx5* clone (accession number AF069396). The *Tbx5*^{en} construct contains a.a.1-274 of the full length *Tbx5* clone fused to a.a. 2-298 of the *Drosophila* engrailed protein (Jaynes and O'Farrell, 1991). The *Tbx5*^{VP16} contains a.a.1-274 of *Tbx5* fused to a duplex of the lambda hinge region and VP16 (Ohashi et al., 1994). Fusion and deletion constructs contain the nuclear localization signal which is sufficient for traslocation of the protein to the nucleus (Collavoli et al., 2003; Zaragoza et al., 2004)

Two full length *Tbx3* viruses were produced; one includes a.a. residues 1-732 and one includes a.a.15-732 of the predicted protein (accession number AF033669). Both forms generated identical results. The first form was produced by inserting a linker into the NcoI site of Slax13. The linker was created by annealing the following oligos: 5'-CATGAATATACCGATGAGAGATCCAGTGAT CCCTGGGACAAG-3' and 5'-CATGCTTGTCCCAGGGATCACTGGATCTCTCA TCGGTATAT T-3'. The *Tbx3*^{EN} contains a.a. 15-289 of Tbx3, which spans the N-terminus and includes the entire DNA-binding T-domain, fused to the engrailed repressor domain (Jaynes and O'Farrell, 1991) while *Tbx3*^{VP16} contains the same Tbx3 a.a. residues fused to two VP16 activation domains (Ohashi et al., 1994). The Gli3ZnF-VP16 construct contains a.a. 471-636 of the human GLI3 (accession number XP_004833) fused to two VP16 activation domains.

11. Retrovirus production and infection

Retrovirus production was carried out using DF1 cells essentially as previously described in Logan and Tabin, 1998. DF1 cells when reached 50-70% confluency were transfected with the appropriate retroviral construct in a 6cm-diameter tissue culture plate (Nunc) using Superfect (Qiagen). The cells were

expanded gradually in a period of two weeks to six 15cm-diameter tissue culture plates. The cells were left to super-confluency and viral supernatants were harvested for three consecutive days. Supernatants were filtered (0.45 μm Nunc filter) and concentrated with ultracentrifugation (swing rotor SW40, 21000 rpm, 4° C). Concentrated virus is then aliquoted and stored at -80° C. The prospective forelimb territories on the right side of the embryo were infected between stages 8-10 with concentrated viral supernatants as previously described (Logan and Tabin, 1998). The left limb served as a contra-lateral control. Each virus produced a limb shift phenotype in approximately 30% of infected embryos. For embryos analyzed before a limb shift phenotype was morphologically obvious batches of infected embryos were analyzed and those with phenotypes scored. For embryos analyzed at later stages, when a shift phenotype was obvious, embryos with a phenotype were selected for further analysis.

12. Whole mount *in situ* hybridisation

Whole mount *in situ* hybridisations were carried out essentially as previously described (Riddle et al., 1993) the only modification being not using glycine after treatment of the samples with proteinase K. All probes have been described previously. *cShh* (Riddle et al., 1993), *mShh* (Echelard et al., 1993), *cMsx* (Ros et al., 1992), *mFgf10* (Bellusci et al., 1997), *mPea3* (Chotteau-Lelievre et al., 2001), *mFgf8* (Crossley and Martin, 1995), *mTbx4* (Bruneau et al., 2001), *mPitx1* (Logan and Tabin, 1999), *cFgf8* (Vogel et al., 1996). *cFgfr1* (Walshe and Mason, 2000), *MyoD, Pax3* (Pourquie et al., 1996), *cHoxb8, cHoxa9, cHoxb9, cHoxc9, cHoxd9, cHoxb4, cHoxc4, cHoxb5, Hoxc5, mHoxc5* (Burke et al., 1995), *cTbx5* (Logan et al., 1998), *cdHand* (Fernadez-Teran et al.,

2000), *cGli3* (Schweizer et al., 2000), *cBmp2* (Schlange et al., 2002) Clones of the chick *Lhx9* and *Tbx15* were isolated from a chick plasmid library (Logan et al., 1998) and their identities were confirmed by sequencing and comparison with published sequences (M. Logan, unpublished).

13. Immunofluorescence assays

To detect cells in mitosis, a rabbit anti-phosphorylated histone H3 primary antibody (Upstate Biotechnology) in 1/1000 dilution and Cy3-conjugated goat anti-rabbit Affipure IgG secondary antibody in 1/250 dilution (Jackson ImmunoResearch) were used following the protocol described previously (Yamada et al., 1993) using 1% BSA, 0.1% Triton in PBS as blocking solution. All washes were performed using PBS. Vectashield mounting medium for fluorescence (Vector) that contains DAPI was then added.

14. Whole mount immunohistochemistry

Whole mount immunohistochemistry was performed essentially as previously described (Kardon G., 1998). Embryos were fixed in 4% paraformaldehyde, 1 hour at 4 °C, washed with PBS and bleached over night 4° C in a solution containing 1 part DMSO, 4 parts methanol and 2.5 parts of hydrogen peroxide. Samples were washed in methanol and were put in a solution that contains 1 part DMSO and 4 parts methanol for further permeabilization. Samples were rehydrated in PBS. Axons were stained using the 3A10 monoclonal antibody to neurofilament-associated antigen diluted 1/100 (Developmental Studies Hybridoma Bank, University of Iowa) followed by an HRP-conjugated goat anti-mouse Affipure IgG secondary antibody in 1/250 dilution (Jackson Immuno-Research). Antibodies were diluted in the following blocking serum: 5% goat

serum (Jackson Immuno-Research), 75% PBS, 20% DMSO. Following extensive washes with PBS (10x 30 min) and DAB staining (Sigma), embryos were fixed in 4% paraformaldehyde, dehydrated in methanol and cleared in a solution of 50% benzyl alcohol, 50% benzyl benzoate (BABB).

15. TUNEL analysis

Apoptotic cell death was assayed with TdT-mediated dUTP nick end labelling (TUNEL). Mouse embryos were fixed overnight in 4% paraformaldehyde and then processed in whole mount using TUNEL reagents (Q-BIOgene) following the manufacturer's protocol with the exception of the following modification: following fixation and washes with PBS, samples were incubated at 65° C in PBT for 30 minutes in order to inhibit endogenous phosphatases. They were then processed for Proteinase K treatment. Chick embryos were fixed overnight in 4% paraformaldehyde, washed in PBT and embedded in OCT (BDH, Merck). Transverse sections (12 μm) were assayed by TUNEL according to the manufacturer's protocol. Sections were fixed in 4% paraformaldehyde, 10 minutes at room temperature then washed with PBS and fixed again with ice cold 1:1 ethanol/acetic acid for 15 minutes at -20° C. Then rehydrated in PBS and equilibriated (equilibriation buffer, Q-biogene) 5 minutes at room temperature. TdT-mediated dUTP nick end labeling reaction was performed at 37° C in a humidified chamber. The reaction was stopped with stop solution (Q-biogene) and three washes, 10 minutes each, with PBS were performed. The samples were then incubated for 45 minutes at room temperature with anti-DIG-Fluorescein antibody followed by five washes, 3 minutes each, at room temperature. Vectashield mounting medium for fluorescence (Vector) that contains DAPI was added.

16. DiI labeling method

DiI crystals (Sigma) were diluted in 100% Ethanol (5 mg/ml). A 10% working solution was prepared in 30% sucrose/PBS solution. Misexpression of retrovirus was performed at stage 8-10 (HH). Approximately 24 hours following retrovirus infection (St. 14) DiI solution was injected into the embryos at several levels in the limb forming region of the LPM and in the adjacent somites, to serve as an axial reference. Equivalent DiI injections were performed in the injected and the contra-lateral, control side of the embryo.

C. RESULTS

CHAPTER ONE

'The role of *Tbx5* in vertebrate limb initiation, outgrowth and patterning'

1. The role of *Tbx5* in vertebrate limb initiation, outgrowth and patterning

To examine the role of *Tbx5* in forelimb development I have undertaken two strategies to disrupt its function in the developing limb bud. I have used a conditional knock-out strategy to delete *Tbx5* function in the developing limbs while leaving the gene intact in other areas of the developing embryo. This approach avoids the complication of phenotypes arising from *Tbx5* loss-of-function in regions of the embryo other than the limb, in particular the heart. The second approach involves using avian retroviruses to misexpress dominant-negative *Tbx5* constructs to interfere with *Tbx5* function in the developing wing bud. As a complementary strategy to misexpression of dominant-negative forms of *Tbx5*, I also misexpressed full length and dominant-active forms of the gene.

1.1 Analysis of *Tbx5* and *Tbx4* expression pattern in the developing chick limbs

The expression pattern of *Tbx4* and *Tbx5* has already been described (Gibson-Brown et al., 1998; Isaac et al., 1998; Logan et al., 1998). However, as a first step towards understanding the function of *Tbx5* I analysed its expression pattern at different stages of chick limb development. I also analysed the expression pattern of *Tbx4. Tbx5* is expressed in the forelimb-forming region prior to overt limb outgrowth but not in the hind forming region (st. 16 HH, Fig.6A). At later stages of development, *Tbx5* is expressed throughout the forelimb mesenchyme but not that of the hindlimb (st.18 HH, Fig.6B). At st.22 HH, the forelimb-restricted expression pattern persists (Fig.6C). *Tbx4* is expressed in the hindlimb-forming region prior to overt limb outgrowth but not in the forelimb region (st.16 HH, Fig.6D). At st.18 HH, *Tbx4* is expressed

throughout the hindlimb mesenchyme but not in the forelimb (Fig.6E). At later stages of development, hindlimb-restricted *Tbx4* expression is retained (Fig.6F).

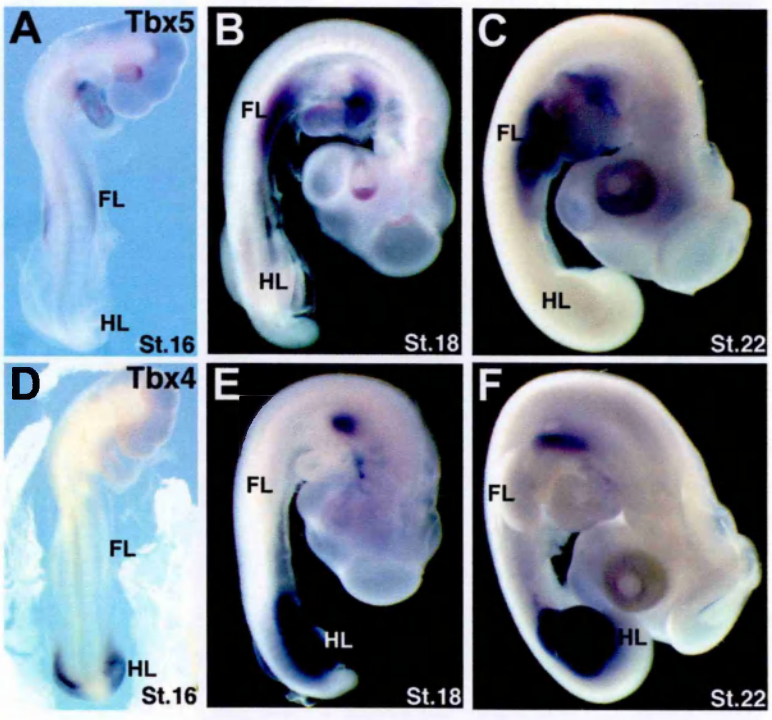

Figure 6. Normal expression patterns of *Tbx4* and *Tbx5* in the chick. **A. .** At St.16 HH, *Tbx5* is expressed in the developing heart and in the LPM of the the presumptive forelimb level. **B.** At St.18 HH *Tbx5* is expressed throughout the forelimb mesenchyme but not in the hindlimb. Expression in the developing heart is also observed. **C.** The forelimb restricted expression persists in later stages of development (St.22 HH). Expression in the heart is still detected.**D.** *Tbx4* is expressed only in the presumptive hindlimb area at st. 16 HH.**E.** By St.18 HH *Tbx4* is expressed throughout the hindlimb mesenchyme and not of the forelimb **F.** The hindlimb restricted expression pattern is observed at later developmental stages (St.22 HH). Abbreviations: FL: forelimb; HL: hindlimb.

1.2 Forelimbs fail to form following deletion of Tbx5 in the cells of the developing forelimb field.

To examine the function of *Tbx5* in forelimb development I genetically inactivated the gene specifically in the limb buds by using mice carrying a *Tbx5* conditional allele, $Tbx5^{lox/lox}$ (Bruneau et al., 2001) (Fig.7C) and a transgene that

expresses the *cre* recombinase enzyme in the limb bud, *Prx1Cre* (Logan et al., 2002) (Fig.7A and 7B). While deletion of *Tbx5* in all cells of the embryo causes embryo lethality by E10 (Bruneau et al., 2001), mice in which *Tbx5* has been deleted specifically in the developing limb die perinatally. The survival of *Tbx5*$^{lox/lox}$;*Prx1Cre* pups throughout the entire gestation period demonstrates that the conditional knock-out approach extends the developmental time window for studying the loss-of function phenotype in the limb.

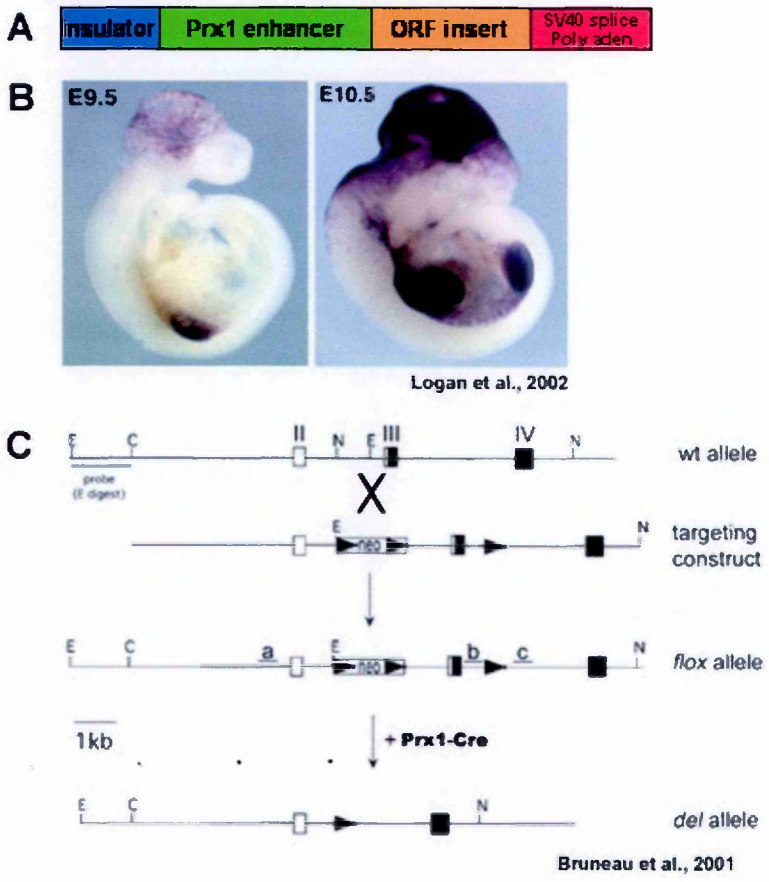

Figure 7. The Cre-deleter line and the conditional allele used for limb-specific inactivation of *Tbx5*. **A.** Schematic showing the transgenic backbone used for the creation of *Prx1-Cre* mice (Logan et al., 2002). A 2.4 Kb fragment of the *Prx1* promoter was cloned upstream of the *Cre* recombinase ORF. An insulator is placed 5' of the promoter fragment and SV40 polyadenylation signal and splice acceptor site is inserted at the 3' end of the transgenic construct. **B.** Cre recombinase activity in *Prx1-Cre* mice, visualized using the Z/AP Cre-reporter mouse. The purple stain indicates where a Cre-catalysed recombination event of the Z/AP reporter transgene leads to expression of alkaline phosphatase. Cre recombinase activity is evident at

E9.5 in the forelimb area. At E10.5 Cre is present In the developing forelimb, hindlimb, interlimb region and craniofacial area. Interestingly, Cre activity is present only in the mesenchyme of the developing forelimb and is excluded from the limb ectoderm and the AER (Logan at al., 2002). **C.** Schematic of the *Tbx5* conditional allele ($Tbx5^{lox/lox}$) indicating the deletion scheme. Exons are shown as boxes while areas that encode the T-domain are solid. Neomycin resistance gene (neo) which is inserted between exon II and exon III and exon III itself are flanked by loxP sites. Following crossing with the Cre-deleter line (*Prx1-Cre*), the neo gene and exon III are deleted.

The forelimbs of newborn (P0) pups are completely absent although the hind limbs are unaffected (Fig.8A). In some examples a small, rudimentary flap of skin is present on one side of the embryo where the forelimb would have formed (Fig.8B). In the majority of cases, however, the skin where the forelimb would normally form is uniform and indistinguishable from the rest of the inter-limb flank. In order to determine that a *Tbx5* deletion event has taken place in the $Tbx5^{lox/lox}$;*Prx1Cre* mice, PCR analysis was used. I was able to identify the presence of the wild-type (wt) and conditional allele (*lox*) in heterozygous $Tbx5^{lox/wt}$ embyos, the conditional allele (*lox*) in the homozygous $Tbx5^{lox/lox}$ embryos and the *lox-out* deleted allele in $Tbx5^{lox/lox}$;*Prx1Cre* limb buds (Fig.8D). All skeletal elements of the forelimb (Fig.8E), including the elements of the pectoral girdle, the clavicle (Fig.8G) and scapula (Fig.8K), are clearly identifiable in control littermates. However, all the elements of the limb proper are absent in $Tbx5^{lox/lox}$;*Prx1Cre* pups at P0 (Fig.8F, 8I, 8M). The skeletal elements of the pectoral girdle, the clavicle (Fig.8I) and the scapula (Fig.8M) do not form. In addition the sternum is completely absent and the rib cage fails to form (Fig.8F, 8I). This may account for the perinatal lethality of the animals because presumably they cannot breathe independently.

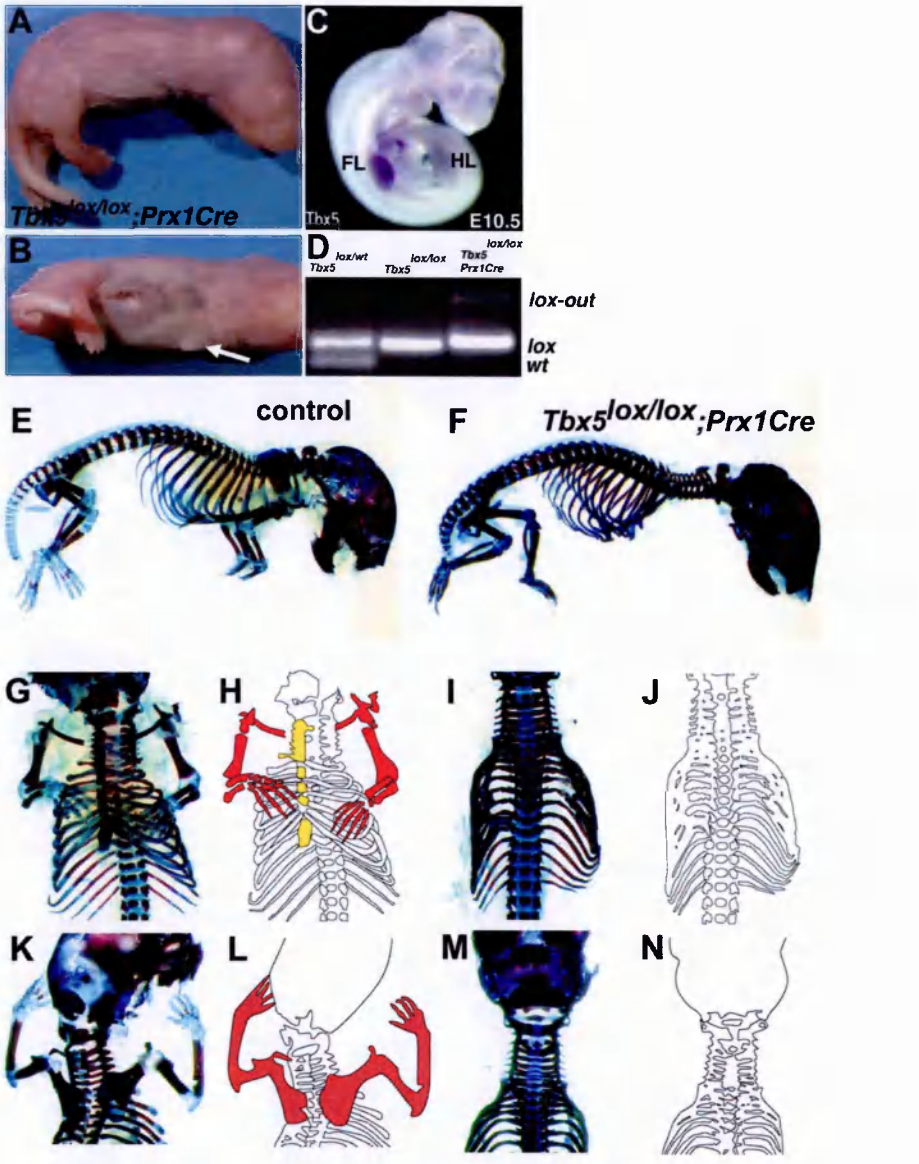

Figure 8. Absence of forelimb skeletal elements in newborn *Tbx5*$^{lox/lox}$;*Prx1Cre* pups. **A.** *Tbx5*$^{lox/lox}$;*Prx1Cre* pup viewed from the side. The forelimb has failed to form although the hindlimb has developed normally. **B.** Ventral view of the embryo shown in **A.** In some occasions a flap of skin (white arrow) is present on one side of the embryo, at the site were the forelimb would normally develop. **C.** Whole mount *in situ* hybridization for *Tbx5*. *Tbx5* expression is detected in the developing forelimb but not the developing hindlimb of an E10.5 mouse embryo. **D.** PCR analysis identifies the presence of the wild-type (wt) and conditional allele (*lox*) in heterozygous *Tbx5*$^{lox/wt}$ embyos, the conditional allele (*lox*) in the homozygous *Tbx5*$^{lox/lox}$ embryos and the *lox-out* deleted allele in *Tbx5*$^{lox/lox}$;*Prx1Cre* limb buds. **E.** Side view of a skeletal preparation of a control littermate. **F.** Side view of a skeletal preparation of a *Tbx5*$^{lox/lox}$;*Prx1Cre* pup showing the absence of forelimb elements. **G.** Ventral view of the skeletal prep of the control in **E**, showing the thoracic region the clavicle and the forelimb skeletal elements. **H.** An

outline diagram of the skeletal preparation shown in **G**. The sternum is highlighted in yellow while the forelimb elements in red. **I.** Ventral view of the skeletal prep shown in **F**. Forelimb skeletal elements are absent. Note that the clavicle and the sternum do not form. **J.** An ouline diagram of the skeleton shown in **I**. **K.** Dorsal view of a skeletal preparation shown in **E** showing the pectoral girdle and forelimb skeletal elements. **L.** An outline diagram of the skeletal preparation shown in **K**. The forelimb skeletal elements are highlighted in red. **M.** Dorsal view of the skeletal preparation showed in **F**. All the elements of the forelimb are absent. The scapula is not present. **N.** An outline diagram of the skeleton shown in **M**. FL:forelimb; HL: hindlimb. Skeletal preps were performed by Malcolm Logan. PCR analysis was performed by Jo Del Buono.

Scanning electron micrographs of control and *Tbx5*$^{lox/lox}$;*Prx1Cre* embryos indicate that the limb defect is manifest by embryonic day 10.5 (E10.5) (Fig 9A, 9B, 9C). In wild-type E10.5 embryos, the limb bud is a prominent outgrowth from the flank of the embryo and the apical ectodermal ridge (AER), the specialised ectodermal structure that runs along the distal extreme of the limb bud, is clearly visible (Fig. 9A, white arrow). In *Tbx5*$^{lox/lox}$;*Prx1Cre* embryos, no limb outgrowth is visible and no morphologically distinguishable AER is present (Fig. 9B, white arrow). In most cases, the region where the forelimb should have formed is indistinguishable from other regions of the embryo flank. In a minority of cases a small tissue mass is present in the forelimb region (Fig. 9C, white arrow). This vestige of the forelimb bud most likely forms in examples where the Cre recombinase has failed to completely remove *Tbx5* function from every cell in the forelimb field. This small mass of tissue may ultimately give rise to the small flap of tissue occasionally observed in *Tbx5*$^{lox/lox}$;*Prx1Cre* P0 pups (Fig. 8B).

1.3 *Tbx5* is required for establishing the signaling centers of the limb bud

While analysis of E10.5 embryos clearly demonstrated a loss of a morphological forelimb in *Tbx5*$^{lox/lox}$;*Prx1Cre* embryos, I was curious to learn if molecular markers of the limb were expressed in the forelimb region. Initiation of the limb bud involves the establishment of key signaling centers within the nascent bud. Classical embryological experiments in the chick have demonstrated the

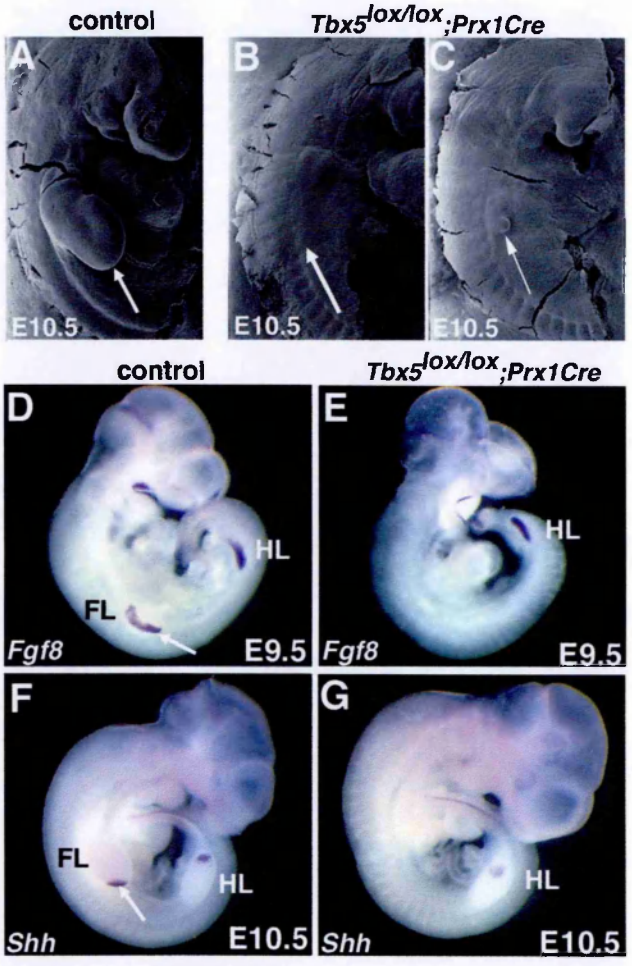

Figure 9. Absence of a forelimb bud in *Tbx5*$^{lox/lox}$;*Prx1Cre* embryos. Scanning electron micrographs of **A.** a control embryo and **B,C.** *Tbx5*$^{lox/lox}$;*Prx1Cre* embryos at E10.5. In **B** no morphological limb bud or AER is present in the forelimb region (arrowed). In **C** a small outgrowth of tissue from the flank is present (arrowed). **D-G.** Expression analysis of limb bud signaling centers markers by whole mount RNA *in situ* hybridisation. **D.** *Fgf8* expression in the AER of the forelimb (arrowed) and hindlimb of a control embryo at E9.5 and **E.** *Fgf8* expression in the hindlimb AER but absence in the forelimb region of a *Tbx5*$^{lox/lox}$;*Prx1Cre* embryo. F) *Shh* expression in the ZPA of the forelimb (arrowed) and hindlimb of a control embryo at E10.5 and

G. *Shh* expression in the hindlimb ZPA but absence in the forelimb region of a *Tbx5*$^{lox/lox}$;*Prx1Cre* embryo. FL: forelimb; HL: hind limb.

requirement of the AER for limb bud outgrowth. Members of the Fibroblast Growth Factor (Fgf) family expressed in the AER have been shown to mediate the effects of this signaling centre (Fallon et al., 1994; Niswander et al., 1993; Sun et al., 2002). At E9.5, *Fgf8* is expressed in the nascent AER in both the forelimb and hindlimb and provides a sensitive molecular marker of this structure (Fig. 9D, white arrow). In the same stage *Tbx5*$^{lox/lox}$;*Prx1Cre* embryo, *Fgf8* expression is not detected in the forelimb region. Expression of *Fgf8* is detected in the AER of the hindlimb bud, consistent with the normal development of the hindlimb in *Tbx5*$^{lox/lox}$;*Prx1Cre* pups (Fig. 9E). *Shh*, expressed by cells of the zone of polarizing activity (ZPA), is essential for normal limb patterning (Echelard et al., 1993; Riddle et al., 1993). At E10.5, *Shh* is expressed in the distal posterior of the limb buds, in the cells of the ZPA (Fig. 9F). However, in *Tbx5*$^{lox/lox}$;*Prx1Cre* embryos, *Shh* is not expressed in the forelimb region although normal expression is detected in the hindlimb (Fig. 9G).

1.4 Hindlimb markers are not expressed in the forelimb region in the absence of *Tbx5*

Previous studies in the chick have suggested that the *Tbx5* and *Tbx4* are important factors implicated in limb-type specification. It has been suggested that *Tbx5* expressed in the prospective forelimb region may repress expression of the closely related gene *Tbx4* which is normally restricted to the hindlimb (Fig.10A) (Takeuchi et al., 1999). I was therefore interested to determine if in the absence of *Tbx5*, hindlimb markers would be ectopically expressed in the

forelimb region. In *Tbx5*$^{lox/lox}$;*Prx1Cre* embryos, *Tbx4* expression is detectable in the hindlimb but is not detected in the forelimb region at E10.5 (Fig.10B, red arrowhead). Similarly, *Pitx1* expression is restricted to the hindlimb in the mouse (Fig.10C). Following deletion of *Tbx5* in the forelimb, *Pitx1* expression remains restricted to the hindlimb and is not expressed in the forelimb region at E10.5 (Fig. 10D, red arrowhead).

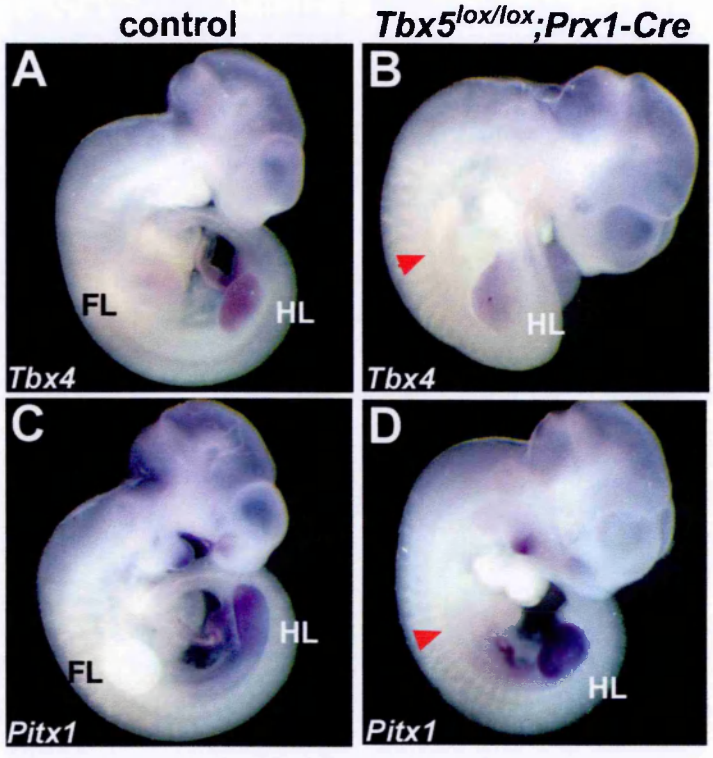

Figure 10. Hindlimb specific markers *Tbx4* and *Pitx1* are not present in the forelimb region following deletion of *Tbx5*. **A.** *Tbx4* expression in the developing hindlimb of a E10.5 control embryo. **B.** *Tbx4* expression in the hindlimb of a E10.5 *Tbx5*$^{lox/lox}$;*Prx1Cre* embryo but absence in the forelimb region (arrowhead). **C.** *Pitx1* expression in a control E10.5 embryo. Expression is detected in the hindlimb and in the LPM at the caudal half part of the interlimb region. **D.** *Pitx1* expression in the hindlimb and LPM of a E10.5 *Tbx5*$^{lox/lox}$;*Prx1Cre* embryo but absence in the forelimb forming region (arrowhead).

These results are in agreement with similar studies in which mice carrying the conditional allele of *Tbx5* (*Tbx5*$^{lox/lox}$) were crossed to *EIIa-Cre* mice so that *Tbx5* function was constitutively deleted in all cells of the developing embryo

(*Tbx5*$^{del/del}$) (Agarwal et al., 2003). Although, the animals do not survive beyond E10 and *Tbx4* and *Pitx1* are present in the hindlimb, no induction of *Tbx4* or *Pitx1* was observed in the presumptive forelimb field of *Tbx5*$^{del/del}$ embryos at E9 or at E9.5. Taken together, this data suggests that *Tbx5* does not normally function to repress the expression of hindlimb markers, *Tbx4* or *Pitx1*, in the forelimb region since in the absence of *Tbx5* the expression patterns of *Tbx4* and *Pitx1* are unaffected.

1.5 *Tbx5* is required for iimb bud outgrowth

My results showed that following deletion of *Tbx5* the absence of any morphological forelimb bud is evident. In addition, molecular markers of two primary signaling centers of the limb bud, *Fgf8* and *Shh* are absent from the forelimb region of *Tbx5*$^{lox/lox}$;*Prx1Cre* embryos. These data indicate a defect at earlier stages of limb development. *Fgf10* is expressed in the lateral plate mesoderm (LPM) of the prospective limb field prior to the expression of *Fgf8* in the prospective AER (Fig.11A, black arrow; 11C, asterisk) (Ohuchi et al., 1997). The functional importance of *Fgf10* in limb formation was demonstrated by the observation that mice carrying a null mutation in *Fgf10* fail to form an AER and P0 pups have severely truncated limbs (Min et al., 1998; Sekine et al., 1999). In the absence of *Tbx5* function, *Fgf10* is not expressed in the prospective forelimb bud mesenchyme by E9.5 (21 somites) (Fig. 11B, arrow and 11D, asterisk). *Pea3* is an *Ets*-related transcription factor that is expressed in the prospective limb mesenchyme (Chotteau-Lelievre et al., 2001) in a similar pattern to *Fgf10* (Fig.11E, black arrow). *Pea3* is thought to directly mediate the nuclear response to Fgf signaling (Raible and Brand, 2001) and it therefore provides a molecular read-out of Fgf signaling. *Pea3* is not expressed in the

forelimb region of *Tbx5*$^{lox/lox}$;*Prx1Cre* embryos by E9.5 (21 somites) (Fig.11F, black arrow) consistent with a failure of *Fgf* signaling in these cells. *Pea3* is also expressed in the intermediate mesoderm lateral and caudal to the forelimb (Fig.11E, red arrow). This expression domain is not affected in *Tbx5*$^{lox/lox}$;*Prx1Cre* embryos (Fig.11F, red arrow) indicating that the effect on *Pea3* is limited to the cells of the prospective forelimb and is not affected at other sites in the developing embryo. *Snail* is a transcriptional repressor that belongs to a superfamily of Zn-finger transcription (Fig.11G, red arrow). Although the expression of *SnR* (*Snail*-related protein, the homologue of *Snail* in the chick) is upregulated rapidly following implantation of beads soaked in Fgfs in the interlimb flank of chick embryos (Isaac et al., 2000), a role for *Snail* in early stages of limb development has not been established. *Snail* is not expressed in the forelimb region of *Tbx5*$^{lox/lox}$;*Prx1Cre* embryos by E9.5 (21 somites) (Fig.11H, red arrow). These results show that in the absence of *Tbx5* early limb mesenchyme markers are absent. Nevertheless, the patterning of the lateral plate mesoderm is intact.

To further examine gene expression in the lateral plate mesoderm in the absence of the forelimb elements, I examined the expression of *Hoxb9* following deletion of *Tbx5. Hoxb9* is expressed in the LPM posterior to the forelimb (Fig.11I, red arrow) and in the posterior and proximal forelimb mesenchyme (Fig.11I, black arrow) (Burke et al., 1995; Cohn et al., 1997). *Hoxb9* is lost from the limb area (Fig.11J). The flap of tissue which is observed in some cases in the site where the forelimb would normally develop does not expressed *Hoxb9* (Fig.11J, black arrow). Nevertheless, expression of *Hoxb9* in the lateral plate mesoderm is intact.

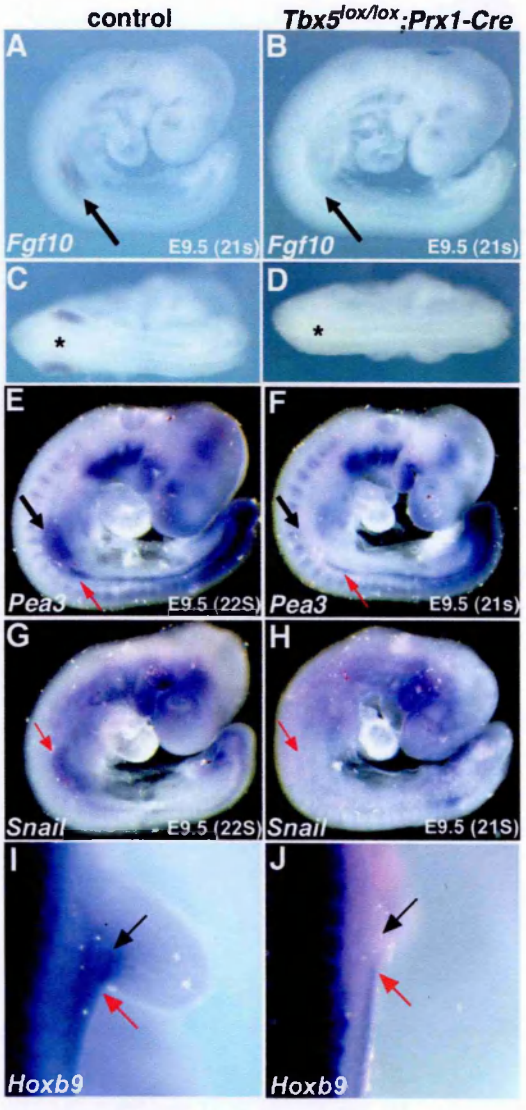

Figure 11. Early markers of the prospective forelimb mesenchyme are absent in *Tbx5*$^{lox/lox}$;*Prx1Cre* embryos. **A.** Expression of *Fgf10* in the forelimb (arrowed) of a control embryo E9.5. **B.** *Fgf10* is not expressed in the forelimb region of a *Tbx5*$^{lox/lox}$;*Prx1Cre* embryo at E9.5. **C.** Dorsal view of the embryo shown in A. *Fgf10* expression in the forelimb buds is indicated by an asterisk. **D.** Dorsal view of the embryo shown in **B**. No *Fgf10* expression is detected in the forelimb-forming region. **E.** Expression of *Pea3* in the forelimb (black arrow) and intermediate mesoderm (red arrow) of a control embryo at E9.5. **F.** *Pea3* is expressed in the intermediate mesoderm (red arrow) but not the forelimb region of *Tbx5*$^{lox/lox}$;*Prx1Cre* embryos at E9.5 (black arrow). **G.** Expression of *Snail* in the forelimb of a control embryo at E9.5 (red arrow). **H.** *Snail* is absent in the forelimb region of *Tbx5*$^{lox/lox}$;*Prx1Cre* embryos at E9.5 (red arrow). **I.** Dorsal view of the forelimb region of a control embryo. *Hoxb9* is expressed in the posterior-proximal forelimb mesenchyme (black arrow) and in the LPM posterior to the forelimb

(red arrow). **J.** Dorsal view of the limb forming region of a *Tbx5*$^{lox/lox}$;*Prx1Cre*. While *Hoxb9* expression is absent in the limb region (black arrow), expression in the LPM is intact.

1.6 Increased programmed cell death following deletion of *Tbx5* and disruption of *Fgf* signaling in the forelimb area

Following deletion of *Tbx5* disruption of *Fgf* signaling is observed. *Fgfs* are important factors for cell survival in the limb mesenchyme. It has been shown that conditional deletion of *Fgf8* and *Fgf4* in the mouse resulted in increased programmed cell death (PCD) in the limb mesenchyme (Sun et al., 2002). I therefore examined cell death in forelimb area of control and *Tbx5*$^{lox/lox}$;*Prx1Cre* embryos. TdT-mediated dUTP nick end labeling (TUNEL) analysis demonstrated that by E9.5 (24 somites) cells in the prospective forelimb region of *Tbx5*$^{lox/lox}$;*Prx1Cre* embryos were first detected to be undergoing an increase in PCD (Fig.12B, arrow) when compared with control embryos at a similar stage (Fig.12A). By E10.5 the domain of cell death in *Tbx5*$^{lox/lox}$;*Prx1Cre* embryos was extensive throughout the forelimb forming region (Fig. 12D, bracket) compared to control embryos (Fig. 12C). These results demonstrate that as a result of *Tbx5* inactivation expression of *Fgf10* is rapidly downregulated and subsequently cells of the prospective forelimb undergo extensive PCD.

1.7 *Tbx5* is required at later stages of limb development

My experiments in the mouse demonstrated an important role for *Tbx5* in limb initiation. During normal development, *Tbx5* is expressed throughout the limb mesenchyme from the earliest stages of forelimb development (Gibson-Brown et al., 1998; Logan et al., 1998). However, this limb-type restricted expression pattern is also maintained during later limb bud development stages, suggesting

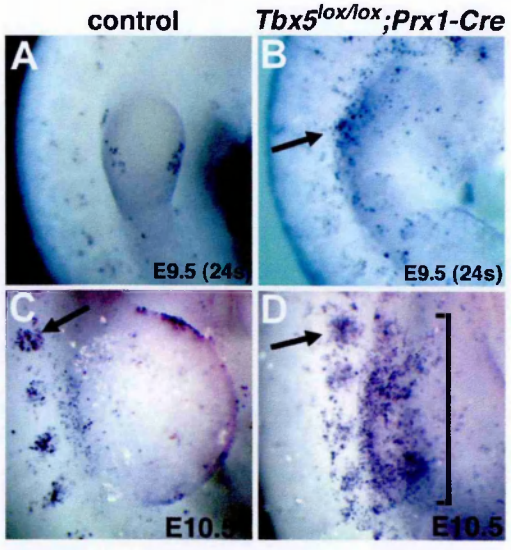

Figure 12. Analysis of programmed cell death (PCD) in the limb by whole mount TUNEL staining. **A.** PCD in the forelimb region of a control embryo at E9.5. **B.** Forelimb region of a *Tbx5*$^{lox/lox}$;*Prx1Cre* embryo at E9.5. A zone of increased PCD is present at the site where the forelimb would normally form (arrowed). **C.** The forelimb region of a control embryo at E10.5. Some PCD is observed in the limb, especially in the AER, and foci of apoptotic cells are observed in the somites (arrowed). **D.** Forelimb region of a *Tbx5*$^{lox/lox}$;*Prx1Cre* embryo at E10.5. A region of increased PCD is present in the forelimb-forming region (bracketed). Foci of apoptotic cells are also observed in the somites in a similar pattern to the control embryo (arrowed). TUNEL staining on E10.5 embryos was performed by Malcolm Logan.

Tbx5 may have additional roles during subsequent stages of limb outgrowth and patterning. To examine these possible later roles of *Tbx5*, I injected avian retroviruses into chick embryos to misexpress dominant-negative and dominant-active forms of *Tbx5* in the developing forelimb, or wing bud. Misexpression of dominant-negative *Tbx5* using this method will cause disruption of *Tbx5* function at later limb bud stages and have a less penetrant down-regulation of *Tbx5* function than the genetic deletion approach I used in the mouse. *Tbx5* is a transcription factor that, by analogy to other members of the *Tbx* family, is thought to mediate its effects by binding to target sites on DNA via the conserved N-terminal, T-domain. The transcriptional effector domain resides in

the C-terminus of the protein (Zaragoza et al., 2004) (Fig.13A). I have generated two putative dominant-negative constructs of *Tbx5*; a truncated construct that contains residues encompassing the N-terminus and T-domain only ($Tbx5^{\Delta}$) and a construct that contains the N-terminus and T-domain fused directly to the transcriptional repressor domain of the *Drosophila* engrailed protein (Jaynes and O'Farrell, 1991), ($Tbx5^{En}$) (Fig.13A). The *engrailed* 'active' repressor domain has been shown to be groucho-dependent (Jimenez et al., 1997) and such fusion proteins have been demonstrated to function as dominant-negative constructs in a range of tissues and organisms (Markel et al., 2002; Yu et al., 2001). In addition, Groucho homologues are present in the limb mesenchyme (Rallis et al., 2003). Both dominant-negative constructs would be expected to compete with endogenous Tbx5 protein for DNA-binding sites upstream of *Tbx5* target genes. The truncated construct would fail to activate expression of target genes, while the engrailed-fusion protein would repress gene expression. As a complementary approach to generating dominant-negative constructs, I also used full-length Tbx5 and generated a dominant-active construct of Tbx5 by fusing the N-terminal portion of the molecule including the DNA-binding T-domain to the VP16 transcriptional activation domain (Fig.13A), (Ohashi et al., 1994). Both full-length and VP16 fusion constructs would be expected to bind to the endogenous DNA binding sites upstream of *Tbx5* target genes and to activate their expression.

To test the activity of my constructs I performed *in vitro* luciferace assays. The reporter plasmid I used contains a glyceraldehyde-3-phosphate dehydrogenase promoter fragment that contains T-box binding sites upstream of the *Renilla* luciferase gene (Alexander et al., 1988). The promoter fragment has been used in other studies and is also responsive to other T-box genes (Carreira et al.,

1998). In these assays, $Tbx5^{FL}$ generates luciferase activity levels 6.5-fold higher than the basal transcription levels. Therefore, in this context Tbx5 is an activator. $Tbx5^{\Delta}$ is transcriptionally inactive presumably due to the absence of the C-terminal region that contains the transactivation domain

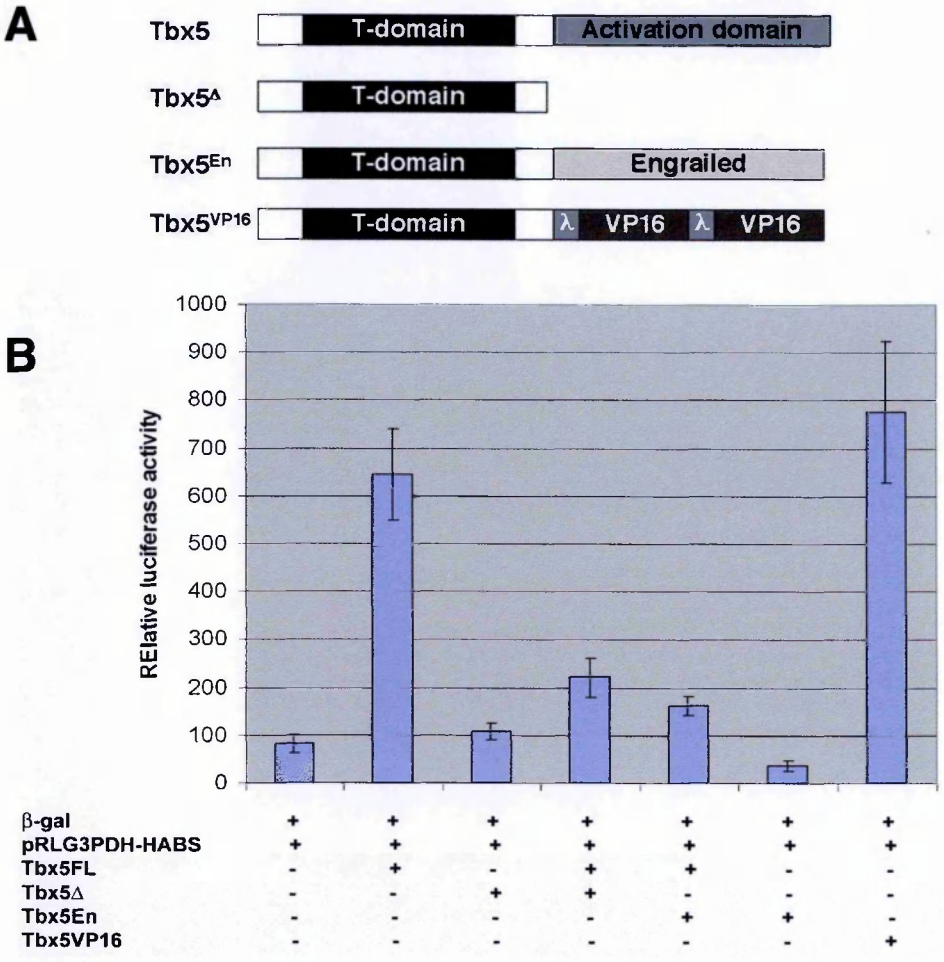

Figure 13. Tbx5 constructs used for the production of replication competent retroviruses and *in vitro* luciferase assays. **A.** Schematic representation of the *Tbx5* full length, truncated and En/VP16-fusion retroviral constructs (see Materials and Methods for details). **B.** Luciferase assays for *Tbx5* constructs performed using cos1 cells. β-gal was used for normalization. Tbx5 activates about 6.5-fold the G3PDH-HABS (High Affinity Binding Sites) promoter. In the absence of the C-terminus domain the Luciferase activity is comparable with the activity seen with the basal transcriptional levels. $Tbx5^{EN}$ construct can repress the basal transcriptional levels about 2.5-fold. Both $Tbx5^{\Delta}$ and $Tbx5^{EN}$ have the ability to compete with the activity of the full length molecule and lower the promoter activity when cotransfected $Tbx5^{FL}$ in equamolar

amounts. Therefore, *in vitro,* the two constructs are expected to act as dominant-negative forms of Tbx5. $Tbx5^{VP16}$ can activate the G3PDH promoter about 8-fold.

(Fig13B). $Tbx5^{EN}$ represses the basal transcription levels (2.5-fold) and $Tbx5^{VP16}$ activates (8-fold) as expected. Significantly, equamolar amounts of $Tbx5^{FL}$ and $Tbx5^{\Delta}$ or $Tbx5^{FL}$ together with $Tbx5^{EN}$ generate intermediate levels of luciferase activity than the Tbx5 construct alone. This shows that $Tbx5^{\Delta}$ and $Tbx5^{EN}$ are able, at least *in vitro*, to interfere with the normal function of Tbx5 (Fig.13B).

In my experiments, misexpression of both dominant-negative constructs produced indistinguishable results ($Tbx5^{\Delta}$: n=87; $Tbx5^{EN}$: n=57) suggesting that both forms had similar effects of blocking endogenous *Tbx5* gene function. Scanning electron micrographs of wing buds injected with dominant-negative forms of *Tbx5* indicate that the injected limb is severely truncated when compared to an uninjected control wing bud (Fig.14A, 14B; n=2/2, 100%). In contrast to the phenotype observed following deletion of *Tbx5* in the mouse, a limb bud does form in the chick following misexpression of dominant-negative forms of *Tbx5.* Presumably this difference is due to incomplete disruption of gene function using this retroviral misexpression technique.

The truncated limbs observed could be generated due to changes in cell proliferation rates and/or apoptosis. I examined the relative rates of cell proliferation in control and dominant-negative *Tbx5* injected limb buds by assaying for phophorylated histone H3 (pH3) a marker of mitotic cells. No differences were found in the frequency of mitotic cells of injected limb buds (Fig.14D; n=3/4, 75%) compared with the contra-lateral uninjected control limb bud (Fig.14C) when regions containing comparable total cell numbers were compared (C'). In contrast, TUNEL staining showed that the frequency of programmed cell death (PCD) is increased in injected limb buds (Fig.14F and

14F' ; n=3/4, 75%) compared with the contra-lateral uninjected control limb bud (Fig. 14E). Taken together these results indicate that the injected limb buds are smaller as a consequence of increased cell death and are not due to a decrease in rates of cell proliferation in the developing forelimb bud. These results are consistent with my observations in *Tbx5*$^{lox/lox}$;*Prx1Cre* mouse embryos and *Fgf4/Fgf8* double knockout embryos that have smaller limbs as a consequence of increased cell death rather than a reduction in cell proliferation (Sun et al., 2002). A common feature in the generation of these similar phenotypes may be the disruption of *Fgf* signaling.

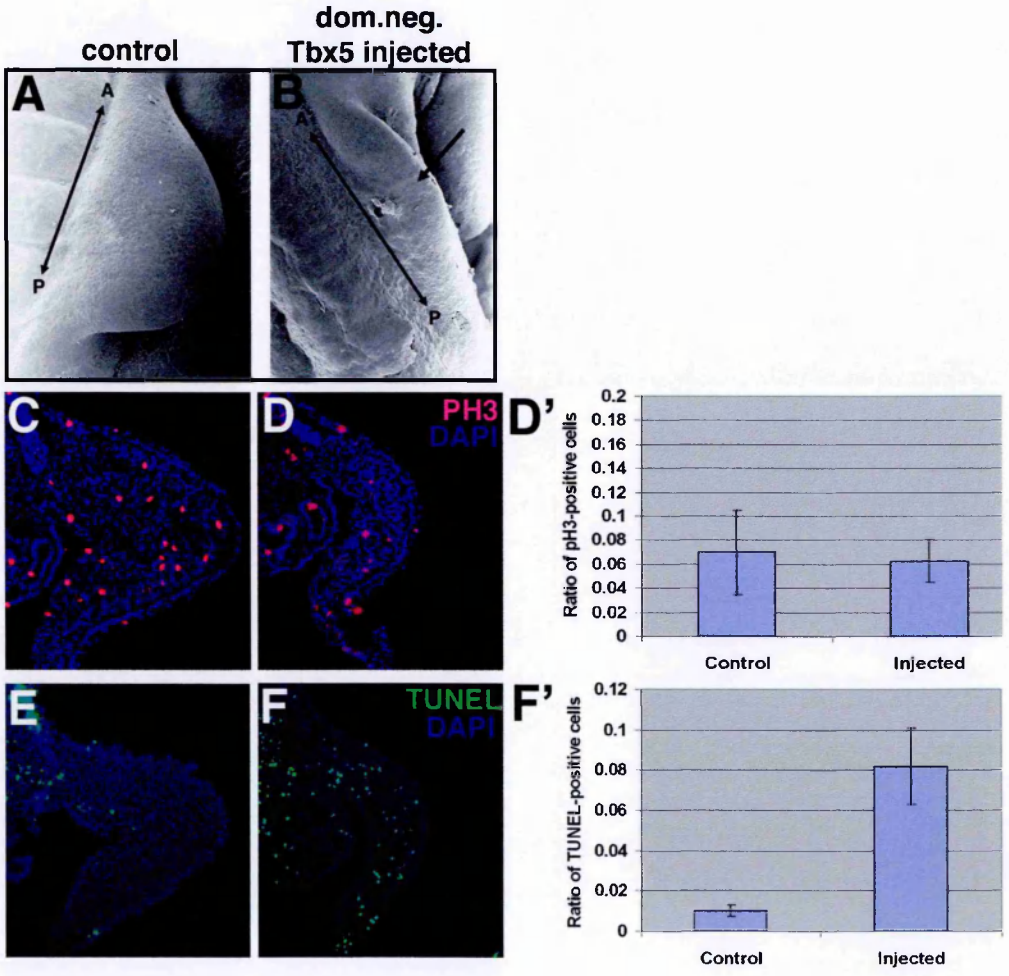

Figure 14. Limb outgrowth is disrupted following misexpression of dominant-negative forms of *Tbx5* in the chick wing bud. Scanning electron micrographs of **A.** control and **B.** dominant-negative *Tbx5* (Tbx5$^{\Delta}$) injected limb buds at st.20 HH shows a dramatic reduction in limb size following Tbx5$^{\Delta}$ misexpression. A:anterior; P:posterior. Transverse sections through **C.** contra-

lateral control and **D.** dominant-negative *Tbx5* (Tbx5$^{\Delta}$) injected limb buds at st.20 HH stained with an antibody against phosphohistone H3 to identify cells undergoing mitosis (pink). **D'.** Statistical analysis of pH3-positive cells in control and injected limbs. No significant difference was observed. Transverse sections through **E.** contra-lateral control and **F.** dominant-negative *Tbx5* (Tbx5$^{\Delta}$) injected limb buds at st.20 stained with TUNEL reagents to identify cells undergoing apoptotic cell death (green). **F'.** Statistical analysis of TUNEL-positive cells in control and injected limb buds. There is a significant increase in cell death (6-fold) following misexpression of dominant-negative *Tbx5*. Sections shown in **C-F** are at 20X magnification.

My experiments in the mouse demonstrated that *Tbx5* is required for the establishment of the AER and the ZPA, signaling centers important in limb outgrowth and patterning of the limb bud. To understand how normal patterning is affected in the truncated forelimbs following dominant-negative *Tbx5* misexpression, I analysed the expression patterns of two markers of the signaling centers of the limb. I observe that *Fgf8* expression is down-regulated in the anterior AER and *Shh* is absent in the injected wing buds (Fig.15B; n=4/12, 33%) compared to control embryos (Fig.15A). If injection of the retrovirus is performed at later stages, lower-level infection of the wing bud results (Logan and Tabin, 1998) and I observe more subtle effects on *Fgf8* and *Shh* expression. In these examples, *Fgf8* expressing cells are still present in the distal, anterior of the limb but in a broader, flattened domain of the ectoderm that has not formed a morphological ridge (Fig.15D, F; n=4/18, 22%) compared with the control wing (Fig.15C, 15E). This broad pattern of *Fgf*8 expression is reminiscent of cells of the immature, nascent AER present in earlier stage limb buds suggesting a delay of AER formation or a failure to maintain the AER. Strikingly, the effect on *Fgf8* expression in the AER was observed predominantly in the anterior of the limb bud (Fig.15B, 15D). In addition, the effect on *Fgf8* expression in the ectoderm must be occurring as a secondary

effect to the knock-down of *Tbx5* function in the limb mesenchyme since Tbx5 is expressed in the forelimb mesenchyme but not the ectoderm. Furthermore, the injection protocol used leads to targeted misexpression in the limb mesenchyme that does not spread to the overlying ectoderm (Logan and Tabin, 1998). In addition the mesenchyme-expressed *Fgf10* is affected following knock-down of Tbx5 function. *Fgf10* is normally expressed in the limb mesenchyme with a pronounced distribution in the distal part presumably as a result of the positive

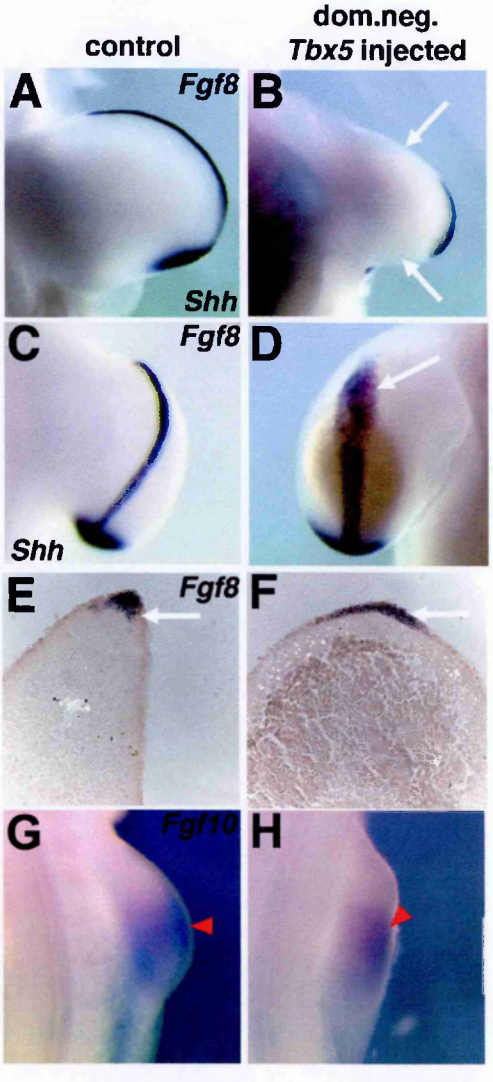

Figure 15. RNA whole mount *in situ* hybridisation analysis of limb buds injected with dominant-negative forms of *Tbx5*. **A.** Dorsal view of the control, uninjected limb bud showing *Fgf8*, expressed in the AER, and *Shh*, expressed in the ZPA at st.23 and **B.** Dorsal view of $Tbx5^{\Delta}$-injected limb. *Fgf8* is not expressed in the anterior of the injected limb and *Shh* expression is not detected in the ZPA. In this example, the injection was done at stage 8 to achieve high-level

infection. In panel A the image of the contra-lateral uninjected control limb has been reversed to provide a clearer comparison with the respective experimental, injected limb in panel **B. C.** Distal view of an uninjected control limb showing *Fgf8* expression in the AER and *Shh* expression in the ZPA and **D.** distal view of the limb injected with $Tbx5^{\Delta}$ virus at st.10 and harvested at st.23. Injection at the later stage produces lower-level infection and a weaker phenotype. Cells expressing *Fgf8* are present in the anterior of the limb in a broader region of flattened ectoderm and have not formed a ridge of cells (arrow). **E.** A transverse section through the anterior of the limb shown in **C.** The *Fgf8*-expressing cells (arrow) form a ridge of cells at the distal tip of the limb. F) Transverse section through the anterior of the limb shown in **D.** The *Fgf8*-expressing cells (arrow) are present in the flattened ectoderm and do not form a ridge. The effect of *Tbx5* misexpression is observed primarily in the anterior mesenchyme. **G.** Dorsal view of the control, uninjected limb bud showing *Fgf10*, expressed in the limb mesenchyme with a zone of higher expression in the distal part under the AER (arrowhead). **H.** Dorsal view of *Tbx5*Δ-injected limb. *Fgf10* is still present in the limb mesenchyme but the proximal-distal distribution of the transcripts is altered.

feedback loop operating between *Fgf10* and *Fgf8* (Fig.15G). Following misexpression of dominant-negative forms of Tbx5 this distribution is altered. *Fgf10* is observed at lower levels in the limb mesenchyme (Fig.15H; n=6/9, 67%). This result suggests a perturbation of the Fgf positive feedback loop that operates between the limb mesenchyme and AER.

Msx1 is a homeobox gene expressed in the AER and in the distal-most mesenchyme cells that lie just under the AER at early limb bud stages (Fig.16A) and (Ros et al., 1992). *Msx1* is a sensitive marker for the influence of the AER on the distal mesenchyme cells since *Msx* expression is rapidly down-regulated upon removal of the AER (Ros et al., 1992). In the dominant-negative *Tbx5* injected wing bud, *Msx1* expression is down-regulated in the anterior while the expression pattern was not significantly affected in the posterior of the limb

(Fig.16B; n=2/5, 40%). To investigate the apparent anterior-bias of the limb truncations produced by the dominant negative *Tbx5* constructs I analysed the effect of expression of markers of the anterior limb mesenchyme. *Lhx9*, a homeodomain transcription factor, is normally expressed in the anterior of the limb bud (Fig.16C) (Retaux et al., 1999). A functional role of *Lhx9* in limb development has not been established (Birk et al., 2000). For my purposes it serves as a marker of anterior limb mesenchyme. Following misexpression of dominant-negative *Tbx5*, *Lhx9* is down-regulated in the anterior mesenchyme (Fig.16D; n=5/9. 56%). The homeobox gene *Hoxc4* is also expressed in the anterior of the forelimb bud (Fig.16E) (Nelson et al., 1996) and is down-regulated significantly in dominant-negative *Tbx5* injected wing buds (Fig.16F; n=4/6, 67%). These results confirm my earlier observations that disruption of *Tbx5* function following misexpression of *Tbx5* dominant-negative forms predominantly affected the anterior mesenchyme of the limb.

Not all markers are downregulated following misexpression of dominant-negative forms of Tbx5. *Fgfr1* (Fgf-receptor 1) is the main receptor for the AER-derived Fgfs expressed by cells in the limb mesoderm (Fig.16G). In addition, previous work has been shown that *Fgfr1* mediates the effects of *Fgf8* in the midbrain-hindbrain boundary (Scholpp et al., 2004). Following misexpression of $Tbx5^{\Delta}$ or $Tbx5^{EN}$, *Fgfr1* is upregulated especially in the anterior mesenchyme (Fig.16H; n=5/8, 63%). Finally, *Snail* which is normally expressed throught limb mesenchyme (Fig.16I) appears unaffected following the knock-down of Tbx5 function (Fig.16J; n=7/7, 100%).

1.8 Tbx5 acts as a transcriptional activator in the limb mesenchyme

As a complementary strategy to misexpressing dominant-negative forms of *Tbx5* to disrupt the gene's function in the limb, I misexpressed dominant-active constructs in the developing chick wing. These constructs are the full-length Tbx5 ($Tbx5^{FL}$) and a Tbx5-VP16 fusion construct ($Tbx5^{VP16}$). As mentioned previously, both full-length and VP16 fusion constructs are able to bind to T-box binding sites and activate the transcription of the luciferase gene *in vitro*.

Following misexpression of dominant-active *Tbx5*, the wing bud is enlarged and expanded anteriorly (Fig.16L,16N,16P,16R,16T). Analysis of *Fgf*8 expression indicates that the domain of Fgf8-expressing cells in the AER extends more anteriorly than in the uninfected wing bud but is not expanded in the posterior of the bud (Fig. 16K, 16L; n=5/7, 71%). In addition, double *in situ* for *Fgf8* and *Shh* (Fig.16M, 16N) indicates that while *Fgf8* expression domain is anteriorly expanded (n=7/10, 70%), *Shh* is normally expressed in the posterior limb mesenchyme and there is no ectopic *Shh* expression in the anterior of the limb bud (Fig.16M, 16N; n=10/10, 70%). I also observe that the domain of *Lhx9* expression is expanded anteriorly but not posteriorly in the wing bud following misexpression of dominant-active *Tbx5* (Fig.16O, 16P; n=4/5, 80%). These results show that following misexpression of dominant-active forms of *Tbx5* both the limb ectoderm and mesoderm are expanded anteriorly. I was curious to examine the expression of the endogenous *Tbx5* transcripts following misexpression of $Tbx5^{VP16}$. I used an *in situ* probe that spans the 3' part of *Tbx5* cDNA that is not included in the retroviral construct. Following misexpression of $Tbx5^{VP16}$ and expansion of the limb mesenchyme, endogenous *Tbx5* is expressed in the anteriorly expanded limb region in addition to the rest of the limb mesoderm (Fig.16Q, 16R; n=5/10, 50%). My experiments in the mouse

showed that *Tbx5* is required for the induction of *Fgf10* in the LPM during limb initiation. Furthermore, disruption of *Tbx5* function in the chick wing following misexpression of dominant-negative forms of *Tbx5* results in downregulation of *Fgf10* expression. *Fgf10* which is normally expressed in the limb mesenchyme (Fig.16S), is upregulated and expressed in the expanded limb region following misexpression of $Tbx5^{VP16}$ (Fig.17T; n=4/10, 40%).

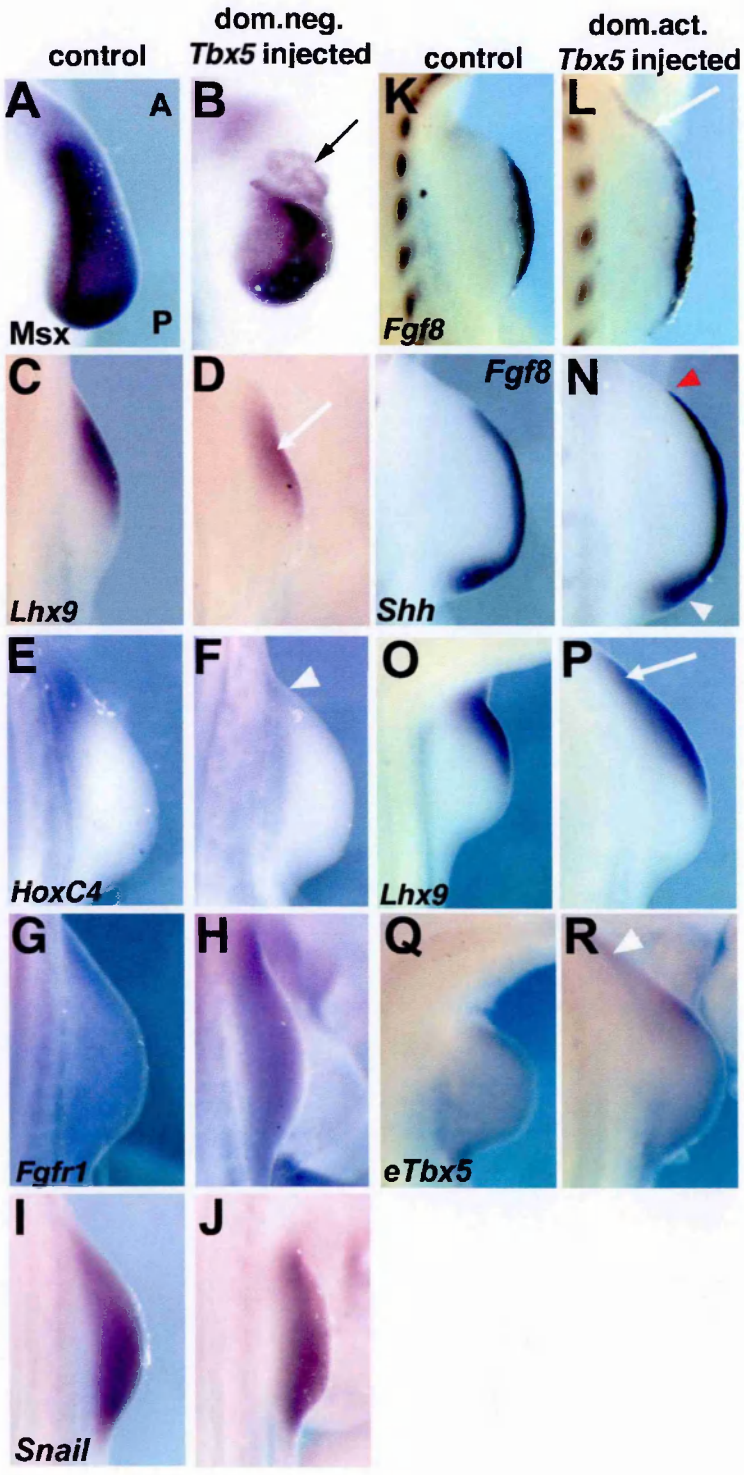

Figure 16. A-F. Misexpression of dominant-negative *Tbx5* leads to down-regulation of anterior mesenchymal markers. **A.** In the contra-lateral control, uninjected limb *Msx* is expressed in the distal mesenchyme of the limb just under the AER at st. 21. **B.** In the dominant-negative *Tbx5*-(Tbx5^{EN}) injected limb, *Msx* is down-regulated in the distal mesenchyme most obviously in the anterior of the limb. **C.** *Lhx9* is expressed in the anterior limb mesenchyme in the control limb at st. 19 and **D.** in the dominant-negative *Tbx5* (Tbx5^{EN}) injected limb expression is down-regulated (arrowed). **E.** *Hoxc4* is expressed in the anterior limb mesenchyme of a control limb (st. 20) and **F.** is down-regulated in the dominant-negative *Tbx5* (Tbx5^{EN}) injected limb. **G.** *Fgfr1* is expressed in throughout the limb mesenchyme of a control limb (st.20) and **H.** is upregulated in the dominant-negative (Tbx5^{EN}) injected wing especially in the anterior. **I.** *Snail* is expressed throughout the limb mesenchyme (st.20) and **J.** is unaffected in the dominant-negative (Tbx5^{EN}) injected wing. **K-R.** Misexpression of dominant-active forms of *Tbx5* (Tbx5^{VP16}) leads to an anterior expansion of the limb. **K.** *Fgf8* expression in the uninjected control limb (st.20). **L.** Following misexpression of a dominant-active *Tbx5* (Tbx5^{VP16}), the domain of cells expressing *Fgf8* in the AER is expanded anteriorly. **M.** *Fgf8* and *Shh* expression in the contra-lateral uninjected wing (st.20). **N.** Following misexpression of dominant-active *Tbx5* (Tbx5^{VP16}) while *Fgf8* expression domain is expanded anteriorly (arrowhead), *Shh* is normally expressed in the posterior limb mesenchyme. **O.** Expression of *Lhx9* in the anterior of the control limb at st.20. L) Following misexpression of dominant-active *Tbx5* (Tbx5^{VP16}), *Lhx9* expression is expanded anteriorly (arrow). **Q.** Endogenous expression of *Tbx5* in the contra-lateral uninjected wing (st.21). **R.** Following misexpression of Tbx5^{VP16} endogenous expression of *Tbx5* is detected throughout the limb mesenchyme including the expanded region. **S.** Normal expression of *Fgf10* in the contra-lateral uninjected wing (st. 19). **T.** Following misexpression of Tbx5^{VP16} *Fgf10* transcripts are present throughout the limb mesenchyme including the anteriorly expanded region. *Fgf10* levels are higher. In panels A and B distal view of the limbs is presented. In the rest of the panels dorsal view is presented. In panels A, C, E, G, I, K, M, O, Q and S the image of the contra-lateral uninjected control limb has been reversed to provide a clearer comparison with the respective experimental, injected limbs in panels B, D, F, H, J, L, N, P, R and T. A:anterior; P:posterior.

Taken together, these results and my loss-of-function data from the mouse, show that *Tbx5* is required for normal *Fgf10* expression during limb initiation and at later stages during limb outgrowth and patterning events. Similar expansion of anterior limb mesenchyme was also obtained following misexpression of the full-length *Tbx5* construct. These findings, in agreement with my *in vitro* luciferase assays and the phenotypes observed with dominant-negative forms of *Tbx5* indicate that *Tbx5* normally functions as a transcriptional activator in the limb.

1.9 Hindlimb-restricted *Tbx4* has similar roles with *Tbx5* in the wing

Tbx5 and *Tbx4* have been implicated in limb-type specification (Gibson-Brown et al., 1998; Isaac et al., 1998; Logan et al., 1998; Takeuchi et al., 1999). My analysis in mouse and chick showed that *Tbx5* has important roles during limb initiation and at later limb outgrowth and patterning events. In addition, *Tbx4* knock-out mice do not survive beyond E10.5 due to failure of chorioallantoic fusion. Induction of the hindlimb seems to occur normally but subsequent development of the hindlimb fails and *Fgf10* expression is not maintained in the hindlimb mesenchyme (Naiche and Papaioannou, 2003).

To investigate a potential similar role for *Tbx4* during limb outgrowth I misexpressed a putative dominant-negative form of *Tbx4* in which the C-terminus of the protein has been replaced by the transcriptional repressor domain of the *Drosophila* engrailed gene, in the chick leg (Fig.17A) (Jaynes and O'Farrell, 1991). Similarly to $Tbx5^{EN}$ I expect this form of Tbx4 to compete with the endogenous Tbx4 protein for downstream targets and repress them instead of them being activated.

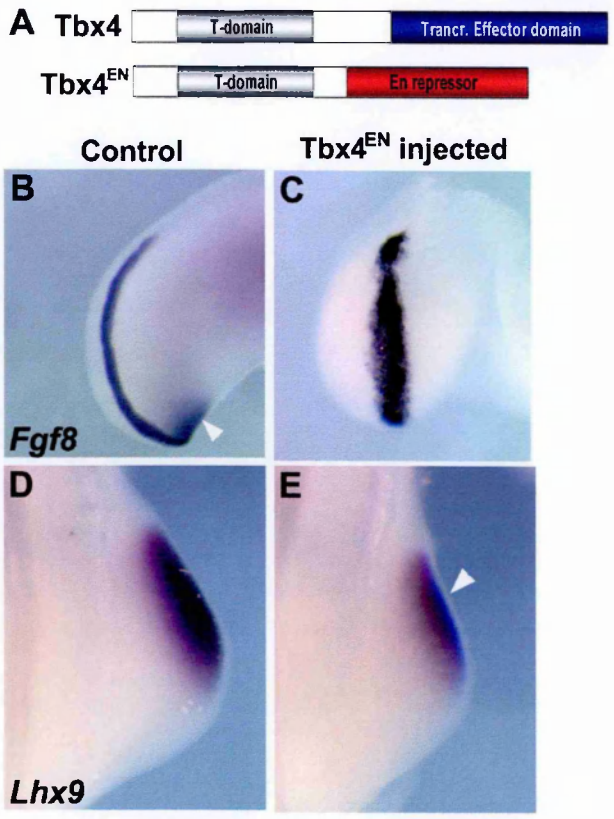

Figure 17. Knock-down of Tbx4 function in the chick leg has similar results as the knock-down of Tbx5 in the wing. **A.** Schematic of the full-length Tbx4 and the Engrailed fusion used for misexpression experiments. Tbx4 shares all the characteristic features of the T-box gene family, namely the T-domain and a putative transcriptional effector domain in the C-terminus of the molecule. In the putative dominant-negative form of Tbx4, the transcriptional effector domain has been replaced by the repressor domain of the *Drosophila* Engrailed protein. **B.** *Fgf8* in the contra-lateral uninjected legs is expressed in the AER. White arrowhead points to the *Shh* expression domain. **C.** Following misexpression of Tbx4^{EN} *Fgf8* expression domain is present in a broader flattened area. **D.** *Lhx9* expression in the anterior mesenchyme of a contra-lateral control leg. **E.** Following misexpression of Tbx4^{EN} *Lhx9* expression is downregulated.

Misexpression of Tbx4^{EN} leads to truncated limbs. While in contra-lateral control limbs *Fgf8* is normally expressed (Fig.17B), in Tbx4^{EN} injected legs, *Fgf8* positive cells are still present but in a broader, flattened area (Fig.18C; n=6/10, 60%) that may represent a failure or delay of the cells to form a ridge. Following misexpression of dominant-negative *Tbx5* forms in the developing forelimb an

anterior limb regions are predominantly affected. I was then curious to learn if anterior markers are affected following misexpression of $Tbx4^{EN}$. *Lhx9*, normally expressed in the anterior hindlimb mesoderm (Fig.17D) is downregulated following $Tbx4^{EN}$ misexpression (Fig.17E; n=6/9, 67%). These data suggest that *Tbx5* and *Tbx4* may have similar roles during wing and leg outgrowth and patterning events respectively.

CHAPTER TWO

'The role of *Tbx3* in positioning the limb along the rostro-caudal axis of the developing vertebrate embryo'

CHAPTER TWO

"The role of Tbx3 in specifying the limb along the antero-

posterior axis of the developing vertebrate embryo"

2. The role of *Tbx3* in positioning the limb along the rostro-caudal axis of the developing vertebrate embryo

Misexpression and gene deletion studies have suggested roles for *Tbx3* during limb bud stages. However, *Tbx3* is expressed in the limb forming region prior to overt limb bud outgrowth. To examine the early role of *Tbx3* in normal limb development I misexpressed full length and dominant-negative constructs of *Tbx3* in the developing forelimb using the avian retroviral system. Here, I provide evidence for a new role for *Tbx3* in participating in the genetic network that positions the limb along the rostro-caudal axis of the vertebrate embryo.

2.1 Analysis of *Tbx3* expression in the developing chick embryo

The expression pattern of chick *Tbx3* has already been described (Gibson-Brown et al., 1998; Logan et al., 1998; Tumpel et al., 2002). However as a first step towards understanding the function of *Tbx3* I analysed its expression pattern at different stages of limb development. Whole mount *in situ* hybridizations were performed between stages 12-25 HH (Fig.18). *Tbx3* shows a dynamic expression pattern as development proceeds. *Tbx3* expression is observed in the future forelimb and hindlimb domains at stages 12-13 HH (Fig. 18A, arrowheads), earlier than previously reported (Tumpel et al., 2002). Just prior to overt limb outgrowth (St.16 HH), *Tbx3* is expressed in the presumptive forelimb and hindlimb areas and expression appears to be more robust in the posterior region (Fig.18B, arrowheads). To analyse *Tbx3* expression in more detail, I performed *in situ* hybridization on sections. *Tbx3* is expressed in the mesoderm and not the ectoderm of the forelimb forming region. In addition expression is observed, in the ventro-lateral lip of dermomyotomal compartment of the somites (Fig.18C, 18E). At the hindlimb level, *Tbx3* is present in the

mesoderm and ectoderm (Fi.18D, 18F). At this stage and at this axial level, expression is not detected in the somites, as was observed in the whole mount

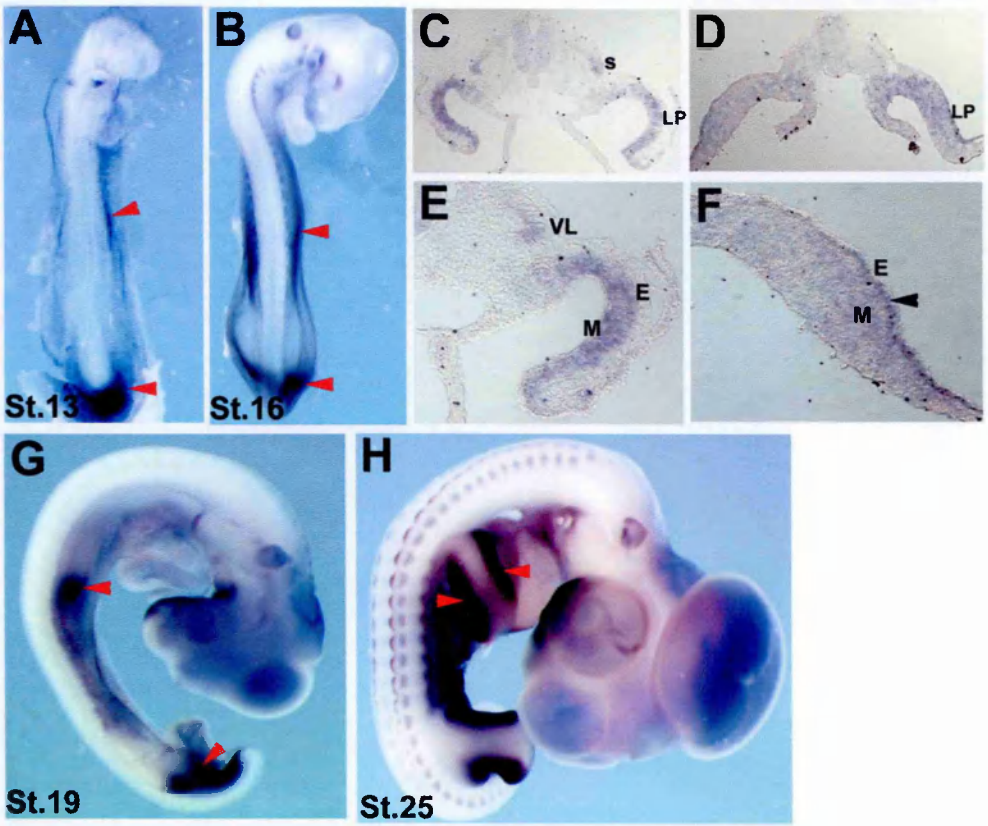

Figure 18. Normal expression of *Tbx3* at different stages of chick development. **A**. At stage 12-13, *Tbx3* is expressed in the presumptive forelimb (FL) and hindlimb (HL) levels. **B**. At stage 16, *Tbx3* expression is located in the presumptive forelimb and hindlimb areas. Expression is more robust in the posterior part of the limb mesenchyme (arrowheads). **C**. St.16 embryo section at forelimb level. *Tbx3* is observed in the lateral plate and somite. **E**. Higher magnification of the section shown in **C**. *Tbx3* is present in the mesoderm and not in the ectoderm of the presumptive wing area. *Tbx3* is also expressed in the ventro-lateral lip of dermomyotome. **D**. St.16 embryo section at the level of the hindlimb-forming region. *Tbx3* is expressed in the lateral plate mesoderm. **F.** Higher magnification of the section shown in **E.** *Tbx3* is expressed in both the mesenchyme and the ectoderm of presumptive hindlimb area. **G.** At st.19, *Tbx3* is located in the posterior forelimb and hindlimb mesenchyme (arrowheads). **H**. At st.25, *Tbx3* is present in the limbs in two stripes in the anterior and posterior limb mesenchyme (arrowheads). S: somite; LP: lateral plate mesoderm; VL: ventral lip of dermomyotome; M: mesoderm; E: ectoderm.

in situ hybridization for *Tbx3* (Fig.18B). At stages when limb buds are evident (St.19 HH), expression is prominent in the posterior of the forelimb and hindlimb (Fig.18G, arrowheads). At later stages (St.25 HH), *Tbx3* transcripts are now detected in two stripes in the anterior and posterior limb mesenchyme in both the forelimbs and the hindlimbs (Fig.18H, arrowheads).

2.2 Multiple isoforms of *Tbx3* have been identified

Two *Tbx3* isoforms have been reported in the mouse (variant 1, accession no: NM_011535 and variant 2, accession no: NM_198052) and human (TBX3+2a, accession no: NM_016569 and TBX3, accession no: NM_005996). These mRNA transcripts differ in a 20 amino-acid insertion in the T-domain of variant 1 (or TBX3+2a) (Fig.19C). The two isoforms are produced by alternative splicing of a 60 bp exon (2a exon). In mouse embryos and adult tissues where *Tbx3* expression is reported, both isoforms are present, with variant 2 (Tbx3) being more abundant in most of the cases (lower band in Fig.19A) (Fan et al., 2004). Recently, experiments performed with mouse embryonic fibroblasts (MEF) showed that the TBX3 isoform is functionally distinct from the TBX3+2a isoform. Overexpression of TBX3 is able to immortalize MEFs while TBX3+2a causes an acceleration of cell senescence. The TBX3 but not TBX3+2a isoform is upregulated in breast cancer cell lines (Fan et al., 2004). In addition, TBX3 but not TBX3+2a, is able to bind to the previously identified T-box binding site in a gel shift assay. The functional differences between the two proteins could be explained by the fact that these two isoforms may have different downstream targets. To determine if two splice variants of chick *Tbx3* are expressed in the embryo at the stages I was interested in, PCR primers were designed that flank the equivalent region of the chick mRNA. Total RNA was isolated from st.19

embryo forelimbs, hindlimbs, head and torso. In addition, total RNA was isolated out from whole st.16 chick embryo. To determine if *Tbx3* isoforms are present in mouse limbs we designed primers complementary for the mouse transcript and total RNA was isolated from mouse E10.5 forelimbs, hindlimbs, head and torso. RT-PCR was carried out. In mouse samples I detect

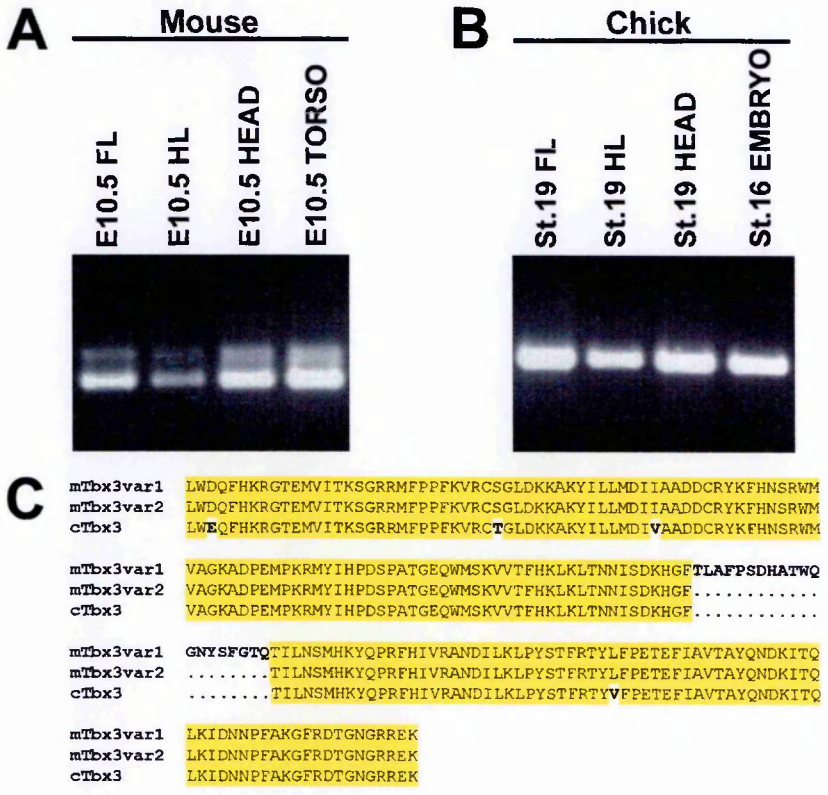

Figure 19. A. RT-PCR for *Tbx3* isoforms using total RNA isolated from mouse E10.5 embryo forelimbs (first lane, E10.5 FL), hindlimbs (second lane, E10.5 HL), head (third lane, E10.5 HEAD) and torso (fourth lane, E10.5 TORSO). Two isoforms are present in all samples. The predominant band represents the variant2 isoform (mTbx3var2 in **C**). **B.** RT-PCR analysis for *Tbx3* isoforms using total RNA isolated from st. 19 chick embryo forelimbs (first lane, St.19 FL), hindlimbs (second lane, St.19 HL), head (third lane, St.19 HEAD) and St.16 whole embryo (fourth lane, St.16 EMBRYO). Only one band is observed in all samples representing *Tbx3* variant2 isoform (cTbx3 in **C**). **C.** Amino-acid sequence alignment of the T-domain of mouse Tbx3 variant 1 (mTbx3var1), mouse Tbx3 variant 2 (mTbx3var2) and chicken Tbx3 (cTbx3). Note the 20 amino-acid residue insertion present in mouse variant 1 (bold) and absent from

mouse variant 2 and chick Tbx3. Four amino-acids are different between the mouse forms and chick sequence. Identical sequences are highlighted in yellow.

two bands that correspond to the two splice variants present (Fig.19A). The predominant band represents splice isoform 2. In samples from chick embryos, a single product is identified that corresponds to the equivalent of mouse variant 2 suggesting that, at least at the stages examined, chick *Tbx3* is represented by a single transcript (Fig.19B). Although my failure to identify a variant 1 transcript cannot demonstrate that it does not exist, following completion of the chicken genome project the genomic sequence of chick *Tbx3* was available. Comparison of the genomic organisation of mouse and chick *Tbx3* showed that mouse *Tbx3* gene has eight exons includind the alternative spliced exon 2a (Fig.20). However, analysis of chick *Tbx3* genomic sequence, indicates that chick *Tbx3* has seven exons. In addition, alternative splice acceptor sites are not predicted in the genomic sequence (Fig.21).

Mouse *Tbx3*

5'upstream sequence

.....ccagcctcctccccggatcccccggcttggatggctgaggcctttcagac

Exon 1

GTAGGCTGAGCTGAGGAGCCGCGGCGAGCTCTCAGGCTGCTGCGAACTCTCTTCTGGATC
AGCCACCTAGAGGCGACTTTGGTGAGCGCGCGGCGCCCTGGTGGCTCCCCGCCCTCCCCT
CTGATCATGTTGACATAAACGCAGGACAGGCCGTAGTACCGCGCGGCGCAGCGACGTTCC
AGTTTCCGACACCTTCTTTTTATAACTCGGCTCTATTCCCCCAGCACTCGACCTGTGAAA
ACCACGCCTATGCAGCCACACAATTGGTCCGAAAGCGTCAAAGAGCCAATCAACAAGCCT
CGGGCTCCCGCAGCCCACAGCGCTGCCGGACCGTCCAGAGCCGCCGAGCAGACGCCCGGG
GAATTCTAGAGGCGGAGGAGGGTGGCGAGGTGCTCGCTCGCTCTCTTTCTCTCTTTCTCT
CCCTCCCTCTACTTGCCTACTCCAGCTCCCAATCACTCCGTTCTCTTCCTTCTTTCCTAT
TTTTTTTTTTTTGCACCCGTCTTCTTGATCCTCCCTCGCCCTGCGTGCCCGGACGCTGAT
TTTTTTTTAATTTATTATTTTTAGGAAAGCGATTTCGCTCACGTTTTTTTAGCACAAGGA
AGACAGCCGGCTCCCCGAGGCAGAAGATCGCAGGCACCATTCGCTCGCCACCCAGACTCT
GCGCGCAGCCCGGAGCCAGAGAGGAGGATCGCGAACCGAAGCCAGCTTCGCAGTTCTAGT
TTTGAAAGCGCCGCTGGAAAGGGGCTTAAATCGCTTTTTTTTTTTTTTTTTTTTAAAGG
AGAGACTTTTCCTCCCCCCCTTGATCTCGCTGCCTGTGAAAGCCAGAGTCTAGCTCAACT
AAGACGCCTCCTGCGAGAAAGCCAGAGAAGAGCTAGGGGGCGGGGGAAGGAGTCGAAAAA
AAGGTTAAAAAAAAAAGTCTCCGAGAACCTTGCGCTTTGGCAACAAAGAGCGTGGGAGCC
GGGGAGCCACCCCGGGAAAGGGCTGCAGTGTCTATTTCCAGCTAAGCCACAGGGCTTGGG
CGCCAGTCGAGCCCCTGCTTGCTGCTTGCCCTACTGAAACCGACTTCCAGGAGCGGCTTT
TCCAACACACTCCACGCACCAGGACAGCCCCTGCAGCGGCTATGTCTCCAGATCTGCTGC
CGCTTTGTCCTCTTTAAAAGCGGCGTTCTCTTCCCCCCAAAGACACTTTCCCCCTCCCTT
TCAAACGCTTTATTTGTAATTTGCCCTCTTTTTTATTTTAAACAAAACTATGCGTCGCTG
TTGAATTTTTTAATTATTATTTTTGAAAAGCAACAACAAAAGCGGAGCCAAGCCAGCAGC
TGCGGACTGGTTCCCTGTCTGGAGTGG**ATGAGCCTCTCCATGAGAGATCCGGTTATCCCT**
GGGACAAGCATGGCCTATCATCCCTTCCTACCTCACCGGGCGCCGGACTTCGCCATGAGC

GCGGTACTGGGCCACCAGCCGCCTTTCTTCCCCGCGCTAACGCTGCCTCCCAACGGCGCC
GCGGCGCTCTCGCTCCCCGGAGCTCTGGCCAAGCCCATCATGGATCAGTTAGTGGGGGCT
GCTGAGACCGGCATCCCTTTCTCATCCCTGGGACCCCAGGCACATCTGAGGCCTCTGAAG
ACCATGGAACCCGAAGAAGACGTAGAAGATGACCCTAAGGTGCACCTGGAGGCCAAGGAA
CTTTGGGACCAGTTTCACAAGCGGGGTACAGAGATGGTCATCACGAAGTCAGGAAG

Intron 1-2 gtaagtaagtaatcagtgggggacc.....tttgccttttctgtgcttttgtag
Exon 2 GCGAATGTTCCCTCCGTTTAAAGTGAGGTGCTCTGGACTGGATAAAAAGGCCAAGTATAT
TTTATTGATGGACATTATAGCTGCTGACGACTGTCGATATAAATTTCACAACTCTCGGTG
GATGGTGGCCGGTAAGGCAGACCCCGAAATGCCAAAGAGAATGTATATACACCCGGACAG
CCCCGCTACGGGGGAGCAATGGATGTCCAAAGTCGTCACTTTCCACAAACTGAAACTCAC
CAACAACATATCGGATAAACACGGATTT

Intron 2-2a gtaagtttcattgactatcatcaat.....tgcatgtttttctctatcttttaag
Exon 2a ACTTTGGCCTTCCCAAGCGATCACGCAACGTGGCAGGGGAATTATAGTTTTGGGACCCAG
Intron 2a-3 gtaggctagggttcaaggtactaat.....tgcaccctcttccctttcttctacag
Exon 3 ACTATACTAAACTCTATGCATAAGTACCAGCCGCGGTTCCACATCGTCAGAGCCAACGAT
ATCCTGAAACTGCCTTACAGTACTTTTCGAACCTACCTGTTCCCGGAAACAGAATTCATC
GCCGTTACTGCCTATCAGAATGACAAG

Intron 3-4 gtaaccaccccaccgggcttgcttc.....tgtcttgcttgtctgtctcctctag
Exon 4 ATAACTCAGTTAAAAATAGACAACAATCCCTTTGCAAAGGGTTTTCGAGACACTGGCAAT
GGCAGGAGAGAAAAAAG

Intron 4-5 gtaagccctgacttttagttgaggg.....aatgggtgggggccccctgttacag
Exon 5 AAAGCAGCTCACACTGCAGTCCATGAGAGTGTTTGAGGAGAGGCATAAGAAGGAGACTTC
GGATGAGTCCTCCAGCGAGCAGGCAGCCTTCAACTGCTTTGCCCAGGCATCCTCTCCTGC
TGTCTCCATCGTGGGGACATCCAACCTCAAAG

Intron 5-6 gtaagtaagtctggccttcttctct.....ttggccttttcctctcctccccaag
Exon 6 ATCTGTGTCCCAGCGAAGCCGAGAGTGACGCCGAGGCTGAGAGCAAGGAGGAGCACGGCC
CTGAGGCCTGCGACGCGGCCAAGATTTCCACCACTACGGCCGAGGAGCCAGGCCGCGACA
AGGGCAGCCCAGCAACCAGGGCGCAGCTGTTCCCCGCGGAGCCCAGCCGGGCCCGCGACA
CCGCGCGTCTGGACAAGGCATCGCCAGACTCGCGCCATAGCCCGGCCACCATCTCGTCCA
GCACGCGAGTTCCGGGAGCTGATGAGCGCAGGAGTCCCGGGCGCGAGGGTCCAGTCGCCA
CCAAGGTGGATGAGGCGCGCGCGATTCCTGCCAAGGACGCCTTCGCTCCACTGTCGGTGC
AGACAGACGCCACCGCGCACCTAGCGCAGGGGCCCCTCCCGGGCTTGGGTTTCGCCCCAG
GCCTTGCGGGCCAGCAGTTCTTCAACGGGCACCCGCTCTTCCTGCACCCGGGCCAGTTCG
CCATGGGCGGCGCCTTCTCTAGCATGGCTGCAGGCATGGGGCCCCTGCTGGCCACAGTAT
CCGGAGCATCCACCGGCGTCTCAGGCCTAGAATCCACAGCCATGGCCTCGGCTGCCGCAG
CGCAGGGACTGTCTGGGGCGTCGGCTGCCACCCTGCCCTTCCACCTCCAACAACACGTTC
TGGCCTCCCAG

Intron 6-7 gtattgcttcctgcctgcccgccta.....tatgtttcttctctctcttccccag
Exon 7 GGCTTGGCTATGTCGCCTTTCGGGAGCCTGTTTCCTTACCCCTACACATACATGGCTGCA
GCAGCTGCAGCCTCCACCGCGGCCGCCTCCAGCTCCGTGCACCGCCACCCGTTCCTCAAT
TTGAACAGCATGCGCCCCAGGCTGCGTTACAGCCCCTATTCCATCCCCGTCCCAGTGCCG
GATAGCAGCAGTTTGCTGGCCACAGCTTTACCATCAATGGCTTCCGCCGCGGGGCCCCTA
GACGGCAAAGCGGCCGCCCTGGCAGCCAGCCCAGCCTCGGTGGCTGTGGACTCGGGGTCG
GAACTGAACAGCCGCTCGTCCACGCTGTCCTCTGGCTCAGTGTCCTTGTCACCCAAACTC
TGCTCCGAGAAGGAGGCGGCTACCAGCGAACTGCAGAGTATCCAGCGGCTGGTCAGTGGC
TTGGAAGCCAAGCCAGACAGGTCTTGCAGCGGGTCCCCTTAAAAACAAGAAAAACAAAAT
CGCCCCCTCCCCCAAGGTCTCTCCATTCCAGTTTGGTCAAATCTGCCAGTGCACTTTGTT
AGATGTAAAATAAACCACGGGCCTTCCACATGGGGTGACCCCCGCCCTGTCCCTTTCAGT
TTTGTCTGGGAGGGAGCACTAAAGCCTTTCCAGAGACTATGCTAGATACCACAGGCCCTG
CCACCATGGGCTGTGTAACCAGGCTGCTGTTGCTTTGAAACGCGGGACTGAGGGGGCGGG
AGGAGTGGTGGCAAACAGGCTTTTGTGTCTAGAGCGACTTTTGTGCAGGCTGGTATGGAA
GTCGGGGCTGAAGAACAAGGTAGCCAGGCCAGCCAGGAGCGCGGGTCTTTGAGAGACTTC
ACCGGAATCTTTCCCCCTTCGTGTGTTTAGTGGAAACATCCCCCCTCCTAAACAAACTAA
CAAAACCAATATGGAGGTGGGGGGAGATGAAGTCCTGTGGAACTGTCTATGAAGACTGAA
ACTCACCAATTGCTGAGTACTTTCGTTGGGGCAGAGAGAAGAGGGGCCTTACCTTGCCCC
ATCTATATTAAAGGAATCCTGTCTTTTTTTGTTTGTTTGTTTTTAAATATTGTGATGTTT
TAAGAGCCGATGCTGGCTTCTTTTTTGCATGTTACAGTTTTCTGGGTTTATTTTGCCCCC
CCCCCCTTTTATGGAAAAACAACGGAAGTCCCATTATCCTCAACCTTGCTCAAGGCGGCA
ACCAGGAGGAAGTGGGGTAAAAGGGGCAGCTATGGGCATGAAACCAACCGAGTTGATTTT
TATCTGAGCGCTTGTAGAGGGCTTCGTGTGCCTGTTGGACCATTAGTTCTTTTAACTGTA
TATGCAATAACAAGGTTTTAAAAGATAATAATAAAGAGGAAACACGACTATTGGACAAAG
TATTTATGTAATTATTTGATATCTCTTGTAAATAGGTGGAATATGACTGCTCAGAAAGTT
AAACTTTAATTTATTGAATTGTACATAGCTGGATGTAAATAGGAGCGTGTCTGTCAGGTT
TTATTCTTGTTTTGCCTTTTGGGTCTTATTTCCAGGTCAGGAGATGGCTAATCCACACTA
GCAAGCCTAGGCATCTTTATTCACATCTCCATGCTTTCAAGTAGAGCTGGCTGCAAAGTT
TTTTTTTTTTTTTCTGATGGAGGGGGTGGGATCGGGAGTACTCCTAACTATTTTCACCAA
AATTGGGGAGGTAATGGCCCTTCCGGGCTCCACTTGAAATTCCCTAAACTCTTGACACCC
CCAGAGGGGTTGAGATTGTTGTGTGAGTAGGGGGGGGGGGGGAACGGCCTTGCGGAGGCC
ACCATAGAACCGTCCTAATTTTTCATAGACTCTGGCATCTTACTAACCCATGTGAGGTTT
TCATTGTTCATCTTTATGGTGTTTTGGATTGGTGTACTGAGAGGGACTTGGTTCAAACGA
CCATGAAAGGCAAAACAAAACAAAAAATTAAAAAAAAAAACAAAAAACAAC

3' downstream sequence aacaaaaaaacaaaaaaaaaacccaagaaggagtattttgtgtttagtct.....

Figure 20. Genomic organization of mouse *Tbx3* modified from ensembl databank. *Tbx3* has 8 exons including the alternatively spliced Exon 2a. 5' and 3' regions are in green. 5' and 3' UTR regions are in purple. Introns sequences are in blue while exon sequences are black

Chick *Tbx3*

5' upstream sequence
.....cccgagggccgaggatgtgccccggctcgggaagttgtaggctgtagaag
Exon 1
TTCTGCCTCTCCCCCATGTACTGTGCTGTTTAGAGCTTGTTTCCCCCCACTTTTTTTTTT
TTTTTTTTTTTTTTCCTTTTTGGTGCTTAATCGTTGTTACTGTTATTATCTTAATTTTTC
TTCTTCATGATGTGCTGTTAGAAACCACTCCAGGACTACTCCAGCAGTAGGAAGACCGAG
GAGTGGAGTGG**ATGAATATACCGATGAGAGATCCAGTGATCCCTGGGACAAGCATGGCTT**
ATCATCCTTTTTTACCTCACCGGGCACCGGACTTTGCCATGAGTGCCGTGCTGGGACATC
AGCCCCCCTTCTTCCCGGCCCTGGCTTTGCCCCCCAATGGGGCGGCCGCCCTCTCCCTCC
CCGGCGCCCTGGCTAAGCCCATTATGGATCAGCTAGTGGGGGCTGCAGAGACTGCTATCC
CCTTTTCTTCCCTGGGCCACCAGGCAGCAGCCCATCTGAGGCCTTTAAAAACTCTGGAGC
CAGAGGAAGAAGTGGAAGACGACCCGAAAGTGCACCTGGAAGCCAAAGAGCTTTGGGAAC
AATTCCATAAAAGAGGCACGGAGATGGTGATCACCAAATCGGGAAG
Intron 1-2
gtaggtgtggggcgggggtcgtgct.....tttatctcctcttctctgcccgtag
Exon 2
GAGAATGTTTCCTCCGTTTAAAGTGAGATGCACTGGACTGGATAAAAAGGCCAAGTACAT
TTTATTGATGGATATTGTGGCGGCTGACGACTGTAGGTACAAATTCCATAATTCCCGGTG
GATGGTAGCCGGCAAAGCTGACCCTGAAATGCCAAAGAGAATGTACATCCACCCGGACAG
CCCGGCCACCGGAGAACAATGGATGTCCAAAGTCGTCACCTTTCACAAGCTGAAGCTCAC
TAACAACATCTCCGACAAGCACGGATTT
Intron 2-3
gtgagtcctttcccctctcccaa.....cctccccggccgctccgcaccgcag
Exon 3
ACCATTTTAAACTCCATGCACAAGTACCAGCCCCGCTTCCACATCGTCCGAGCGAACGAT
ATTCTCAAGCTTCCCTACAGCACGTTCCGGACCTACGTGTTCCCGGAGACTGAATTCATC
GCAGTGACCGCATACCAGAATGATAAG
Intron 3-4
gtaaggagattaagaaaggatttgt.....ctttttttttcttctctccttgtag
Exon 4
ATCACTCAATTAAAAATTGACAACAACCCCTTTGCCAAAGGTTTTCGCGACACTGGGAAT
GGAAGGAGGGAAAAAAG
Intron 4-5
gtgagtctggaaacattatatacgg.....cccagcagctccgtgtgcccggcag
Exon 5
GAAGCAGCTGACCCTGCAATCCATGCGGGTGTACGACGAGAGGCAGAAGAAAGAAAACCC
CACTTCGGACGAATCGTCCAACGAGCAGACAGCCTTCAAGTGCTTCGCGCAGTCCTCCTG
CCCCGCCGTGCCCGCCGTCGGCACCTCCAGCCTCAAAG
Intron 5-6
gtgagcgctgagccccggccctgtg.....gccccgggccgtctttgtcttgcag
Exon 6
ATCTCTGTCCCAGCGAGGGTGACAGCGATGCCGACAGCAAAGACGACCCTTTGCTAGAAG
CCAGCGAGTCGGGCAAAATCAGCACGACCACGGCCACCACCCCC
Intron 6-7
g
Exon 7
CGCCAGCCAGCTCCGGGGCGGCCGCGAGTGACGACCCTCGGGACAAAGGGGGCAGCCCTT
CCAAAAGCCACTTCTTCCCCAGCGACTCGGCGACGAGCCGGAGCCGGGAGAGGACGGAAA
AGGCCCCCCCGGACTCCAGGCACAGCCCGGCCACCATCTCCTCCAGCAGCCGGGGGGGAG
GCTTGAGCGGCGAGGAACTGAAAAGCCCCCTCCGGGACGGCCCTAAAGTAGACGAGAACC
GGCTGCTGGGCAANGAGCCCTTCGCCCCCCTCCCGGTCCAGNCCGNCNGCCCGGCGCGCC
TGAGCCAGGGACCTTTGCNGNNCCTGGGGTTCCCCCCCGCCCTGGCCGGCCNGCCGTTCT
TCTTCCCGCTGGGGCGCTGGAAGGGGCTGCTGCTGCACCCCGGGCAGTTCGCTGGGTGTA
AAGGGGTCTCCGGCATGGCCGCGGGCAGGGGTCCGCTGCTCG
3' downstream sequence
gaannnnnnnnnnnnnnnnnnnnnnnnnnnnnnnnnnnnnnnnnnnnn.....

Figure 21. Genomic organization of chick *Tbx3* modified from ensembl databank. *Tbx3* has 7 exons. An exon 2a is not present and a unique transcript is predicted. 5' and 3' regions are in green. 5' and 3' UTR regions are in purple. Introns sequences are in blue while exon sequences are black.

2.3 Tbx3 is a transcriptional repressor *in vitro*

In vitro data suggest that human *TBX3* is a transcriptional repressor (Carlson et al., 2001). To determine if chick *Tbx3* can act as a repressor, I generated three constructs; full-length Tbx3 (Tbx3), that contains the N-terminus and T-domain fused to the VP16 transcriptional activator domain (Ohashi et al., 1994) ($Tbx3^{VP16}$), and a construct in which the N-terminus and the T domain of the protein are fused directly to the repressor domain of the *Drosophila engrailed* gene (Jaynes and O'Farrell, 1991) ($Tbx3^{EN}$) (Fig.22A). The $Tbx3^{VP16}$ construct is expected to compete with the endogenous Tbx3 protein for binding sites and activate target genes. The Tbx3 and $Tbx3^{EN}$ are expected to suppress target genes. To test the transcriptional properties of these three Tbx3 constructs, I performed *in vitro* luciferase assays using a reporter plasmid containing a single T-box binding site (Kispert et al., 1995). Both Tbx3 and $Tbx3^{EN}$ fusion

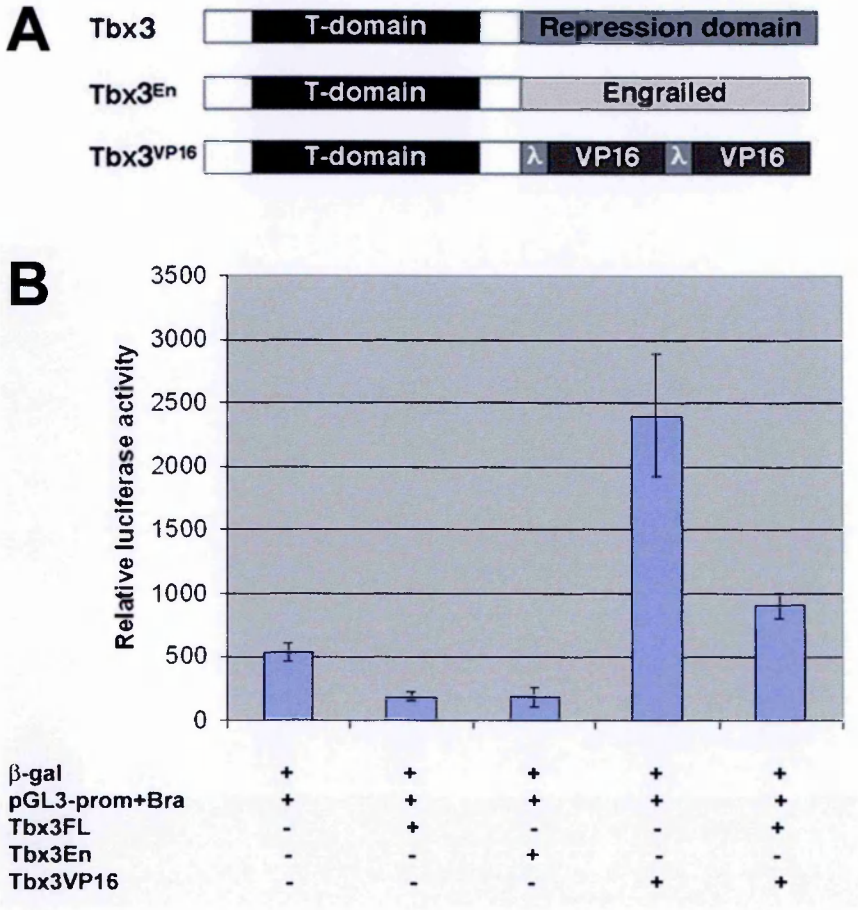

Figure 22. A. Schematic representation (not to scale) of *Tbx3* full length, truncated and En/VP16-fusion retroviral constructs (see Materials and Methods for details). **B.** *In vitro* Luciferase assays for *Tbx3* constructs. After cotransfection with the reporter plasmid there is a 2.5-fold repression on the luciferase activity levels. In the absence of the C-terminus domain ($Tbx3^{\Delta}$) of Tbx3 the repressor activity is abolished. $Tbx3^{en}$ represses luciferase expression to comparable levels with full length Tbx3 while $Tbx3^{vp16}$ activated luciferase expression 5-fold. Cotransfection of equamolar amounts of $Tbx3^{\Delta}$ and $Tbx3^{FL}$ results in increased luciferase activation compared with the $Tbx3^{FL}$ alone but still at lower levels than basal levels. Cotransfection of equamolar amounts of $Tbx5^{vp16}$ and $Tbx3^{FL}$ abolish the repressive activity of $Tbx3^{FL}$ and lead to increased activation of the luciferase gene compared to basal levels.

constructs repress expression to an almost equal extent (2.5-fold). In contrast, the $Tbx3^{VP16}$ fusion construct activates expression (5-fold) (Fig.22B). Co-transfection of Tbx3/$Tbx3^{VP16}$ generates luciferase activity at intermediate levels between those achieved with Tbx3 or $Tbx3^{VP16}$ alone (Fig.22B). Taken together, the data demonstrate that Tbx3 functions as a transcriptional repressor *in vitro*.

2.4 Misexpression of *Tbx3* can be targeted to the prospective limb forming region

I have investigated the role of *Tbx3* in normal limb development using the chicken retroviral system to misexpress the gene throughout the pre-limb bud territory. To determine the targeting, timing of virus-derived transgene expression and progression of virus infection, I performed *in situ* hybridization using a probe that recognizes the viral transcript (Logan and Tabin, 1998). Following our retroviral targeting strategy (see Materials and Methods) we could first detect virus from st.12 HH (Fig.23A) and broadly in the limb-forming region from st.14 HH onwards (Fig.23B). At st.16 HH the virus transcript levels are increased (Fig.23C). By st.17 HH (Fig.23D) the viral transcripts are highly

expressed throughout the forelimb region. At st.19 HH transcripts are detected throughout the limb bud (Fig.23E).

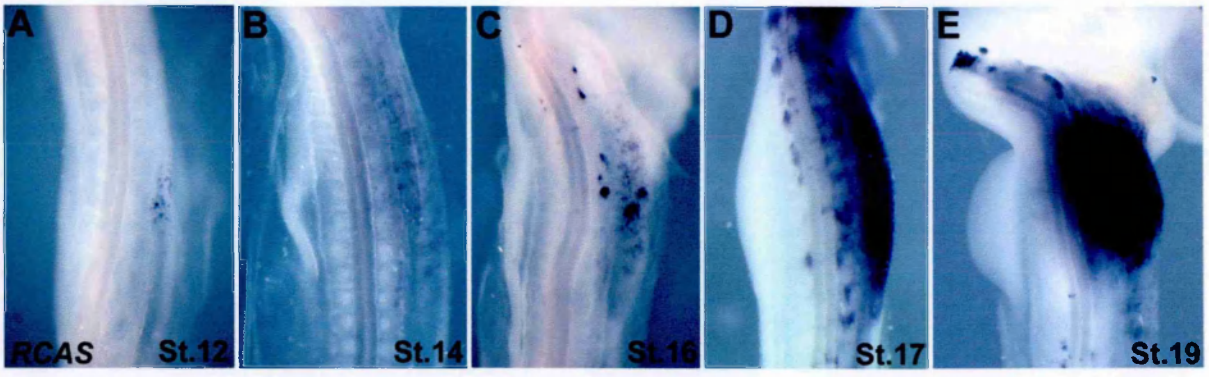

Figure 23. *In situ* hybridization for viral transcripts in different timepoints, following *Tbx3* retrovirus injections at St.8-10 (HH). **A.** Viral transcripts are first detected at st.12. **B.** At st.14, viral transcripts are observed throughout the limb-forming region. **C.** At st.16 the viral transcripts have increased in the presumptive forelimb mesenchyme. **D.** At st.17, the virus has infected in a large number of cells. **E.** By st.19, viral transcripts are detected in the whole limb mesenchyme.

2.5 Misexpression of *Tbx3* can alter limb position

Strikingly, misexpression of full-length Tbx3 shifted the axial position of the injected limb rostrally along the rostro-caudal axis of the embryo (Fig.24A; embryos with rostral limb shift phenotype: n=142; phenotype frequency 25-30%). Identical results were produced with $Tbx3^{EN}$ (embryos with phenotype n= 82, phenotype frequency 25-30%), further suggesting that Tbx3 normally functions as a transcriptional repressor. Comparison of *MyoD* expression, which is expressed in the dermomyotomal compartment of each somite and serves as an axial reference, and *Shh*, which marks the zone of polarizing activity (ZPA) in the posterior limb, demonstrates the rostral shift in limb position following *Tbx3* misexpression (limb on right), relative to contra-lateral control limbs (on left in all cases shown) (Fig.24A; n=6/6, 100%). The shift in axial position can extend

over the distance of one to three somites, however the limb itself is otherwise morphologically normal.

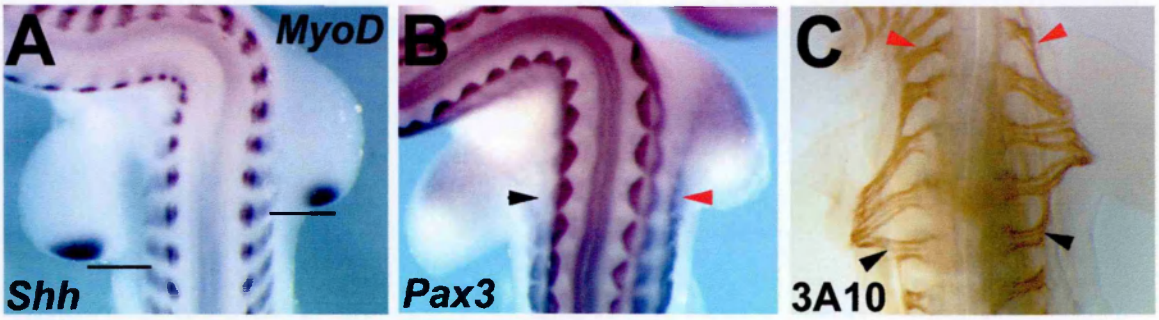

Figure 24. Misexpression of *Tbx3* and *Tbx3*^{EN} causes a rostral shift in limb position along the body axis. In all panels a dorsal view of the embryo is presented, the injected side is on the right and contra-lateral control side on the left. Rostral is top. A. Whole mount *in situ* hybridization with *MyoD* marking the somites and *Shh* marking the ZPA. There is one somite level shift in axial limb position (compare level of left and right bar). B. Whole mount *in situ* hybridization with *Pax3* marking myoblasts that migrate from the lateral lip of dermomyotome into the limb mesenchyme. *Pax3* is not detected in the lateral lip of dermomyotome in somites at levels that normally contribute to limb musculature (black arrowhead) as these cells have migrated into the limb. Following a limb shift, these *Pax3*-expresssing cells are still present in somites at the same level (red arrowhead). C. Whole mount immunohistochemistry for the neurofilament-associated antigen (3A10). Axons from axial levels that normally innervate the limb now fail to send projections to the limb (black arrowheads). At more rostral levels, following mislocation of the limb, axons that do not normally innervate the limb, now project into the limb mesenchyme (red arrowheads). Chick stages: A. 22, B. 23, C. 24,

Pax3 is a paired-homeobox transcription factor expressed in the dermomyotome of the developing somites and the migrating myoblasts (Williams and Ordahl, 1994). Following misexpression of *Tbx3* and mislocation of the limb to a more rostral position along the embryo axis, myoblasts that migrate into the shifted limb are derived from somites at a more rostral level. Myoblasts at more caudal levels that normally migrate into the limb, no longer

contribute to the limb musculature and remain within the ventro-lateral lip of the dermomyotome (Fig.24B; n=7/7, 100%). Both delamination and migration of the myoblasts into the limb depend on the c-met receptor and its ligand HGF, also called scatter factor, produced by non-somitic mesoderm (Dietrich et al., 1999). Following shift of the limb from its normal position, the source of HGF is presumably also shifted, leading to migration of myoblasts from somites at the incorrect axial level.

The neurons that innervate the wing and form the brachial plexus originate from the 16^{th} to 19^{th} spinal ganglia (Lillie, 1927). Transplantation of a limb to the interlimb region results in the migration of neuron axons from the spine into the ectopic limb from axial levels that normally do not contribute to limb innervation (Hamburger, 1939). Consistent with transplantation studies, following *Tbx3* misexpression, the shifted limb is innervated by neurons from the 15^{th} to 18^{th} spinal ganglia (Fig.24C; n=6/6, 100%). Therefore, following rostral shift of the limb, neuron axons that normally would not participate in innervation of the wing, are recruited into the limb and axons that would normally enter the limb mesenchyme no longer do so (Fig.24C). Therefore, following the mislocation of the limb to a more rostral position, several cell-types undergo changes in their normal developmental program and contribute to different regions of the body.

2.6 The limb shifted by *Tbx3* misexpression is patterned normally

It has been reported that misexpression of *Tbx3*, and the closely related gene *Tbx2*, in the developing hindlimb, results in changes in antero-posterior patterning of digits suggesting that these genes have a role in specifying digit identity (Suzuki et al., 2004). To determine if patterning of the shifted limb is

altered, I analyzed the expression patterns of genes that are regionally restricted within the limb. *Fgf8* is expressed in the AER of the injected wing in a pattern indistinguishable from the control limb (Fig.25A; n=5/5, 100%). *Msx1* which is expressed in the AER and in the distal limb mesenchyme is normal in Tbx3-injected embryos (Fig.25B; n=5/5, 100%). *Bmp2*, which is expressed in the AER and in the posterior of the limb as a response to Shh signaling from the ZPA (Francis et al., 1994), is expressed in an identical pattern in injected and uninjected limbs (Fig.25C; n=5/5, 100%). This is consistent with the normal distribution of *Shh* expression in *Tbx3*-injected limbs (Fig.24A). Expression of other T-box genes are also unaffected within the shifted limb despite the rostral mislocation; *Tbx5* is expressed throughout the limb mesenchyme (Fig.25D; n=7/7, 100%), *Tbx15* is expressed in medial regions of the limb (Fig.25E; n=6/6, 100%) and *Tbx2* is expressed in anterior and posterior stripes, in a similar pattern to *Tbx3* (Fig.25F; n=6/6, 100% compare with Fig.18C). *Hoxc5,* which is expressed in proximal regions of the limb mesenchyme (Burke et al., 1995), is unaffected in the injected limb (Fig.25G; n=6/6, 100%). Finally expression of *Sox9* is normal in st.25 HH embryos following misexpression of Tbx3 (Fig.25H; n=6/6, 100%). However, cartilage precursors of the scapula marked by *Sox9*, are located in a more rostral axial position in the injected side (right) compared to the contra-lateral control side (left) (Fig.25H, red arrowheads).

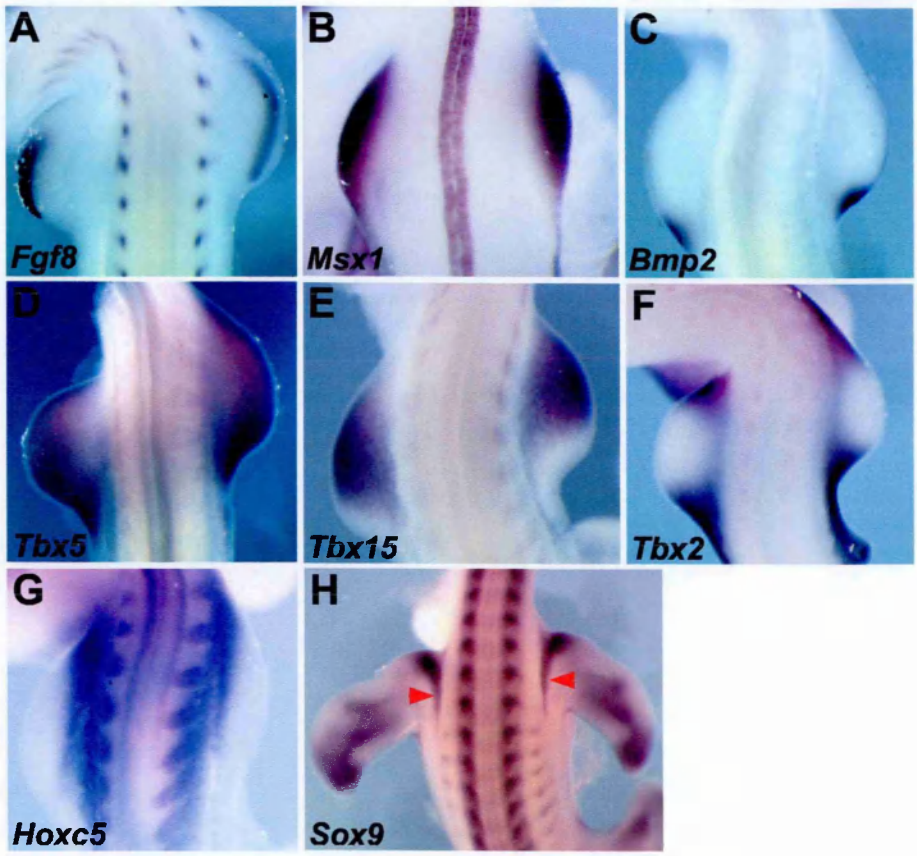

Figure 25. The limb shifted by misexpression of Tbx3 repressor forms is patterned normally. While a rostral shift in axial limb position is apparent *Fgf8* (**A**), *Msx1* (**B**), *Bmp2* (**C**), *Tbx5* (**D**), *Tbx15* (**E**) and *Tbx2* (**F**), *Hoxc5* (**G**), *Sox9* (**H**) are all expressed in their normal pattern in the shifted limb. Red arrowheads in H point to the scapula precursors which are located in more rostral position. Chick stages: **A**: 21,**B**: 19, **C**-**F**: 21, **H**: 25.

To determine if the normal patterning observed using molecular markers expressed at limb bud stages results in normal skeletal patterning, I performed *in situ* hybridization with *Sox9* at st.27 HH. Following misexpression of repressor forms of Tbx3 the expression pattern of *Sox9* in injected forelimbs (Fig.26B; n=8/8, 100%) and hindlimbs (Fig.26D; n=7/7, 100%) is indistinguishable from the contra-lateral uninjected fore- (Fig.26A) and hindlimbs (Fig.26C).

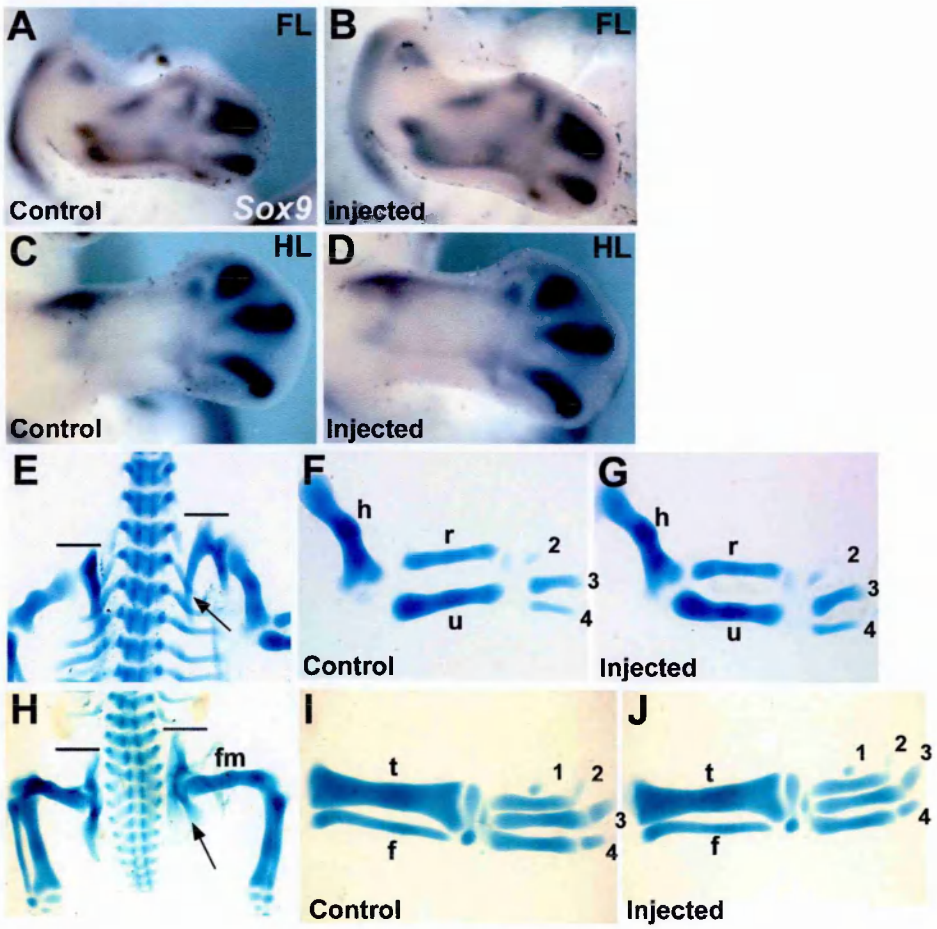

Figure 26. Normal digit patterning following misexpression of Tbx3 repressor forms. **A-D.** *In situ* hybridization for *Sox9* in forelimbs (**A-B**) and hindlimbs (**C-D**). *Sox9* expression is not altered following misexpression of Tbx3 repressor forms. **E-J.** Skeletal preparations of *Tbx3*-injected embryos. **E.** While the limb is shifted (compare bar levels between left and right side), no alterations are observed in the vertebral column. **F.** Skeletal preparation of contra-lateral control forelimb and **G**. injected forelimb. There is no alteration in the pattern of the limb elements. **H.** Following misexpression of Tbx3 in the presumptive leg region there is a rostral shift in axial hindlimb position (compare bar levels between left and right side). **I.** Skeletal preparation of control and **J**. injected hindlimb. No alteration in skeletal elements is observed. The arrows in E and H indicate the scapula and ischium respectively. Digits are numbered. FL: forelimb, HL: hindlimb, h: humerus, r: radius, u: ulna, fm: femur, t: tibia, f: fibula. Chick stages: **A-D**: St.27, **E-J**: St.29

In addition, embryos with a shift phenotype that were allowed to develop to later stages (st.29 HH) in order to analyze their limb skeletal elements using

histological staining with alcian blue. In these examples, the vertebral column of the embryos is normal (Fig.26E, 26H). However, the limb skeletal elements including the scapula are mislocated rostrally, although there is no alteration in their morphology (Fig.26E; n=10/10, 100%). Moreover, the morphology of the digits in the shifted wing (Fig.26G) is normal compared with those in the contra-lateral control limb (Fig.26F). Similar results were obtained following misexpression of *Tbx3* in the developing hindlimbs (Fig.26H; n=10/10, 100%). The axial position of the injected limb is shifted rostrally along the rostro-caudal axis, but hindlimb digit morphology (Fig.26J) is indistinguishable from the digits in the contra-lateral control leg (Fig.26I).

2.7 Axial Hox gene expression is unaffected following *Tbx3* misexpression

To understand the mechanism underlying the rostral shift in limb position, I investigated the effects of *Tbx3* misexpression at stages prior to morphological limb shifts (St. 15-16 HH). Although there is no direct evidence that axial Hox gene expression controls the position of the limb primordia, the axial position at which the limbs develop is fixed across species and correlates with the expression of several Hox genes in the LPM (Burke, 2000; Burke et al., 1995; Cohn et al., 1995; Cohn et al., 1997; Rancourt et al., 1995). Experiments performed in the chick suggested that the Hox9 paralogues may be important in limb positioning along the rostro-caudal axis of the developing embryo and in limb-type specification (Cohn et al., 1997). I, therefore, examined the expression pattern of *Hoxa9*, *Hoxb9*, *Hoxc9* and *Hoxd9* on st.16 embryos following misexpression of Tbx3 repressor forms. No alteration was observed in the expression pattern of these genes in the LPM of the forelimb-forming area. The rostral expression boundary *Hoxa9* is not altered (Fig.27A; n=16/16,

100%). The expression border of *Hoxb9,* which is reported to be just caudal to the region of the LPM which will give rise to the posterior forelimb mesenchyme (Burke et al., 1995; Cohn et al., 1997), is at the same level on the rostro-caudal axis of the embryo in both the control and injected side (Fig.27B; n=27/27, 100%). The same result is obtained with *Hoxc9* (Fig.27C; n=18/18, 100%). *Hoxd9* is expressed in the limb mesenchyme of the forelimb but not of the

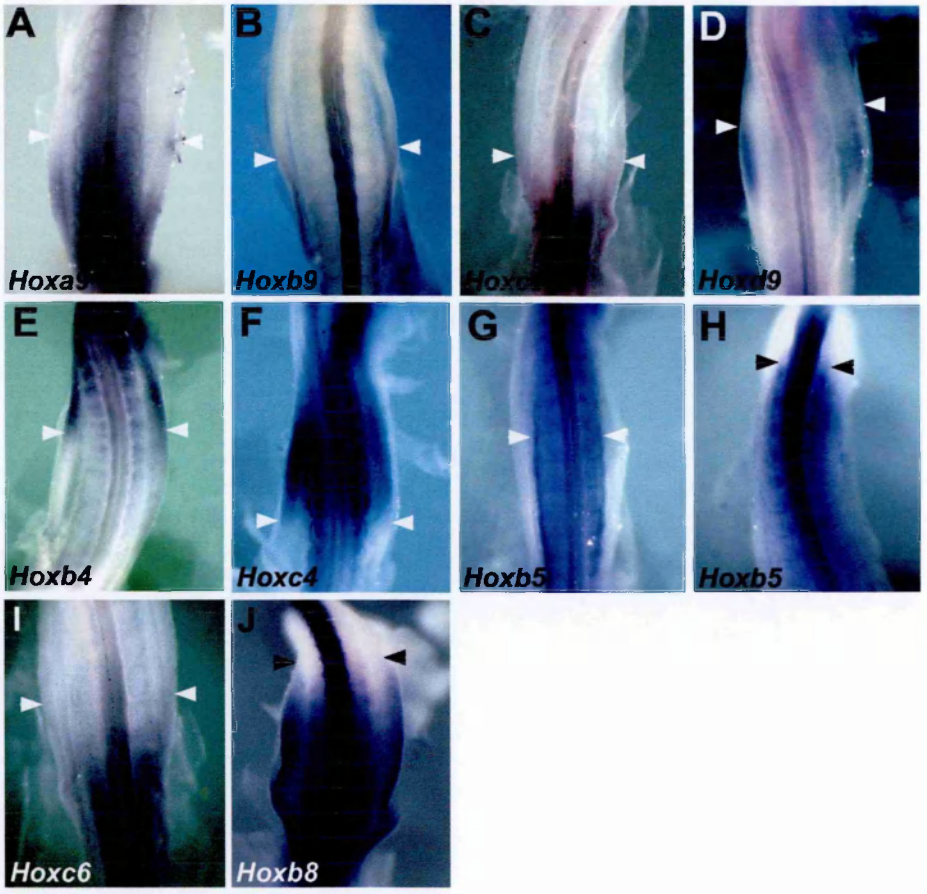

Figure 27. Hox gene expression following misexpression of Tbx3 repressor forms. Expression of *Hox* genes examined is not altered. **A-D.** *In situ* hybridization for *Hox9* paralogues. **A.** *Hoxa9* **B.** *Hoxb9* **C.** *Hoxc9* and **D.** *Hoxd9*. **E.** *Hoxb4* and **F.** *Hoxc4* which are expressed in more rostral regions are not altered following Tbx3 misexpression. **G.** *Hoxb5* is normally expressed in the somites and intermediate mesoderm in both the injected and contra-lateral control side in the level of the forelimb-forming region, while its rostral expression border in the cervical level **H.** is not altered. **I.** *Hoxc6* whick is expressed in the thoracic region is not altered following Tbx3 misexpression. **J.** *Hoxb8* rostral expression border, observed in the anterior limb mesenchyme,

is also unchanged. Arrowheads indicate rostral expression borders except in **G** where normal expression of *Hoxb5* is observed in the forelimb-forming region.

hindlimb. *In situ* hybridization for *Hoxd9* shows that following misexpression of *Tbx3* its expression is not altered and the anterior border of its expression in the limb-forming region is at the same level in the injected side (right) compared to the contra-lateral control side (left) (Fig.27D; n=16/16, 100%). After the examination of *Hox* genes expressed within or caudally to the limb forming regions I was curious to examine *Hox* gene expression located at more rostral regions. *Hoxb4* and *Hoxc4* are expressed in the cervical region and in the LPM that will give rise to anterior forelimb mesenchyme (Burke et al., 1995). The caudal boundary of *Hoxb4* (Fig.27E; n=17/17, 100%) and *Hoxc4* (Fig.27F; n=20/20, 100%) is not altered following misexpression of Tbx3-repressor forms. *Hoxb5* expression, observed in the IM at the level of the limb forming region, is not altered (Fig.27G; n=19/19, 100%). In addition, its rostral expression boundary located in the cervical level of the developing embryo, is at the same level in the injected area compared with the contra-lateral control side (Fig.27H). Forelimbs normally develop at the cervical-thoracic junction (Burke et al., 1995). I therefore examined the expression of *Hoxc6*. The rostral border of *Hoxc6* is reported to mark the cervical-thoracic boundary (Burke et al., 1995). Following misexpression of Tbx3-repressor forms, *Hoxc6* expression is not altered (Fig.27I; n=15/15, 100%) indicating that the cervical-thoracic boundary is not changed and the axial body plan is not affected. *Hoxb8* is reported to be important for anteroposterior patterning of the limb (Stratford et al., 1997) and its rostral border coincides with the anterior limb mesenchyme. *Hoxb8* expression is unchanged following misexpression of Tbx3 repressor forms (Fig.27J; n=30/30, 100%). These results suggest that the mechanism that alters

the position of the forelimb in the *Tbx3*-injected embryos lies downstream of a theoretical axial Hox code that provides positional information to cells of the prospective limb-forming LPM.

2.8 Effects of *Tbx3* misexpression on limb mesenchyme markers

The secreted factor *Wnt2b* is expressed in the prospective forelimb region prior to limb bud formation and misexpression experiments in the chick have suggested that this gene has a role in limb initiation (Kawakami et al., 2001). Following misexpression of *Tbx3*, the domain of *Wnt2b* expression is unaffected (Fig.28A; n=15/15, 100%). Experiments in the mouse, chick and zebrafish have established that *Tbx5* is required for forelimb initiation (Agarwal et al., 2003; Ahn et al., 2002; Ng et al., 2002; Rallis et al., 2003; Takeuchi et al., 2003). Following misexpression of *Tbx3,* expression of *Tbx5* is expanded to more rostral regions of the LPM, whereas the more caudal expression domain, that would normally give rise to the posterior limb mesenchyme, is initially unaffected (Fig.28B; n=6/19, 32%). Expression of *Hoxc5*, which is also expressed in the early limb bud mesenchyme, is also expanded rostrally while the caudal domain remains fixed (Fig.28C; n=7/20, 35%). These data demonstrate that the rostral shift in the limb is preceded by a rostral expansion in the expression of genes present in the limb mesenchyme, while their caudal domain in unchanged. However, at later stages of development, the expression domains of *Hoxc5* and *Tbx5* within the limbs are shifted rostrally (Fig.25D, 25G).

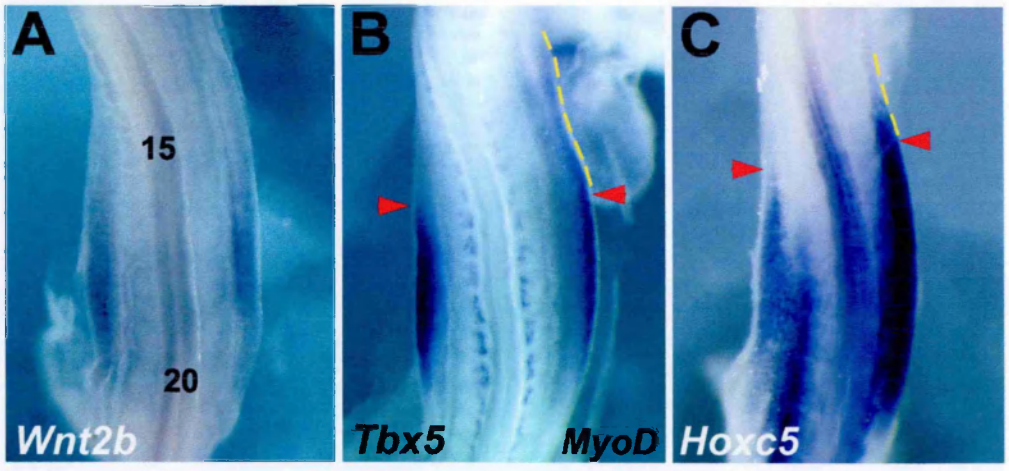

Figure 28. Effects of Tbx3 misexpression on early limb mesenchyme markers. **A.** *Wnt2b* expression domain is not changed in the injected area compared with the contra-lateral control right side. **B.** A dramatic rostral expansion in *Tbx5* expression domain is observed compared with the control side. **C.** *Hoxc5* an early marker of the limb-forming region is upregulated and expanded rostrally, in a similar way to *Tbx5*. Yellow lines in **B** and **C** indicate the area of expanded gene expression. Red arrowheads in **B**, **C** show the sites of the normal rostral border of gene expression. Embryo stages: **A**-**C**: st.16

2.9 Cell movement does not account for the limb-shift phenotype

To investigate whether cell movement accounts for the shifted limb phenotype, I performed DiI labeling experiments to follow the fates of cells of the prospective limb-forming region. Viral injections were performed at st.8-10 (HH) (Fig.29A). Twenty-four hours later and at stages before the expansions of *Tbx5* and *Hoxc5* occur, DiI dye was injected in the LPM at the 17th and 20th somitic level that corresponds to the medial and posterior wing mesenchyme. DiI was also injected in adjacent somites for axial reference. Identical injections were performed in the contra-lateral control side (Fig.29B). The embryos were left until stages when the limb shift phenotype is apparent and then harvested and fixed (Fig.29C). On the level of 17th somite, labeled cells are part of the medial limb mesenchyme. Cells at the level of the 20th somite, while in the contra-lateral control (left) side are found in the posterior-proximal limb mesenchyme,

in the injected side they contribute to the interlimb flank.

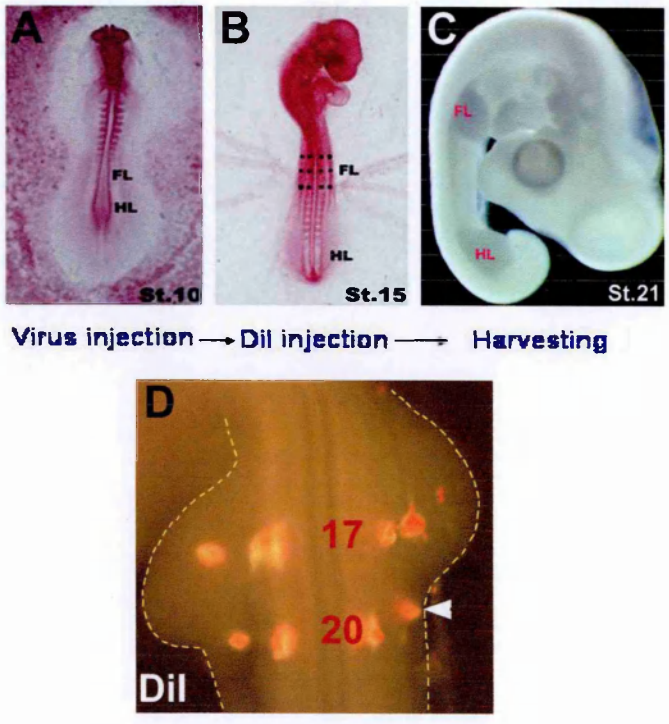

Figure 29. DiI labeling experiment in order to follow the fates of the limb-forming cells in the LPM. **A.** At st.8-10 (HH), Tbx3 virus is injected *in ovo* in the presumptive forelimb territory, and the embryo is left to develop. **B.** At st.15, DiI is injected in the LPM in sites where the wings are going to develop and in adjacent somites for an axial reference. The egg is then sealed and the embryo is left to develop until stages that the phenotype is apparent (st.18-20, HH). **D.** Cell movement does not account for the limb shift phenotype. Embryo injected with Tbx3 virus and DiI, exhibiting the phenotype. On the level of 17th somite, labeled cells are part of the medial limb mesenchyme. Cells at the level of the 20th somite, while in the contra-lateral control (left) side are part of the posterior-proximal limb mesenchyme, in the injected side they contribute to the interlimb flank. FL: forelimb, HL: hindlimb. 17th and 20th somites are indicated in D. The embryo is outlined for better visualization of the phenotype.

Therefore, following misexpression of *Tbx3,* cells of the future posterior limb that would normally contribute to the limb mesenchyme no longer do so and instead become incorporated into the interlimb flank (Fig.29D; n=5/5, 100%). Cells in more rostral locations, which would not normally contribute to the limb

are recruited to form (anterior) limb. Therefore, the shift in the limb position cannot be attributed to migration of cells in the LPM.

2.10 *Tbx3* and positioning of the ZPA

A shift in the axial position of the limb is demonstrated by the expression of *Shh* in the posterior of the limb bud at an inappropriate axial level (Fig.24A). I therefore examined the expression of *dHand* and *Gli3*, genes which are involved in pre-patterning the anterior-posterior axis of the limb and establishing the position of *Shh* expression in the ZPA (Charite et al., 2000; Fernandez-Teran et al., 2000; te Welscher et al., 2002a). During limb induction stages, *dHand* (also referred to as *Hand2*), a bHLH transcription factor, is expressed throughout the limb-forming region (Fig.30A, 30D) (Charite et al., 2000; Fernandez-Teran et al., 2000). Subsequently, *Gli3*, a zinc-finger transcription factor, is expressed throughout almost the entire limb mesenchyme in an anterior-to-posterior graded fashion (Fig.30B) (Schweitzer et al., 2000). Genetic antagonism between *Gli3* and *dHand* results in down-regulation of *dHand* expression in the anterior limb mesenchyme. At later stages, *dHand* and *Gli3* are expressed in the anterior and posterior limb mesenchyme, respectively, with an overlapping domain of co-expression in the medial limb (Fig.30C). The interactions between *dHand* and *Gli3* ultimately position the ZPA prior to *Shh* signaling (te Welscher et al., 2002a; Zuniga and Zeller, 1999). Following misexpression of *Tbx3, dHand* is expressed throughout the limb-forming region, while in the control side *dHand* is restricted to the posterior limb mesenchyme (Fig.30E; n=7/22, 32%). In addition, there is a downregulation of *Gli3* throughout the injected limb and the caudal border of its graded expression domain shifts rostrally (Fig.30G; n=8/22, 36%). However, at later stages, when

the shift phenotype is obvious, *dHand* is expressed normally in the posterior mesenchyme of the shifted limb (Fig.30F; n=7/7, 100%) and *Gli3* has a normal distribution in the anterior mesenchyme (Fig.30H; n=8/8, 100%). These data show that following misexpression of *Tbx3*, the normal restriction of *dHand* expression to the posterior limb mesenchyme and *Gli3* to anterior is disrupted. However, at later stages, after the position of the limb has been shifted, *dHand* and *Gli3* expression is normal within the limb mesenchyme.

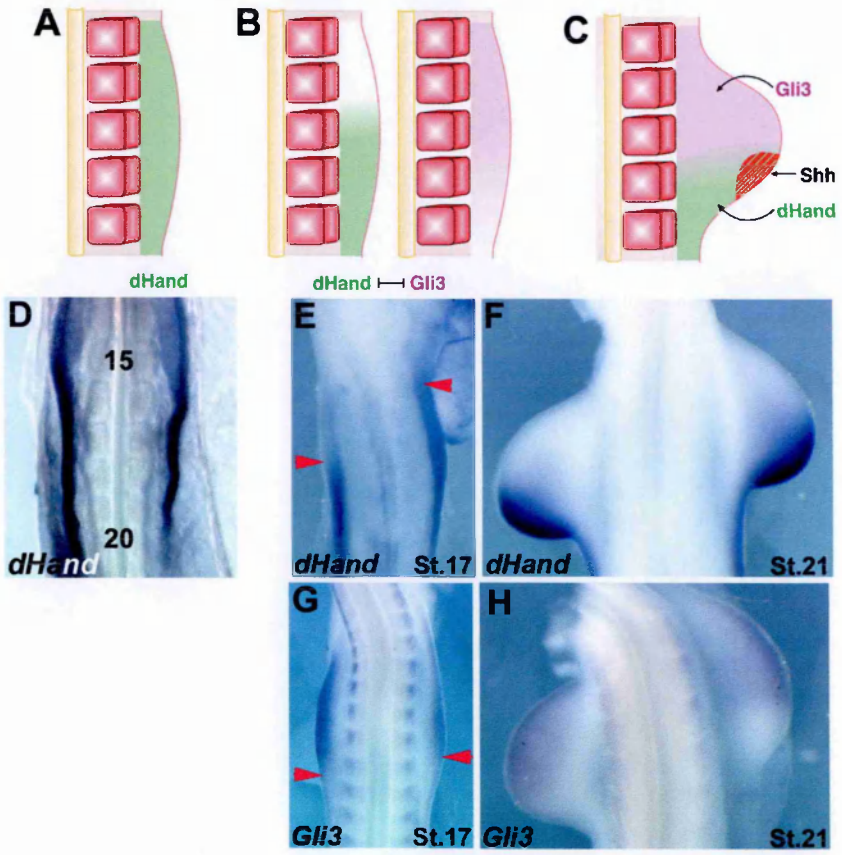

Figure 30. Effects of *Tbx3* and *Tbx3*^{EN} misexpression on *dHand* and *Gli3* expression. Schematics of the limb-forming region at st. 16 (**A**), st. 17 (**B**) and st. 18 (**C**) **A**. *dHand* is present throughout the limb forming region. **B**. High levels of *dHand* expression are observed only in the posterior limb mesenchyme due to repression by *Gli3*, expressed at higher levels in the anterior. **C**. *Gli3* is expressed in the anterior limb mesenchyme, while *dHand* in the posterior is required for the establishment of *Shh* expression in the ZPA. **D**. Normal expression of *dHand* in the presumptive forelimb-forming region at st.16 (HH). **E.** At St.17 HH *dHand* is restricted in the posterior limb mesenchyme in the control side (left, arrowhead shows rostral border of expression) while in the injected side, *dHand* is expressed throughout the limb-forming region

(right, arrowhead). **F.** At stage 21, normal expression of *dHand* is observed within the limb mesenchyme of the shifted limb. **G**. At st.17, *Gli3* is downregulated in the injected side (right arrowhead) compared with the control side (left arrowhead). A rostral shift in the graded *Gli3* expression domain is observed (compare left and right arrowhead levels). **H**. At later stages (st.21) *Gli3* is expressed normally within the mesenchyme of the shifted limb.

In summary, following misexpression of transcriptional repressor forms of *Tbx3* in the limb-forming region, early markers of the limb mesenchyme are expanded (Fig.31B). The initial expansion is followed by an alteration in the mechanism that positions the ZPA so that it is now positioned in a more rostral location along the rostro-caudal axis of the embryo that ultimately leads to limb shifting to a more rostral location (Fig.31C).

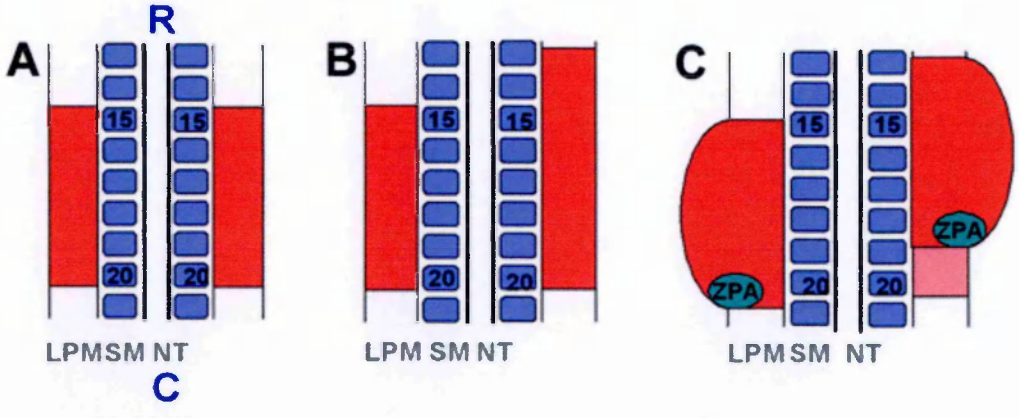

Figure 31. Summary of events that take place following misexpression of repressor forms of *Tbx3*. **A.** In the chick, forelimbs develop at the level of the 15th and 20th somites. **B.** Following misexpression of *Tbx3* an expansion in the domain of limb mesenchyme markers. **C.** At later stages the injected wings are not expanded. They shift in more rostral location along the rostro-caudal axis of the embryo. Signaling centers such as the ZPA are normally formed although they are displaced rostrally in their axial position. Cells that would normally contribute to posterior limb mesenchyme (pink box) are now part of the interlimb flank.

2.11 Misexpression of Tbx3^{VP16} can shift the limb caudally in axial position

As a complementary approach to misexpressing transcriptional repressor forms of Tbx3, I misexpressed Tbx3^{VP16} in the presumptive forelimb area. Tbx3^{VP16} is a transcriptional activator in my *in vitro* assays (Fig.22B). Moreover, Tbx3^{VP16} has the ability to interfere with the repressor activity of Tbx3 (Fig.22B). Following misexpression of Tbx3^{VP16}, the injected limb is displaced caudally in axial position (embryos with caudal limb shift phenotype n=42; frequency of phenotype 30%). Analysis of the expression pattern of *MyoD* and *Shh* demonstrates the caudal shift in axial position (Fig.32A, n=7/7, 100%). The limb displacement can extend over the distance of one to three somites but, as seen with rostral limb shifts, the limb itself is otherwise morphologically normal. I examined the expression of *dHand* and *Gli3* at pre-limb bud stages, following misexpression of Tbx3^{VP16}. While in the control, *dHand* expression is restricted to the posterior mesenchyme of the limb-forming region, following misexpression of Tbx3^{VP16} there is a caudal displacement of the expression domain of *dHand* (Fig.32B, n=9/30, 33%). In addition, there is an up-regulation of *Gli3* expression (Fig.32C, n=8/25, 32%). These results show that by misexpressing Tbx3^{VP16} I am able to generate a limb shift in the opposite direction to that obtained using Tbx3 and Tbx3^{EN}.

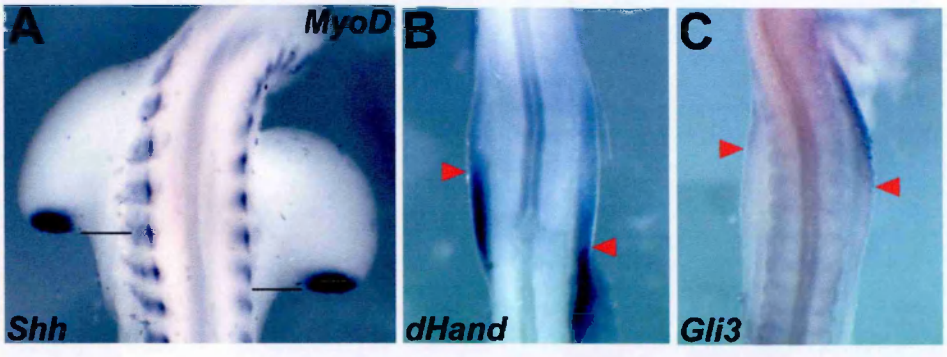

Figure 32. Misexpression of Tbx3^{VP16} causes a caudal shift in axial limb position. **A**. *MyoD* expression marks the somites and *Shh* marks the ZPA. There is one somite level caudal shift (marked by bars) in the injected limb (right). **B**. *dHand* expression at st.17 following Tbx3^{VP16}

misexpression. *dHand* is restricted to the posterior limb mesenchyme in the control side (left, arrowhead shows rostral expression border), while in the injected side, the *dHand* expression domain is displaced caudally (right, arrowhead). **C.** *Gli3* expression at st.17 following $Tbx3^{VP16}$ misexpression. *Gli3* is upregulated in the injected side (right) compared with the control side (left). The graded domain of *Gli3* expression is displaced caudally (compare left and right arrowheads).

2.12 Gli3 is implicated in positioning the limb

Following misexpression of *Tbx3*, *Gli3* mRNA levels appear to be decreased within the limb mesenchyme and the caudal border of its expression is shifted rostrally (Fig.30G). The effect of *Tbx3* misexpression on *Gli3* is observed at stages prior to Shh expression when Gli3 is predicted to be acting as a repressor (Litingtung et al., 2002; Wang et al., 2000). To investigate whether *Gli3* can directly alter limb positioning, I misexpressed a form of Gli3 that contains the DNA binding domain of the protein fused with two VP16 activation domains (Gli3ZnF-VP16, Fig.33A). Gli3ZnF-VP16 has the ability to bind Gli3 binding sites and activate transcription (J. Briscoe, pers. comm). Misexpression of this form of Gli3 is predicted to compete with the endogenous Gli3 repressor (Gli^R) for binding sites and to activate, rather than repress, target genes and thereby lower the repressor activity of endogenous Gli3. Misexpression of Gli3ZnF-VP16 generated a phenotypically similar result to that obtained following misexpression of Tbx3 (embryos with rostral limb shift phenotype n=48; phenotype frequency: 35-40%). A rostral shift in axial limb position is evident by comparing *MyoD* and *Shh* expression domains (Fig.33B, n=7/7, 100%). The rostral shift in axial position can extend from one to three somites. Following misexpression of Gli3ZnF-VP16, the *Tbx3* expression domain is expanded rostrally in the injected side compared with the contra-lateral control

side (Fig.33C, n=6/16, 38%). A similar expansion is observed in *dHand* expression (Fig.33D, n=5/14, 36%). In contrast, the endogenous expression of *Gli3* is decreased following misexpression of Gli3ZnF-VP16 (Fig.33E, n=5/13, 38%).

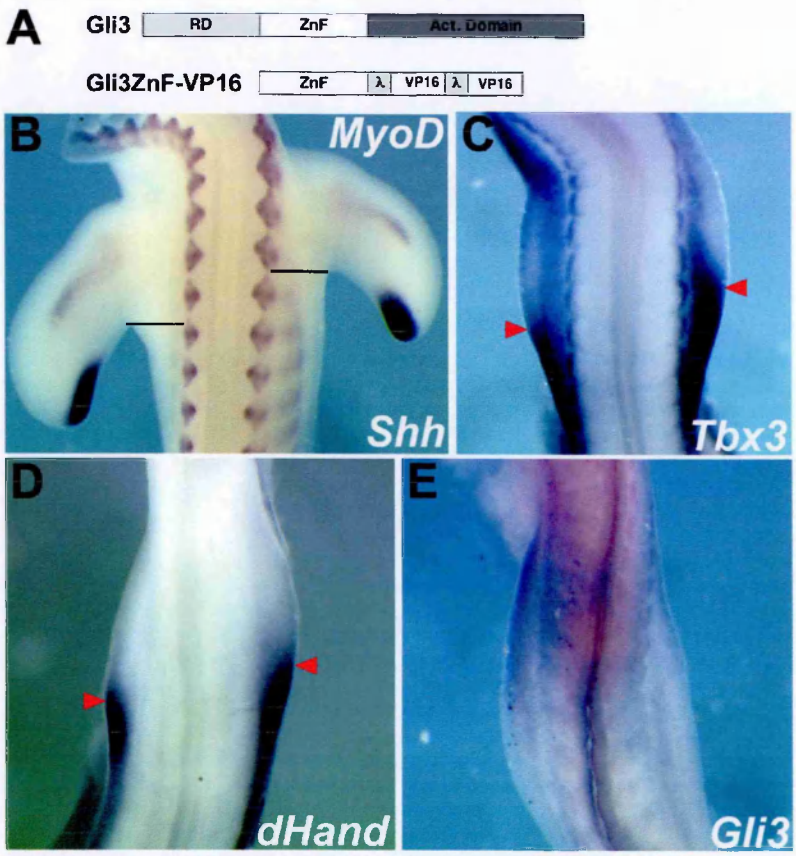

Figure 33. Misexpression of a Gli3ZnF-VP16 activator form of *Gli3* influences limb positioning. **A**. Schematic of full-length Gli3 protein (Gli3) and a Gli3ZnF-VP16 activator form. Full-length Gli3 protein contains an N-terminal repression domain (RD), a zinc finger DNA-binding domain (ZnF), and an activation domain in the C-terminus (Act. Domain). The Gli3 activator form contains the ZnF fused with two VP16 activation domains. Panels **B-E** show dorsal views of the embryo. The right limb has been injected with Gli3ZnF-VP16 virus. **B**. Whole mount *in situ* hybridization with *MyoD* indicates the somites and *Shh* marks the ZPA. There is a one somite level shift in limb position (Compare level of left and right bars). **C**. The anterior border of the *Tbx3* and **D.** *dHand* expression domains in the forelimb region at st.17, have been displaced rostrally (arrowheads). **E**. *Gli3* expression is down-regulated.

2.13 The limb-shift phenotype is generated by specifically manipulating *Tbx3* function

Other *Tbx* genes such as *Brachyury*, *Tbx15* and *Tbx2* are expressed in the limb mesenchyme. I was curious to investigate if the limb-shift phenotype was generated by specifically manipulating *Tbx3* function. I therefore misexpressed *Tbx15* and *Tbx2* in the developing chicken wing using replication-competent retroviruses.

2.13.1 Misexpression of *Tbx15* in the limb mesenchyme does not generate limb-shift phenotype

In order to determine if *Tbx15* is able to generate a limb-shift phenotype, I misexpressed full-length *Tbx15* in the developing chick wing. In no case a limb-shift was observed following misexpression of *Tbx15* (n=41) (Fig. 34).

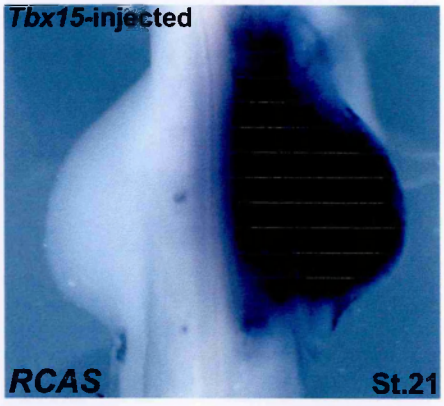

Figure 34. *In situ* hybridization for viral transcripts following *Tbx15* retrovirus infection at st.8-10 HH. While the virus is present throughout the limb mesenchyme, a shift in axial limb position is not observed. The dorsal view of the embryo is presented.

2.13.2 Analysis of *Tbx2* expression pattern in the developing chick embryo

The expression pattern of *Tbx2* in the developing limbs has already been analysed (Gibson-Brown et al., 1998; Logan et al., 1998). However as a first

step in understanding the role of *Tbx2* in limb development I analysed its expression pattern at different stages of chick development. *Tbx2* is expressed in the forelimb and hindlimb region prior to overt limb outgrowth (Fig.35A, st.16 HH). Its expression differs from that of *Tbx3* at this stage (Fig.18B). *Tbx3* expression is more robust in the posterior limb mesenchyme while *Tbx2* expression is uniform. *Tbx2* expression is also detected in the IM (Fig.35A, arrowhead). At later stages of development (st.19 HH), *Tbx2* expression is

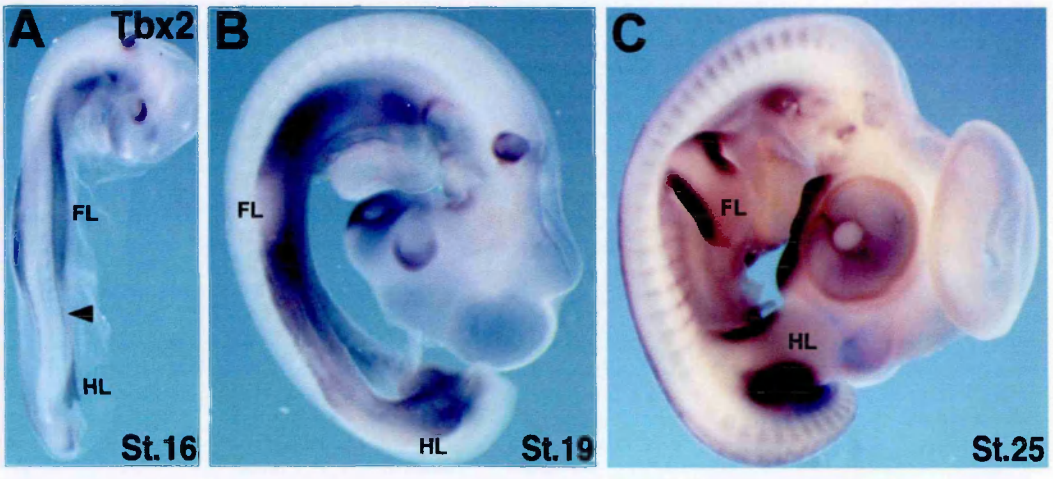

Figure 35. Analysis of *Tbx2* expression in the developing chick embryo. **A.** *Tbx2* is expressed in the forelimb and hindlimb forming regions of the LPM prior to overt limb outgrowth (st.16 HH). *Tbx2* is expressed in the IM (arrowhead). **B.** At st.19 HH, *Tbx2* expression is downregulated in the medial limb mesenchyme but persists in the anterior and posterior regions of the forelimb. In the hindlimb and at this stage, *Tbx2* is expressed in a uniform pattern. **C.** At later stages of development (st.25 HH), *Tbx2* transcripts are present in two stripes in the anterior and posterior forelimb and hindlimb mesenchyme. Abbreviations: FL: forelimb; HL: hindlimb.

downregulated in the medial region of the limb mesenchyme but it is detected in the anterior and posterior limb mesenchyme (Fig.35B). At this developmental stage, *Tbx3* expression is detected at the posterior limb mesenchyme (Fig.18G). At later stages (st.25 HH), *Tbx2* transcripts are detected in two stripes in the anterior and posterior forelimb and hindlimb mesenchyme

(Fig.35C). *Tbx3* has a similar expression pattern at the same stage. However, *Tbx3* stripes are broader than those observed in the case of *Tbx2.*

2.12.3 Misexpression of *Tbx2* in the developing wing leads to increased limb size

Tbx2 protein shares all the characteristic features of the T-box family, namely, the T-domain (DNA binding/dimerization domain) and a transcriptional effector domain in the C-terminal part of the molecule (Fig.36A).

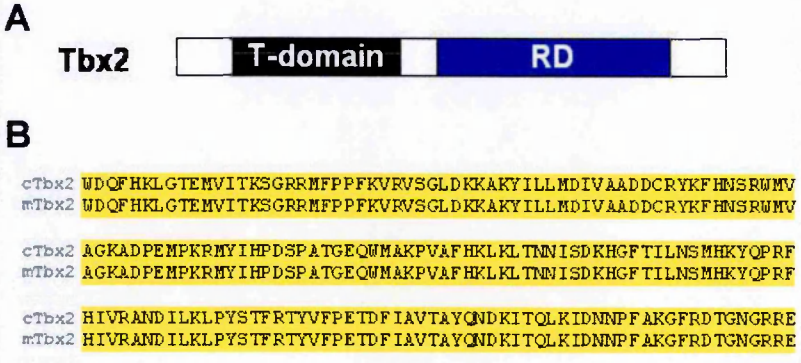

Figure 36. A. Schematic of the Tbx2 protein. Tbx2 shares all the features of the T-box gene family, the T-domain and a transcriptional effector domain in the C-terminal part. In the case of Tbx2 a repression domain lies at this part of the molecule. **B.** Sequence alignment of the T-domain of mouse and chick Tbx2. 100% identity is observed between the mouse and the chick protein.

Tbx2 has been reported to act as a transcriptional repressor (Carreira et al., 1998; Lingbeek et al., 2002; Prince et al., 2004). In order to examine the role of *Tbx2* in normal limb development I misexpressed full-length mouse *Tbx2* in the wing using replication competent retroviruses. The mouse and chick Tbx2 sequences are 100% identical in the T-domain (Fig.36B).

Two days after the injections are performed a dramatic effect on limb size is observed following misexpression of full-length *Tbx2* in the limb mesenchyme.

Tbx2-injected limbs are larger compared to the contra-lateral control wings (Fig.37). Misexpression of *Tbx2* never generated a limb-shift phenotype (n=57).

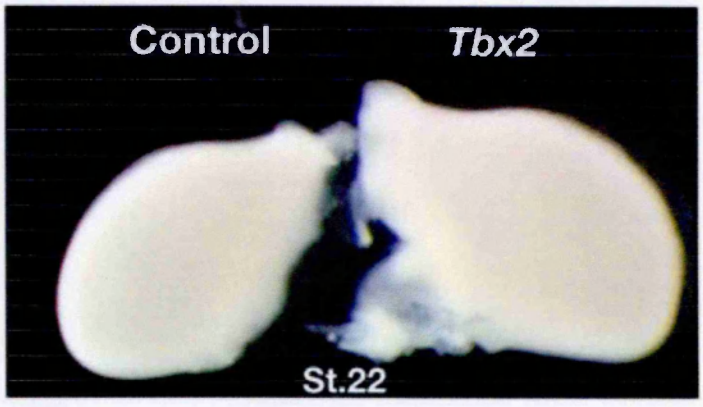

Figure 37. *Tbx2* misexpression generates larger limbs. Comparison of *Tbx2*-injected limb with its contra-lateral control.

2.13.4 *Tbx2* misexpression affects both cell proliferation and program cell death rates in the limb mesenchyme

The larger limbs may be generated due to an increase in cell proliferation rates or decrease in cell death rates. In order to examine cell proliferation, I performed immunohistochemistry on sections using an antibody that recognizes phosphorylated histone 3 (pH3), a marker of mitotic cells (G2-M transition). An increase in cell proliferation rate was observed in the *Tbx2*-injected limbs (Fig.38B), compared to the uninjected contra-lateral control limbs (Fig.38A) when regions containing the comparable cell numbers where compared. Statistical analysis of the numbers of pH3-positive cells showed that the difference between control and injected limbs is significant (Fig.38C).

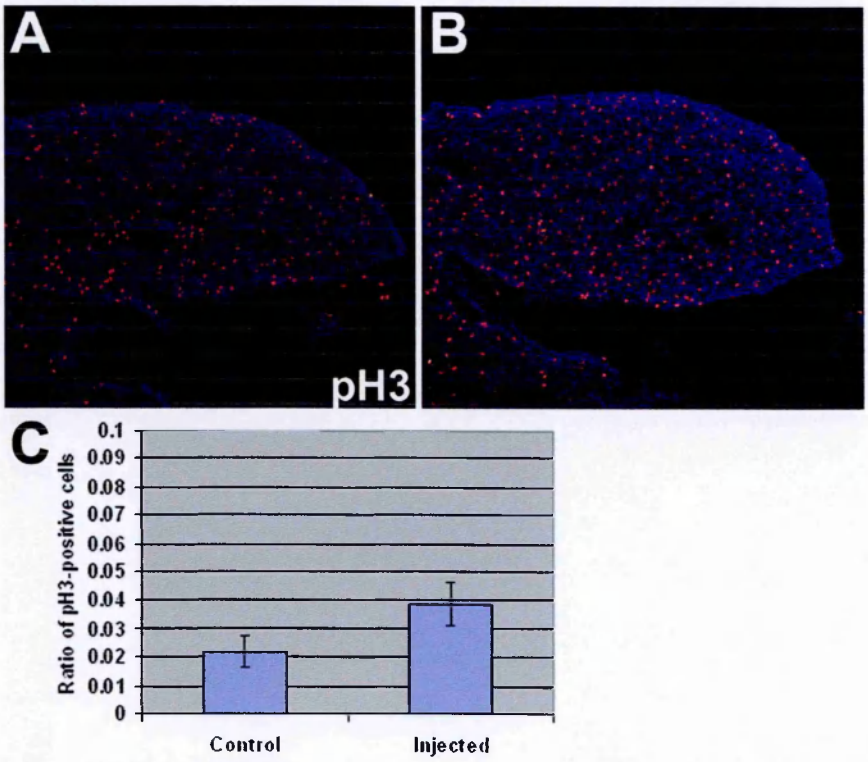

Figure 38. Cell proliferation rates increase following misexpression of *Tbx2*. Transverse sections through **A.** contra-lateral control and **B.** *Tbx2*-injected limb buds at st.22 HH stained with an antibody against phosphohistone H3 to identify cells undergoing mitosis (pink). **C.** Statistical analysis of the ratio of pH3-positive cells in control and injected limbs. The difference observed is significant.

I examined the rates of programmed cell death (PCD) following misexpression of *Tbx2* using TUNEL staining. PCD is dramatically decreased in *Tbx2*-injected limbs (Fig.39B) compared to the contra-lateral control limbs (Fig.39A). Statistical processing of the numbers obtained from cell counting demonstrate the statistical significance of the decreased PCD in *Tbx2*-injected wings (Fig.39C).

Taken together, these data indicate that the limbs are larger as a result of an increase in cell proliferation and decrease in PCD rates.

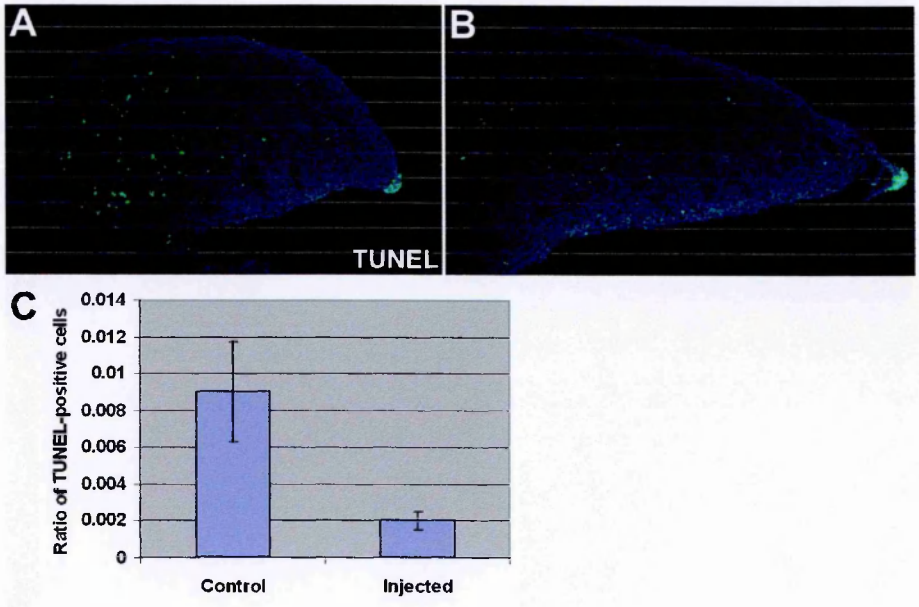

Figure 39. PCD rate is decreased following misexpression of *Tbx2*. Transverse sections through **A.** contra-lateral control and **B.** *Tbx2*-injected limb buds at st.22 HH following TUNEL staining.**C.** Statistical analysis of the TUNEL-positive cells in control and injected limbs. A significant decrease in apoptosis is observed following misexpression of *Tbx2* in the limb mesenchyme.

2.13.5 *Tbx2* and cell cycle progression in limb mesenchyme

Tbx2 has been implicated in cell cycle and cancer (Carreira et al., 1998; Lingbeek et al., 2002; Prince et al., 2004). *Tbx2* is shown to directly regulate $p21^{WAF}$, a gene required for G1-S progression. I examined the expression of cell cycle progression genes in the limb mesenchyme following misexpression of *Tbx2. Nmyc* and *cyclinD1* are genes important for G1-S progression (Hipfner and Cohen, 2004). Following misexpression of *Tbx2*, *Nmyc* is upregulated compared to the contra-lateral control limbs. *CyclinD1* expression is also upregulated following *Tbx2*-misexpression (Fig.40).

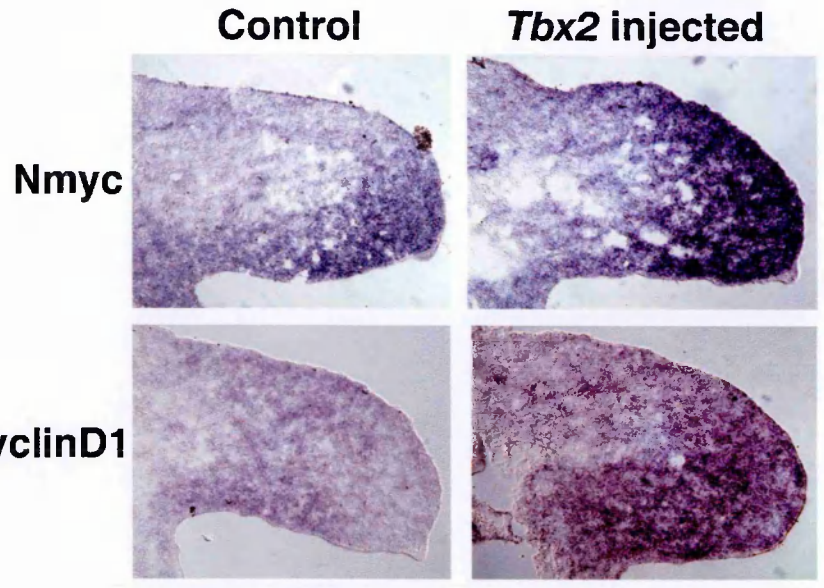

Figure 40. Expression of genes implicated in cell cycle regulation following misexpression of *Tbx2* in the limb mesenchyme. Both *Nmyc* and *CyclinD1* are upregulated following *Tbx2* misexpression.

Further examination will be required to understand the role of *Tbx2* in cell cycle progression and patterning of the developing limb. *Tbx2* directly regulates $p21^{CIP1}$ and is able to dimerise with RB protein. Further experiments will be required to determine if *Tbx2* directly regulates Myc and Cyclin D proteins (Fig.41).

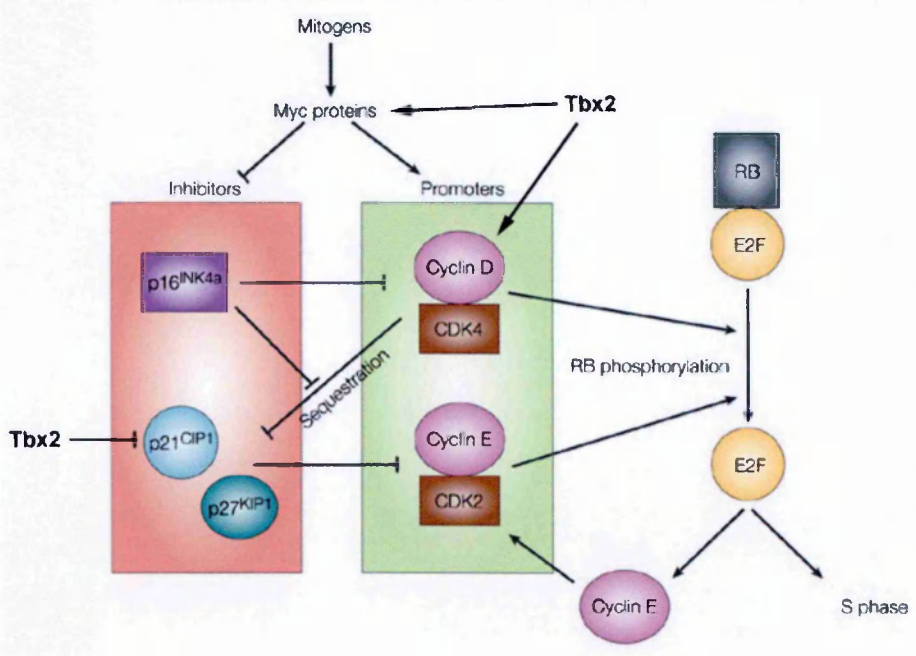

Figure 41. Schematic showing interactions required for cell cycle progression. It has been demonstrated that Tbx2 directly represses p21. However, our results indicate that it may also be implicated in the positive regulation of Myc and CyclinC.

D. DISCUSSION

PART ONE

'The role of *Tbx5* in limb development'

1. The role of *Tbx5* in limb development

I have taken two approaches to investigate the role of *Tbx5* in limb-type specification and outgrowth. The first is a conditional knock-out method in the mouse where I inactivated *Tbx5* specifically in the developing forelimbs. As a complementary strategy I injected dominant-negative and dominant-active forms of *Tbx5* in the developing chicken wing using replication-competent avian retroviruses.

1.1 *Tbx5* is required for forelimb bud development

Tbx5 is expressed in the prospective forelimb-forming territory of the lateral plate mesoderm prior to overt limb bud outgrowth and coincident with the time that these cells are specified to their limb-type fate (Gibson-Brown et al., 1998; Isaac et al., 1998; Logan et al., 1998; Ohuchi et al., 1998). *Tbx5* expression proceeds that of *Fgf10* (Agarwal et al, 2003) and *Tbx5* transcripts are present in the limb-forming region of *Fgf10* knock-out mice (Min et al., 1998; Sekine et al., 1999). In my experiments, *Tbx5* is inactivated in cells of the prospective forelimb at early limb induction stages, E9-E9.5, using the *Prx1Cre* transgene. As a result, *Fgf10* is never expressed and a morphological limb bud is never formed, demonstrating that *Tbx5* is required to initiate *Fgf10* expression in cells of the prospective forelimb. These results are consistent with data from inactivation of *Tbx5* in all the cells of the developing mouse embryo and with *in vitro* data that have shown the presence of *Tbx5* binding sites in the promoter of *Fgf10* and that this promoter is *Tbx5* responsive (Agarwal et al., 2003). My analysis of *Pea3* and *Hoxb9* expression patterns demonstrated that of LPM patterning is intact in the absence of the forelimbs. TUNEL staining of mutant embryos indicated that as a consequence of the failure to establish the positive

feedback loop of *Fgf* signaling between the limb mesenchyme and overlying ectoderm leads to programmed cell death of the prospective forelimb bud. Together, these data establish *Tbx5* in a genetic hierarchy essential for forelimb initiation (Fig.42). Although we know that *Fgf10* is downstream of *Tbx5*, factors that lie upstream of *Tbx5* have remained elusive. *Tbx5* may be expressed in the LPM as a result to an axial cue such as Wnt2b.

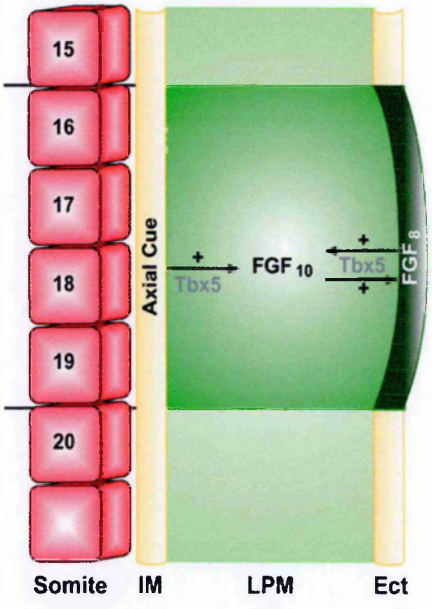

Figure 42. A model for *Tbx5* function in the developing limb bud. *Tbx5* is first expressed as limb bud initiation commences in response to axial cues. *Tbx5* is acting genetically upstream of *Fgf10* and is required for *Fgf10* expression in the limb mesenchyme. Later, *Tbx5* is also required for the positive inductive loop between *Fgf8*, expressed by cells in the AER, and *Fgf10*, expressed by cells of the distal mesenchyme.

1.2 *Tbx5* is required for formation of all skeletal elements of the limb

A striking observation of conditional knock-out of *Tbx5* in limb mesenchyme is the complete absence of all the elements of the appendicular skeleton. *Tbx5* is therefore required for the formation of the clavicle and scapula of the pectoral girdle in addition to the skeletal elements of the limb proper. This phenotype is more severe than that observed in the forelimb of *Fgf10* null mice. This

indicates that *Tbx5* has a broader influence on forelimb development than *Fgf10* and is absolutely required for the formation of all limb elements. Skeletal elements of the limb proper and most of the pectoral girdle are formed from lateral plate tissue where *Tbx5* is normally expressed. However, the proximal portion of the scapula blade is derived from the somites that lie medial and adjacent to the forelimb (Burke, 2000; Huang et al., 2000). *Tbx5* expression is never detected in the somites and is not present in the scapula precursors that are somite-derived. Following limb ablation in the chick, the somite-derived hypaxial myoblasts that form the limb musculature, are never recruited to the limb field (Gumpel-Pinot et al., 1984). By extension, the most likely explanation for the loss of the proximal portion of the scapula in $Tbx5^{lox/lox}$;*Prx1Cre* embryos is that, following deletion of *Tbx5* in the limb mesenchyme and the failure of early limb bud formation, the somite-derived non-*Tbx5*-expressing, scapula precursors are not recruited into the limb field.

1.3 Different mechanisms of *Tbx5* action are suggested between lower and higher vertebrates

Development of the zebrafish pectoral fin involves the directed migration and condensation of lateral plate mesodermal cells to the future limb-bud-forming region (Ahn et al., 2002). Recently, the requirement of *tbx5* for the formation of the pectoral fin in zebrafish has been demonstrated using morpholino antisense oligonucleotides to knock-down *tbx5* function (Ahn et al., 2002; Garrity et al., 2002). In *tbx5* morpholino-injected embryos, *tbx5* expression is normally initiated. However, LPM cells are loosely organized and remain dispersed and pectoral fins fail to form. However, in higher vertebrates, cells in the LPM destined to form the limbs do not exhibit a similar migration (Saunders et al.,

1957; Saunders et al., 1959; Searls, 1967; Searls and Janners, 1969). The only migratory cells that contribute to the limbs are the myoblasts which derive from the somites and not from the LPM. Although my results and those of Ahn et al. are phenotypically similar, in that embryos lacking *Tbx5* function fail to form a forelimb, my results demonstrate a different mechanism for *Tbx5* action. While in lower vertebrates *tbx5* may have a role in directed migration of limb precursor cells, in higher vertebrates *Tbx5* is required for the induction of *Fgf10*, essential for limb bud initiation.

1.4 Tbx5 is required for continued limb outgrowth and patterning

My misexpression experiments in the chick demonstrate that *Tbx5* is not only required for limb initiation but is also required at later stages of limb development for continued outgrowth and patterning. *Fgf10* expressed in the lateral plate mesoderm is initially required for the induction of *Fgf8* in cells of the nascent AER (Ohuchi et al., 1997; Yonei-Tamura et al., 1999). *Fgf8* expressed by cells of the AER is required, in turn, for the maintenance of *Fgf10* in distal mesenchyme underlying the AER. Following AER formation, a positive feedback loop is established between *Fgf8*-expressing cells in the AER and cells of the distal mesenchyme expressing *Fgf10* (Ohuchi et al., 1997). Knock-down of *Tbx5* function by misexpression of dominant-negative forms of the protein, leads to downregulation of *Fgf10* and disruption of the AER. The AER is induced but consequently, it regresses. In cases of lower levels of infection with dominant-negative *Tbx5* constructs, AER cells are present in a flattened area, reminiscent of an AER at earlier stages, suggesting a failure of AER maturation. These observations strongly suggest a perturbation of the *Fgf8/Fgf10* positive feedback loop and are consistent with a requirement for *Tbx5* in the AER-

mediated maintenance of *Fgf10* expression in the distal mesenchyme at later stages of development. This role for Tbx5 can be placed within our current models of limb outgrowth (Fig.42). A direct, positive regulatory relationship between a T-box gene and a *Fgf* gene has previously been demonstrated between *brachyury* and *eFgf* during mesoderm induction in *Xenopus* (Schulte-Merker and Smith, 1995). My results suggest that this regulatory relationship has been conserved and reused in the context of the limb. Following misexpression of Tbx5 dominant-negative forms, while *Fgf8* is downregulated in the AER, the expression of its receptor *Fgfr1*, expressed by mesodermal cells, is upregulated. The effect of *Tbx5* knock-down on *Fgfr1* expression is presumably indirect. However, it may uncover a negative auto-regulatory loop for *Fgfr1* expression. In this scenario, ligand binding and *Fgf* signaling pathway activation, could lead to repression of receptor expression. Following misexpression of dominant-negative forms of *Tbx5*, downregulation of *Fgf10* in the mesenchyme and *Fgf8* (the *Fgfr1* ligand) in the ectoderm, results in limited binding and pathway activation. This could lead to the break-down of the Fgfr1 negative auto-regulatory loop and can increased the levels of *Fgfr1* transcripts (Fig.43).

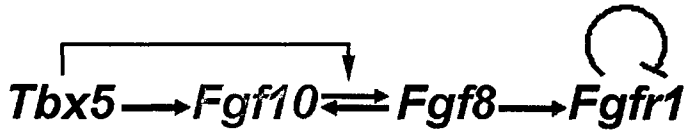

Figure 43. Model for *Tbx5* function and *Fgf* signaling in the developing limb bud. *Tbx5* is required for the induction of *Fgf10* and for the maintenance of the *Fgf8/Fgf10* positive feedback loop. A negative auto-regulatory loop may function in the case of Fgfr1. Fgf8 binding to Fgfr1 and activation of the Fgf signaling pathway, may lead to repression of Fgfr1 expression. Knock-down of Tbx5 function results in *Fgf10* downregulation, perturbation of the positive feedback

loop and downregulation of *Fgf8*. Limited ligand and pathway activation could result in the break-down of the negative auto-regulatory loop and increased *Fgfr1* transcripts.

1.5 A molecular context into understanding HOS deformities

In human, mutations in *TBX5* are associated with Holt-Oram syndrome. Disruption of the *Fgf8/Fgf10* epithelial-mesenchymal positive feedback loop would lead to severe truncation of limb outgrowth and could explain the reduction deformities observed in HOS which, in the most severe cases, result in phocomelia, an almost complete absence of all elements of the limb. The more commonly observed characteristic features of HOS phenotypes are deformities of anterior elements of the limb, such as the thumb, thenar elements or radius. Following knock-down of *Tbx5* by misexpression of dominant-negative constructs, I observed defects in AER formation and maintenance, primarily in the anterior of the infected wing bud. Loss of *Fgf8* expression is observed in the anterior AER and a concomitant failure of *Fgf*-mediated signaling to the underlying mesenchyme is indicated by the down-regulation of *Msx1* expression in the anterior-distal mesenchyme. The reduction of anterior mesenchyme is also demonstrated by the loss of *HoxC4* and *Lhx9* expression in the anterior of the limb. Misexpression of dominant-negative forms of *Tbx5* generated a phenotype consistent with the characteristic abnormalities presented in human HOS patients. Interestingly, following misexpression of dominant-negative forms of *Tbx5 Fgfr1* transcripts are elevated especially in the anterior. Transgenic mice in which Fgfr1 function is elevated throughout the limb bud, exhibit preaxial polydactyly with iterations of digit I (the equivalent of the thumb in human) (Hajihosseini et al., 2004), a complimentary phenotype to that observed in HOS patients. Future studies will be necessary to determine the exact role of Fgfr1 in the formation of anterior limb elements and whether

there is any connection between the phenotypes observed following disruption of *Tbx5* and Fgfr1 function.

Misexpression of full length Tbx5 or constructs containing the T-domain of Tbx5 fused to the VP16 transcriptional activation produced complimentary phenotypes to those observed with dominant-negative constructs. Therefore, the effects on markers in the anterior limb ectoderm and mesenchyme provides a molecular context to understand the genesis of HOS deformities. Unfortunately, I was unable to analyse the skeletal deformities that would result following misexpression of dominant-negative or dominant-active *Tbx5* forms, because continued spread of the replication-competent retrovirus produces heart defects that lead to embryonic lethality.

1.6 *Tbx5* is required for sternum formation

An interesting observation of the conditional knock-out of *Tbx5*, is the complete absence of the sternum. In the mouse, the sternum is first evident around E12.0 dpc. Studies in the chick showed that the sternum originates independently from the ribs and the pectoral girdle (Fell, 1939). In the mouse, the sternum precursors appear as two bands of mesenchymal condensations in the dorso-lateral body wall that is close to the forelimb region (Chen, 1952a; Chen, 1952b). These bands lengthen in a caudal direction, move towards each other, and eventually fuse in the ventral midline. The structure that is formed is then attached to seven pairs of ribs. While *Prx1Cre* transgene expression in the developing limbs has been determined, further studies will be required to characterize the spatial and temporal expression of the *Prx1Cre* transgene in the body wall. This study, has focused on the role of *Tbx5* in the developing limbs. Future studies will be necessary to characterize the normal expression of

Tbx5 in the body wall and sternum precursors and to provide a temporal progression of the sternum defects.

1.7 Tbx5 acts as a transcriptional activator

My *in vitro* luciferase assays, demonstrated that *Tbx5* can act as a transcriptional activator. In addition, deletion of the C-terminal domain of *Tbx5* resulted in abolishment of its ability to activate reporter gene expression showing that the transactivation domain lies in this part of the Tbx5 protein. Misexpression of both types of dominant-negative *Tbx5* constructs produced essentially identical results and are consistent with defects observed due to haploinsufficiency of *TBX5* in HOS (Basson et al., 1997; Li et al., 1997) and defects in the *Tbx5* heterozygous knock-out mice (Bruneau et al., 2001). In the converse experiment, misexpression of full length *Tbx5* or constructs containing the T-domain of Tbx5 fused to the VP16 transcriptional activation produced identical results. Moreover, the phenotypes observed, compliment those observed with dominant-negative constructs. Together, my *in vitro* and *in vivo* observations support the conclusion that *Tbx5* is acting as a transcriptional activator in the developing forelimb. My results are consistent with reports demonstrating that *Tbx5* can transactivate expression from constructs containing a portion of the *Fgf10* promoter (Agarwal et al., 2003).

1.8 *Tbx5* and *Tbx4* have similar roles during limb development

Following misexpression of a putative dominant-negative form of *Tbx4* in the developing hindlimb, the anterior limb mesenchyme marker *Lhx9* is downregulated and *Fgf8* positive cells are expressed in a broad domain reminiscent of earlier stage expression pattern, showing a retardation in the

maturation of the AER. These phenotypes are strikingly similar with those of the *Tbx5*-dominant negative injected wings and may suggest that *Tbx4* has similar roles to *Tbx5* during limb outgrowth. *Tbx4* may, as we have shown for *Tbx4*, be important for the maintenance of the *Fgf8/Fgf10* positive feedback loop. In this experiment a large portion of the Tbx4 protein has been replaced by the engrailed repressor domain. It is possible that I have removed residues of the Tbx4 protein that distinguish it from the closely related Tbx5 protein. However, genetic data in the mouse from others in the lab, have demonstrated that *Tbx4* and *Tbx5* play similar roles in the initiation of outgrowth of the developing hindlimb and forelimb respectively (Minguillon, Del Buono and Logan, *Dev. Cell* in press). In these experiments, the conditional knock-out allele of *Tbx5,* the Cre-deleter line (Prx1Cre) and a transgenic line in which *Tbx4* is ectopically expressed in the forelimb (*Prx1-Tbx4*) are combined. In this way, *Tbx5* is replaced with *Tbx4* in the forelimb. *Tbx4* is able to rescue the 'no-limb phenotype' following deletion of *Tbx5.* The rescued limb has the molecular profile and the morphology of a forelimb, showing that, *Tbx4* and *Tbx5* do not specify limb-type identity and have a common role in limb initiation. Taken together, these results suggest that *Tbx4* and *Tbx5* may have similar roles during initiation of limb outgrowth and at later stages during limb patterning events.

PART TWO

'The role of *Tbx3* in limb development'

2. The role of *Tbx3* in limb development

I have used misexpression strategies in the chick to study the function of Tbx3 in the developing limb.

2.1 *Tbx3* acts as a transcriptional repressor in the limb

My *in vitro* luciferase experiments demonstrate that Tbx3 can act as a transcriptional repressor *in vitro* and that the repressor domain lies in the C-terminal part of the Tbx3 protein (Fig.22B). These results are consistent with data showing that human *TBX3* is able to act as a transcriptional repressor in many cell types (Carlson et al., 2001). Misexpression of Tbx3 and $Tbx3^{EN}$ in the forelimb region produces identical phenotypes. In the converse experiment, misexpression of $Tbx3^{VP16}$ generates the opposite phenotype. Taken together, data from *in vitro* and *in vivo* experiments strongly suggest that Tbx3 acts as a transcriptional repressor in the developing limb bud.

2.2 *Tbx3* participates in mechanisms that position the limb along the body axis

Following misexpression of *Tbx3*, molecular markers of the forelimb-forming region of the LPM are initially expanded rostrally. This expansion is followed by a shift in limb position. My fate mapping shows that the altered contribution to the limbs is not simply explained by migration of limb bud precursors. Cells of the flank, rostral to the limb, which would not normally contribute to the limb, now become incorporated into the limb. Furthermore, cells that normally form posterior limb mesenchyme now no longer contribute to the limb. Strikingly, these cells had presumably initially expressed *Tbx5*, a gene required and apparently sufficient for limb initiation (Agarwal et al., 2003; Ahn et al., 2002; Ng

et al., 2002; Rallis et al., 2003; Takeuchi et al., 2003). Interestingly, the size of the shifted limb is the same as that of the normal limb suggesting that a mechanism, yet to be determined, is functioning to regulate limb size. An attractive possibility is that the width of the limb bud may be controlled by the range of signaling from the polarizing region at the posterior limb mesenchyme. Other members of the T-box gene family have been reported to alter the extent of the limb but limb-shift phenotypes similar to those I observed following *Tbx3*-misexpression are never generated. *Tbx18* is expressed in the limbs from st.17 HH. When *Tbx18* is misexpressed in the presumptive wing bud region, an anterior expansion of the wing bud associated with enhanced expression of *Tbx5* and *SnR* is observed. The wing bud is extended rather than shifted in position. This extension is however only transient and at later stages limbs are morphologically normal (Tanaka and Tickle, 2004). Brachyury, the prototypical T-box transcription factor, is expressed in the LPM at the onset of limb formation and at later stages of limb development, in the distal limb mesenchyme that lies underneath the AER. Misexpression of *Brachyury* in the chick resulted in anterior expansion of the AER (Liu et al., 2003). Skeletal abnormalities include anterior digit duplications, posterior transformations of anterior digits and rarely the anterior-most metatarsal was thickened. Significantly, in no cases did misexpression of these genes result in any alterations in limb position along the rostro-caudal axis of the embryo. Misexpression of *Tbx5*-activator forms demonstrates an anterior expansion in the ectoderm and mesoderm of the injected wing (Rallis et al., 2003). However, the expansions described, are evident at later stages of limb development than those observed with *Tbx3* and a shift in axial limb position is not observed. I have also performed injections with dominant-negative and dominant-active

forms of *Tbx15* and a limb-shift phenotype is not generated (Fig.34). Finally, *Tbx2* the closely related gene to *Tbx3* is expressed in a similar pattern to *Tbx3.* In addition *Tbx2* has been reported to act as a transcriptional repressor like *Tbx3.* Interestingly, *Tbx2* misexpression does not result in a limb-shift phenotype but dramatically affects limb size (Fig.37). I conclude that the phenotypes observed following misexpression of *Tbx3* forms, are generated by specifically manipulating *Tbx3* function.

2.3 Hox genes in limb position

Tbx3 misexpression does not affect the pattern of axial Hox gene expression. A role for *Hox* genes in limb positioning is suggested largely by the nested expression patterns of various *Hox* genes and by the *Hoxb5* knock-out mice which exhibit a unilateral or bilateral rostral shift in axial forelimb position (Rancourt et al., 1995). However, the phenotype in *Hoxb5*$^{-/-}$ mice differs in several aspects from that obtained with *Tbx3* or *Tbx3*^{EN} misexpression. In *Hoxb5*$^{-/-}$ mice, alterations in the axial skeleton are observed, namely anteriorizing homeotic transformation of the cervico-thoracic vertebrae from C6 through T1. The clavicle in *Hoxb5* mutant mice, retains a medial articulation with its normal target, the sternum, resulting in a V-shaped shoulder girdle. Furthermore, in *Hoxb5* mutants, neurons from the brachial plexus that normally enter the medial limb originate from the spinal cord at the normal axial level but instead enter the posterior limb mesenchyme. In *Tbx3*-shifted limbs, neurons that innervate the limb are derived from the brachial plexus at ectopic rostral sites. The alteration in limb position in the *Hoxb5*$^{-/-}$ mice is therefore associated with a transformation of the entire axial skeleton. In contrast, the limb-shift

phenotype generated by misexpression of *Tbx3* is restricted to the developing limbs and axial patterning is not affected.

The *Hox9* paralogues have been implicated in the specification of limb position and limb-type identity through a correlation in their expression patterns and the position of the developing forelimb and hindlimb (Cohn et al., 1997). However, in Hox gene misexpression and deletions experiments reported to date, no alteration in limb position independent of the axial skeleton has been observed. The absence of an effect of *Tbx3* on the expression of Hox9 paralogues is particularly significant because it shows that *Tbx3* may mediates its effects on limb position downstream or independently of any potential axial Hox code.

2.4 Normal limb patterning following misexpression of *Tbx3* forms

Tbx3 and the closely related gene *Tbx2* have been implicated in specifying posterior digit identity via *Shh* and *Bmp* signaling (Suzuki et al., 2004; Tumpel et al., 2002). In this study, following misexpression of *Tbx2* and *Tbx3* in the developing hindlimb, the expression pattern of *Bmp2* and *HoxD* genes are altered. These changes in gene expression are followed by apparent anterior transformations of posterior digits. I therefore analyzed the expression pattern of *Shh* and *Bmp2* in the shifted limb. However, the expression of these genes is unaffected in our experiments and in skeletal preparations of *Tbx3*-injected embryos, digit identity is unchanged. I also performed injections of *Tbx3* in the hindlimb-forming region and obtained the same result as seen in forelimbs: the injected hindlimb is shifted rostrally, while the digit array is unaffected.

One difference between my experiments and those of Suzuki et al. is the timing of the viral injections; I performed our injections at st.8-10 while in Suzuki et al. the virus was injected at st. 11-12. Injections at later stages may account for

their failure to generate limb shifts. Nevertheless, it is not clear why different effects on limb patterning were observed in these two sets of experiments. Suzuki et al., claim that *Tbx2* and *Tbx3* are downstream of Bmps. Nevertheless, in *Bmp2/Bmp7* double mutants *Tbx2* and *Tbx3* are normally expressed. Furthermore, the authors suggest a model in which *Tbx2* and *Tbx3* regulate digit identity through Bmp signaling. However, *Bmp2* conditional knock-out mice exhibit syndactyly of digit 2 and 3, consistent for the role of Bmps in regulating interdigital cell death but not digit identity. *Bmp4* conditional knock–out mice, have normal digit array while *Bmp7*-deficient mice do not have any limb phenotype. Double knock out of *Bmp2/7* and *Bmp2/4* does not disrupt digit identity but instead proximal limb elements are deleted. Preliminary results have also shown that the triple knock-out *Bmp2/4/7* mice do not exhibit any changes in digit identity (C. Tabin communication of unpublished results). These data strongly suggest that Bmps do not have a role in the regulation of digit identity in contrast to the model suggested by Suzuki et al. Finally, mice in which *Tbx3* has been inactivated do not exhibit any changes in digit identity (Davenport et al., 2003). Recent data have shown that mice in which *Tbx2* has been inactivated do not exhibit any disruption in digit identity (Harrelson et al., 2004)

2.5 A genetic interplay between *Tbx3*, *dHand* and *Gli3* prior to *Shh* expression

Some of the earliest changes observed following misexpression of *Tbx3* forms are in the expression patterns of *dHand* and *Gli3*. At these stages, *Gli3* is acting as a repressor (Wang et al., 2000), while *dHand* is shown to be a transcriptional activator (Dai and Cserjesi, 2002; Dai et al., 2002). Misexpression of *Tbx3* leads

to an expansion or failure of repression of the *dHand* expression domain, potentially through an interaction between *Tbx3* and *Gli3* (Fig.44). Since I have demonstrated both *in vivo* and *in vitro* that *Tbx3* acts as a transcriptional repressor we predict that it is normally repressing *Gli3* expression in the future posterior limb mesenchyme. Repression by *Tbx3* could be responsible for generating the anterior-to-posterior graded expression of *Gli3* in the developing limb primordium. This model is consistent with the observation in *Tbx3* mutant mice that *dHand* is downregulated in the forelimbs and absent in the hindlimbs which subsequently leads to a disruption in *Shh* expression. My model would predict that downregulation of *dHand* is due to high *Gli3* expression that is no longer restricted to the anterior limb primordium and expands to the posterior (Fig.44).

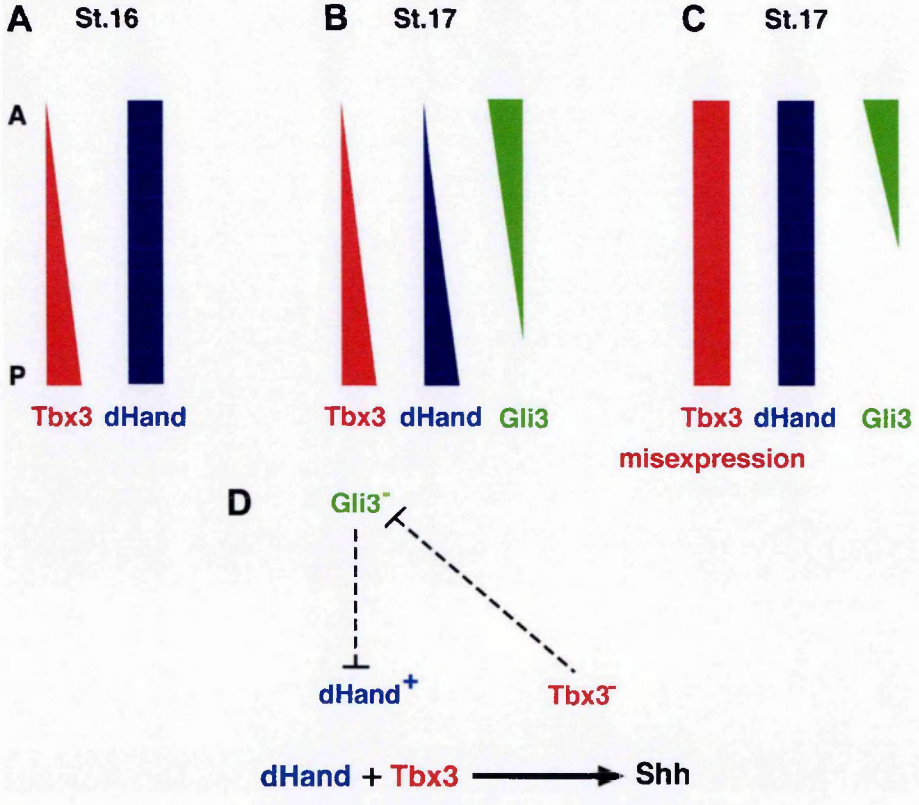

Figure 44. Models for the interactions between *dHand*, *Gli3* and *Tbx3*, in the limb forming-region at stages prior to *Shh* expression, that refine limb position along the rostro-caudal axis of the embryo. **A**. At st.16, *Tbx3* is expressed throughout the limb-forming region but expression is

more robust in the future posterior limb mesenchyme. *dHand* is expressed throughout the limb-forming region. **B.** At st. 17, *Gli3* is expressed throughout the limb mesenchyme with higher levels in the anterior. *dHand* expression is restricted posteriorly. **C.** Ectopic expression of *Tbx3* in more anterior regions leads to a repression of *Gli3*, resulting in a de-repression of *dHand* and expansion of its expression domain. **D.** The genetic antagonism between *dHand* and *Gli3* that positions the future ZPA is mediated through *Tbx3*. – and + symbols indicate the transcriptional repressor and activator function of each protein, respectively. *Tbx3* and *dHand* co-operate to lead to induction of *Shh* and thereby specify the position of the ZPA and posterior limb mesenchyme. A=anterior, P=posterior

Misexpression of $Tbx3^{VP16}$ produces the opposite phenotype to that obtained with Tbx3 and $Tbx3^{EN}$ such that the limb forms in a more caudal position than normal. *Gli3* expression is upregulated and expanded caudally in the $Tbx3^{VP16}$ injected limbs, lending further support to a model in which *Tbx3* normally functions to restrict *Gli3* to the anterior mesenchyme. As a consequence of this *Gli3* expansion, the *dHand* expression domain is shifted caudally. In contrast, in Tbx3- and $Tbx3^{EN}$-injected embryos, disruption of the normal repression of *dHand* by *Gli3* resets the rostro-caudal position of the ZPA to a more rostral position and this ultimately results in the limb shift phenotype. In $Tbx3^{VP16}$ injected embryos, de-repression of *Gli3* shifts the expression domain of *dHand* and this ultimately leads to the ZPA forming more caudally. My data demonstrate that the signals required for pre-patterning the A-P axis of the limb and setting the position of the ZPA can influence the position of the limb along the rostro-caudal axis of the embryo.

2.6 *Gli3* and limb positioning

I predict that the effects of Gli3ZnF-VP16 on *dHand* and *Tbx3* are caused by a disruption of endogenous Gli^R activity. Misexpression of Gli3ZnF-VP16 leads to

the expansion of *Tbx3* and *dHand* expression domains rather than the induction of ectopic patches of expression. This may indicate a non-cell autonomous action of *Gli3* on *dHand* and presumably also on *Tbx3* since Gli3ZnF-VP16 is misexpressed throughout the limb mesenchyme. A regulatory relationship between *Gli3* and *Tbx3* has been demonstrated during lung organogenesis (Li et al., 2004). *Tbx3* is normally expressed in the mouse lung in the presence of *Shh*. In this environment, *Gli3* acts as an activator of *Tbx3* transcription. In $Shh^{-/-}$ animals, where *Gli3* acts as a repressor, *Tbx3* transcripts are significantly reduced. However, in $Shh^{-/-}/Gli3^{-/-}$ animals, de-repression of *Tbx3* is observed and *Tbx3* expression is, at least partially, restored (Li et al., 2004). These results, together with my own, suggest that regulatory relationships between *Tbx3* and *Gli3* may exist broadly during embryogenesis.

My data implicate *Gli3* in a genetic network that can influence limb position, yet mice mutant for *Gli3* (*Extra toes*, Xt^J), are not reported to exhibit any shift in axial limb position (Buscher et al., 1997; Buscher et al., 1998; Hui and Joyner, 1993; Litingtung et al., 2002). In Xt^J/Xt^J mice (that lack all Gli3 activity), *dHand* is expressed throughout the limb and subsequently *Shh* is expressed ectopically in the anterior limb mesenchyme. Misexpression of *dHand* alone, at limb bud stages, is capable of inducing *Shh* expression but only in the anterior limb mesenchyme rather than medial locations (Charite et al., 2000; Fernandez-Teran et al., 2000). These results suggest that anterior and posterior limb mesenchyme may express a 'licensing factor' required together with *dHand* for the induction of *Shh* and that this factor is absent from the medial limb mesenchyme. *Tbx3* is expressed in two stripes in the anterior and posterior limb mesenchyme at later stages of limb development (Fig.18H) and may normally

act as such a factor. A requirement for *Tbx3* to establish or re-set the domain of *Shh*-expressing cells in the ZPA may also explain why no limb shift phenotype is observed in Xt^J/Xt^J mice. *Tbx3* expression is not expanded in Xt^J/Xt^J mice (Tumpel et al., 2002). Without the presence of both *Tbx3* and *dHand*, the position of the limb is not altered. In *Tbx3* misexpression experiments, however, *Tbx3* can repress *Gli3* and this leads to an expansion of *dHand*. The co-expression of *Tbx3* and *dHand* can, in turn, 'license' ectopic *Shh* expression, which in turn, alters the position of the limb (Fig.44).

Mice in which *Tbx3* is inactivated and humans with UMS who are haploinsufficient for *TBX3* are not reported to exhibit any shift in axial limb position. This is consistent with the model I propose for the role of *Tbx3* in the early limb bud. In $Tbx3^{-/-}$ mouse embryos, the expression domains of *dHand* and *Shh* are down-regulated or even eliminated (Davenport et al., 2003) consistent with *Tbx3* being required for their normal expression. This finding supports my conclusions that, although not strictly required to fix limb position, *Tbx3* is an important component of the signals establishing the position of the domain of *Shh* expressing cells that comprise the ZPA in the posterior limb.

2.7 The *Luxate mutant*

Luxate (*Lx*) is a spontaneous, dominant mutation in the mouse, mapped to the proximal region of chromosome 5 (Lane, 1967). *Lx* mutant mice exhibit preaxial polydactyly, which is restricted to the hindlimbs. Homozygotes show polydactyly, oligodactyly, hemimelia with shortened tibias, and sacralization of the 26^{th} vertebra. Most importantly, *Luxate* mutants show a rostral shift in the axial position of the hindlimbs. Analysis using molecular markers showed that

dHand and *Gli3* are altered. *dHand* is expanded anteriorly while the posterior border of *Gli3* expression has moved rostrally. In *Lx* embryos, the *Shh* positive cells appear in more rostral position. The authors conclude that the molecular mechanism that positions the ZPA might relate with the positioning of the hindlimbs. The striking similarities between the phenotypes of *Lx* and *Tbx3*-injected limbs suggest a possible link between *Lx* and *Tbx3. Lx* and *Tbx3* are localized on the same chromosome (mouse chromosome 5), however *Lx* mutation has been mapped 22cM from the centrosome, while *Tbx3* is located 65cM from the centrosome. Nevertheless, genetic interaction between *lx* and *Tbx3* is not excluded. *Lx* mutation could be located in a regulatory region that may influence *Tbx3*. Alternatively, *Lx* may be located in a region that encodes for a factor participating in the same or parallel genetic pathway to *Tbx3.*

2.8 Roles of Gli3 repressor and activator function in the patterning of the developing limb

Gli3ZnF-VP16 injected embryos exhibit a rostral shift in axial limb. I suggest that the shift is a result of a knock-down of $Gli3^{R}$ activity during limb initiation stages. Nevertheless, the shifted limbs are normally patterned. There is no ectopic *Shh* expressing cells in the anterior limb mesenchyme and no sign of polydactyly is observed. In vertebrates *in vitro* and *in vivo* experiments have shown the requirement of both the activator ($Gli3^{FL}$) and repressor function of Gli3 ($Gli3^{R}$) in the context of the developing neural tube (Bai et al., 2004; Lei et al., 2004; Persson et al., 2002). *In vitro* experiments in the mouse have shown that both $Gli3^{FL}$ and $Gli3^{R}$ are present in the limb. $Gli3^{R}$ forms an anterior-to-posterior concentration gradient, while $Gli3^{FL}$ a posterior-to-anterior gradient. Nevertheless, the requirement for both activator and repressor forms for the

patterning of the developing limbs is not clear. Production of the $Gli3^{FL}$ form in the presence of *Shh* could be a part of a de-repression mechanism for downstream targets. Such a model (the de-repression model) can explain the absence of AP defects in Gli3ZnF-VP16 limbs since the formation of an anterior-to-posterior gradient of $Gli3^{R}$ is the crucial event while the full-length (activator) form of Gli3 does not play an important role in AP patterning.

3. Perspectives

Previous experiments in which *Tbx5* is misexpressed in the developing hindlimb suggested a role in limb-type specification. In this study, using a conditional knock-out approach in the mouse a role for *Tbx5* in limb initiation is established. However, the absence of all limb elements does not indicate a role for *Tbx5* at later stages of limb development. By misexpressing dominant-negative and dominant-active forms of *Tbx5* in the developing chick wing, I reveal the requirement for *Tbx5* during limb outgrowth and patterning events. In addition, the phenotypes obtained provide a molecular context into understanding HOS deformities.

Tbx3 gene deletion studies in the mouse showed a requirement of this gene in normal limb patterning. However, using misexpression experiments in the chick, a new role for *Tbx3* in positioning the limbs along the rostro-caudal axis of the embryo is suggested. Using a range of experimental approaches different gene functions have been revealed and steps to understanding the role of T-box genes in limb development and disease have been made.

REFERENCES

Agarwal, P., Wylie, J. N., Galceran, J., Arkhitko, O., Li, C., Deng, C., Grosschedl, R. and Bruneau, B. G. (2003). Tbx5 is essential for forelimb bud initiation following patterning of the limb field in the mouse embryo. *Development* **130**, 623-33.

Agulnik, S. I., Garvey, N., Hancock, S., Ruvinsky, I., Chapman, D. L., Agulnik, I., Bollag, R., Papaioannou, V. and Silver, L. M. (1996). Evolution of mouse T-box genes by tandem duplication and cluster dispersion. *Genetics* **144**, 249-54.

Ahn, D. G., Kourakis, M. J., Rohde, L. A., Silver, L. M. and Ho, R. K. (2002). T-box gene tbx5 is essential for formation of the pectoral limb bud. *Nature* **417**, 754-8.

Alexander, M. C., Lomanto, M., Nasrin, N. and Ramaika, C. (1988). Insulin stimulates glyceraldehyde-3-phosphate dehydrogenase gene expression through cis-acting DNA sequences. *Proc Natl Acad Sci U S A* **85**, 5092-6.

Arman, E., Haffner-Krausz, R., Gorivodsky, M. and Lonai, P. (1999). Fgfr2 is required for limb outgrowth and lung-branching morphogenesis. *Proc Natl Acad Sci U S A* **96**, 11895-9.

Bai, C. B., Stephen, D. and Joyner, A. L. (2004). All mouse ventral spinal cord patterning by hedgehog is Gli dependent and involves an activator function of Gli3. *Dev Cell* **6**, 103-15.

Barrow, J. R., Thomas, K. R., Boussadia-Zahui, O., Moore, R., Kemler, R., Capecchi, M. R. and McMahon, A. P. (2003). Ectodermal Wnt3/beta-catenin signaling is required for the establishment and maintenance of the apical ectodermal ridge. *Genes Dev* **17**, 394-409.

Basson, C. T., Bachinsky, D. R., Lin, R. C., Levi, T., Elkins, J. A., Soults, J., Grayzel, D., Kroumpouzou, E., Traill, T. A., Leblanc-Straceski, J. et al. (1997). Mutations in human TBX5 [corrected] cause limb and cardiac malformation in Holt-Oram syndrome. *Nat Genet* **15**, 30-5.

Basson, C. T., Huang, T., Lin, R. C., Bachinsky, D. R., Weremowicz, S., Vaglio, A., Bruzzone, R., Quadrelli, R., Lerone, M., Romeo, G. et al. (1999). Different TBX5 interactions in heart and limb defined by Holt-Oram syndrome mutations. *Proc Natl Acad Sci U S A* **96**, 2919-24.

Bellusci, S., Grindley, J., Emoto, H., Itoh, N. and Hogan, B. L. (1997). Fibroblast growth factor 10 (FGF10) and branching morphogenesis in the embryonic mouse lung. *Development* **124**, 4867-78.

Birk, O. S., Casiano, D. E., Wassif, C. A., Cogliati, T., Zhao, L., Zhao, Y., Grinberg, A., Huang, S., Kreidberg, J. A., Parker, K. L. et al. (2000). The LIM homeobox gene Lhx9 is essential for mouse gonad formation. *Nature* **403**, 909-13.

Bongers, E. M., Duijf, P. H., van Beersum, S. E., Schoots, J., Van Kampen, A., Burckhardt, A., Hamel, B. C., Losan, F., Hoefsloot, L. H., Yntema, H. G. et al. (2004). Mutations in the human TBX4 gene cause small patella syndrome. *Am J Hum Genet* **74**, 1239-48.

Bose, J., Grotewold, L. and Ruther, U. (2002). Pallister-Hall syndrome phenotype in mice mutant for Gli3. *Hum Mol Genet* **11**, 1129-35.

Boulet, A. M., Moon, A. M., Arenkiel, B. R. and Capecchi, M. R. (2004). The roles of Fgf4 and Fgf8 in limb bud initiation and outgrowth. *Dev Biol* **273**, 361-72.

Brummelkamp, T. R., Kortlever, R. M., Lingbeek, M., Trettel, F., MacDonald, M. E., van Lohuizen, M. and Bernards, R. (2002). TBX-3, the gene mutated in

Ulnar-Mammary Syndrome, is a negative regulator of p19ARF and inhibits senescence. *J Biol Chem* **277**, 6567-72.
Bruneau, B. G., Logan, M., Davis, N., Levi, T., Tabin, C. J., Seidman, J. G. and Seidman, C. E. (1999). Chamber-specific cardiac expression of Tbx5 and heart defects in Holt-Oram syndrome. *Dev Biol* **211**, 100-8.
Bruneau, B. G., Nemer, G., Schmitt, J. P., Charron, F., Robitaille, L., Caron, S., Conner, D. A., Gessler, M., Nemer, M., Seidman, C. E. et al. (2001). A murine model of Holt-Oram syndrome defines roles of the T-box transcription factor Tbx5 in cardiogenesis and disease. *Cell* **106**, 709-21.
Burke, A. C. (2000). Hox genes and the global patterning of the somitic mesoderm. *Curr Top Dev Biol* **47**, 155-81.
Burke, A. C., Nelson, C. E., Morgan, B. A. and Tabin, C. (1995). Hox genes and the evolution of vertebrate axial morphology. *Development* **121**, 333-46.
Buscher, D., Bosse, B., Heymer, J. and Ruther, U. (1997). Evidence for genetic control of Sonic hedgehog by Gli3 in mouse limb development. *Mech Dev* **62**, 175-82.
Buscher, D., Grotewold, L. and Ruther, U. (1998). The XtJ allele generates a Gli3 fusion transcript. *Mamm Genome* **9**, 676-8.
Capdevila, J., Tsukui, T., Rodriquez Esteban, C., Zappavigna, V. and Izpisua Belmonte, J. C. (1999). Control of vertebrate limb outgrowth by the proximal factor Meis2 and distal antagonism of BMPs by Gremlin. *Mol Cell* **4**, 839-49.
Carlson, H., Ota, S., Campbell, C. E. and Hurlin, P. J. (2001). A dominant repression domain in Tbx3 mediates transcriptional repression and cell immortalization: relevance to mutations in Tbx3 that cause ulnar-mammary syndrome. *Hum Mol Genet* **10**, 2403-13.
Carreira, S., Dexter, T. J., Yavuzer, U., Easty, D. J. and Goding, C. R. (1998). Brachyury-related transcription factor Tbx2 and repression of the melanocyte-specific TRP-1 promoter. *Mol Cell Biol* **18**, 5099-108.
Carreira, S., Liu, B. and Goding, C. R. (2000). The gene encoding the T-box factor Tbx2 is a target for the microphthalmia-associated transcription factor in melanocytes. *J Biol Chem* **275**, 21920-7.
Charite, J., McFadden, D. G. and Olson, E. N. (2000). The bHLH transcription factor dHAND controls Sonic hedgehog expression and establishment of the zone of polarizing activity during limb development. *Development* **127**, 2461-70.
Chen, J. M. (1952a). Studies on the morphogenesis of the mouse sternum. I. Normal embryonic development. *J Anat* **86**, 373-86.
Chen, J. M. (1952b). Studies on the morphogenesis of the mouse sternum. II. Experiments on the origin of the sternum and its capacity for self-differentiation in vitro. *J Anat* **86**, 387-401.
Chiang, C., Litingtung, Y., Harris, M. P., Simandl, B. K., Li, Y., Beachy, P. A. and Fallon, J. F. (2001). Manifestation of the limb prepattern: limb development in the absence of sonic hedgehog function. *Dev Biol* **236**, 421-35.
Chotteau-Lelievre, A., Dolle, P., Peronne, V., Coutte, L., de Launoit, Y. and Desbiens, X. (2001). Expression patterns of the Ets transcription factors from the PEA3 group during early stages of mouse development. *Mech Dev* **108**, 191-5.
Cohn, M. J., Izpisua-Belmonte, J. C., Abud, H., Heath, J. K. and Tickle, C. (1995). Fibroblast growth factors induce additional limb development from the flank of chick embryos. *Cell* **80**, 739-46.

Cohn, M. J., Patel, K., Krumlauf, R., Wilkinson, D. G., Clarke, J. D. and Tickle, C. (1997). Hox9 genes and vertebrate limb specification. *Nature* **387**, 97-101.

Collavoli, A., Hatcher, C. J., He, J., Okin, D., Deo, R. and Basson, C. T. (2003). TBX5 nuclear localization is mediated by dual cooperative intramolecular signals. *J Mol Cell Cardiol* **35**, 1191-5.

Crossley, P. H. and Martin, G. R. (1995). The mouse Fgf8 gene encodes a family of polypeptides and is expressed in regions that direct outgrowth and patterning in the developing embryo. *Development* **121**, 439-51.

Crossley, P. H., Minowada, G., MacArthur, C. A. and Martin, G. R. (1996). Roles for FGF8 in the induction, initiation, and maintenance of chick limb development. *Cell* **84**, 127-36.

Dai, Y. S. and Cserjesi, P. (2002). The basic helix-loop-helix factor, HAND2, functions as a transcriptional activator by binding to E-boxes as a heterodimer. *J Biol Chem* **277**, 12604-12.

Dai, Y. S., Cserjesi, P., Markham, B. E. and Molkentin, J. D. (2002). The transcription factors GATA4 and dHAND physically interact to synergistically activate cardiac gene expression through a p300-dependent mechanism. *J Biol Chem* **277**, 24390-8.

Davenport, T. G., Jerome-Majewska, L. A. and Papaioannou, V. E. (2003). Mammary gland, limb and yolk sac defects in mice lacking Tbx3, the gene mutated in human ulnar mammary syndrome. *Development* **130**, 2263-73.

De Moerlooze, L., Spencer-Dene, B., Revest, J., Hajihosseini, M., Rosewell, I. and Dickson, C. (2000). An important role for the IIIb isoform of fibroblast growth factor receptor 2 (FGFR2) in mesenchymal-epithelial signalling during mouse organogenesis. *Development* **127**, 483-92.

Deschamps, J., van den Akker, E., Forlani, S., De Graaff, W., Oosterveen, T., Roelen, B. and Roelfsema, J. (1999). Initiation, establishment and maintenance of Hox gene expression patterns in the mouse. *Int J Dev Biol* **43**, 635-50.

Dietrich, S., Abou-Rebyeh, F., Brohmann, H., Bladt, F., Sonnenberg-Riethmacher, E., Yamaai, T., Lumsden, A., Brand-Saberi, B. and Birchmeier, C. (1999). The role of SF/HGF and c-Met in the development of skeletal muscle. *Development* **126**, 1621-9.

Dobrovolskaia-Zavadskaia, N. (1927). Sur la modification spontanee dela queue che la suris nouveau-nee at sur l'existence d'un charactere (facteur) hereditaire 'non-viable'. *C.R.Seanc.Soc Biol* **97**, 114-116.

Dudley, A. T., Ros, M. A. and Tabin, C. J. (2002). A re-examination of proximodistal patterning during vertebrate limb development. *Nature* **418**, 539-44.

Echelard, Y., Epstein, D. J., St-Jacques, B., Shen, L., Mohler, J., McMahon, J. A. and McMahon, A. P. (1993). Sonic hedgehog, a member of a family of putative signaling molecules, is implicated in the regulation of CNS polarity. *Cell* **75**, 1417-30.

Eswarakumar, V. P., Monsonego-Ornan, E., Pines, M., Antonopoulou, I., Morriss-Kay, G. M. and Lonai, P. (2002). The IIIc alternative of Fgfr2 is a positive regulator of bone formation. *Development* **129**, 3783-93.

Fallon, J. F., Lopez, A., Ros, M. A., Savage, M. P., Olwin, B. B. and Simandl, B. K. (1994). FGF-2: apical ectodermal ridge growth signal for chick limb development. *Science* **264**, 104-7.

Fan, W., Huang, X., Chen, C., Gray, J. and Huang, T. (2004). TBX3 and its isoform TBX3+2a are functionally distinctive in inhibition of senescence and are overexpressed in a subset of breast cancer cell lines. *Cancer Res* **64**, 5132-9.
Fernandez-Teran, M., Piedra, M. E., Kathiriya, I. S., Srivastava, D., Rodriguez-Rey, J. C. and Ros, M. A. (2000). Role of dHAND in the anterior-posterior polarization of the limb bud: implications for the Sonic hedgehog pathway. *Development* **127**, 2133-42.
Francis, P. H., Richardson, M. K., Brickell, P. M. and Tickle, C. (1994). Bone morphogenetic proteins and a signalling pathway that controls patterning in the developing chick limb. *Development* **120**, 209-18.
Ganan, Y., Macias, D., Basco, R. D., Merino, R. and Hurle, J. M. (1998). Morphological diversity of the avian foot is related with the pattern of msx gene expression in the developing autopod. *Dev Biol* **196**, 33-41.
Garrity, D. M., Childs, S. and Fishman, M. C. (2002). The heartstrings mutation in zebrafish causes heart/fin Tbx5 deficiency syndrome. *Development* **129**, 4635-45.
Gibson-Brown, J. J., Agulnik, S. I., Silver, L. M., Niswander, L. and Papaioannou, V. E. (1998). Involvement of T-box genes Tbx2-Tbx5 in vertebrate limb specification and development. *Development* **125**, 2499-509.
Gumpel-Pinot, M., Ede, D. A. and Flint, O. P. (1984). Myogenic cell movement in the developing avian limb bud in presence and absence of the apical ectodermal ridge (AER). *J Embryol Exp Morphol* **80**, 105-25.
Habets, P. E., Moorman, A. F., Clout, D. E., van Roon, M. A., Lingbeek, M., van Lohuizen, M., Campione, M. and Christoffels, V. M. (2002). Cooperative action of Tbx2 and Nkx2.5 inhibits ANF expression in the atrioventricular canal: implications for cardiac chamber formation. *Genes Dev* **16**, 1234-46.
Hajihosseini, M. K., Lalioti, M. D., Arthaud, S., Burgar, H. R., Brown, J. M., Twigg, S. R., Wilkie, A. O. and Heath, J. K. (2004). Skeletal development is regulated by fibroblast growth factor receptor 1 signalling dynamics. *Development* **131**, 325-35.
Hamburger, V. (1939). The development and innervation of transplanted limb primordia of chick embryos. *J Exp Zool* **80**, 347-389.
Hamburger, V. and Hamilton, H. L. (1951). A series of normal stages in the development of the chick embryo. *J. Exp. Morph.* **88**, 49-92.
Harfe, B. D., Scherz, P. J., Nissim, S., Tian, H., McMahon, A. P. and Tabin, C. J. (2004). Evidence for an expansion-based temporal shh gradient in specifying vertebrate digit identities. *Cell* **118**, 517-28.
Harrelson, Z., Kelly, R. G., Goldin, S. N., Gibson-Brown, J. J., Bollag, R. J., Silver, L. M. and Papaioannou, V. E. (2004). Tbx2 is essential for patterning the atrioventricular canal and for morphogenesis of the outflow tract during heart development. *Development* **131**, 5041-52.
Harrison, R. G. (1918). Experiments on the development of the fore-limb of Amblystoma, a self differentiating equipotential system. *Journal of Experimental Zoology* **25**, 413-461.
Hipfner, D. R. and Cohen, S. M. (2004). Connecting proliferation and apoptosis in development and disease. *Nat Rev Mol Cell Biol* **5**, 805-15.
Hoogaars, W. M., Tessari, A., Moorman, A. F., de Boer, P. A., Hagoort, J., Soufan, A. T., Campione, M. and Christoffels, V. M. (2004). The transcriptional repressor Tbx3 delineates the developing central conduction system of the heart. *Cardiovasc Res* **62**, 489-99.

Hsu, D. R., Economides, A. N., Wang, X., Eimon, P. M. and Harland, R. M. (1998). The Xenopus dorsalizing factor Gremlin identifies a novel family of secreted proteins that antagonize BMP activities. *Mol Cell* **1**, 673-83.
Huang, R., Zhi, Q., Patel, K., Wilting, J. and Christ, B. (2000). Dual origin and segmental organisation of the avian scapula. *Development* **127**, 3789-94.
Hui, C. C. and Joyner, A. L. (1993). A mouse model of greig cephalopolysyndactyly syndrome: the extra-toesJ mutation contains an intragenic deletion of the Gli3 gene. *Nat Genet* **3**, 241-6.
Isaac, A., Cohn, M. J., Ashby, P., Ataliotis, P., Spicer, D. B., Cooke, J. and Tickle, C. (2000). FGF and genes encoding transcription factors in early limb specification. *Mech Dev* **93**, 41-8.
Isaac, A., Rodriguez-Esteban, C., Ryan, A., Altabef, M., Tsukui, T., Patel, K., Tickle, C. and Izpisua-Belmonte, J. C. (1998). Tbx genes and limb identity in chick embryo development. *Development* **125**, 1867-75.
Jacobson, A. G. and Sater, A. K. (1988). Features of embryonic development. *Development* **104**, 341-359.
Jaynes, J. B. and O'Farrell, P. H. (1991). Active repression of transcription by the engrailed homeodomain protein. *Embo J* **10**, 1427-33.
Jimenez, G., Paroush, Z. and Ish-Horowicz, D. (1997). Groucho acts as a corepressor for a subset of negative regulators, including Hairy and Engrailed. *Genes Dev* **11**, 3072-82.
Kaufman, M. H. (1992). The atlas of mouse development: Academic press.
Kawakami, Y., Capdevila, J., Buscher, D., Itoh, T., Rodriguez Esteban, C. and Izpisua Belmonte, J. C. (2001). WNT signals control FGF-dependent limb initiation and AER induction in the chick embryo. *Cell* **104**, 891-900.
Khokha, M. K., Hsu, D., Brunet, L. J., Dionne, M. S. and Harland, R. M. (2003). Gremlin is the BMP antagonist required for maintenance of Shh and Fgf signals during limb patterning. *Nat Genet* **34**, 303-7.
Kieny, M. (1964). Etude du mecanisme de la regulation dans le development du bourgeon de membre de l'embryon de poulet II. Regulation des deficiences dans les chimeres 'aile-patte' et 'patte-aile'. *Journal of Embryology and Experimental Morphology* **12**, 357-371.
Kispert, A. and Hermann, B. G. (1993). The Brachyury gene encodes a novel DNA binding protein. *Embo J* **12**, 4898-9.
Kispert, A., Koschorz, B. and Herrmann, B. G. (1995). The T protein encoded by Brachyury is a tissue-specific transcription factor. *Embo J* **14**, 4763-72.
Krumlauf, R. (1994). Hox genes in vertebrate development. *Cell* **78**, 191-201.
Lamonerie, T., Tremblay, J. J., Lanctot, C., Therrien, M., Gauthier, Y. and Drouin, J. (1996). Ptx1, a *bicoid*-related homeo box transcription factor involved in transcription of the pro-opiomelanocortin gene. *Genes and Development* **10**, 1284-1295.
Lanctot, C., Moreau, A., Chamberland, M., Tremblay, M. L. and Drouin, J. (1999). Hindlimb patterning and mandible development require the Ptx1 gene. *Development* **126**, 1805-10.
Lane, P. W. (1967). Linkage groups 3 and XVII in the mouse and the position of the light-ear locus. *J Hered* **58**, 21-4.
Laufer, E., Nelson, C. E., Johnson, R. L., Morgan, B. A. and Tabin, C. (1994). Sonic hedgehog and Fgf-4 act through a signaling cascade and feedback loop to integrate growth and patterning of the developing limb bud. *Cell* **79**, 993-1003.

Lei, Q., Zelman, A. K., Kuang, E., Li, S. and Matise, M. P. (2004). Transduction of graded Hedgehog signaling by a combination of Gli2 and Gli3 activator functions in the developing spinal cord. *Development* **131**, 3593-604.
Lewandoski, M., Sun, X. and Martin, G. R. (2000). Fgf8 signalling from the AER is essential for normal limb development. *Nat Genet* **26**, 460-3.
Li, Q. Y., Newbury-Ecob, R. A., Terrett, J. A., Wilson, D. I., Curtis, A. R., Yi, C. H., Gebuhr, T., Bullen, P. J., Robson, S. C., Strachan, T. et al. (1997). Holt-Oram syndrome is caused by mutations in TBX5, a member of the Brachyury (T) gene family. *Nat Genet* **15**, 21-9.
Li, Y., Zhang, H., Choi, S. C., Litingtung, Y. and Chiang, C. (2004). Sonic hedgehog signaling regulates Gli3 processing, mesenchymal proliferation, and differentiation during mouse lung organogenesis. *Dev Biol* **270**, 214-31.
Lillie, F. R. (1927). The development of the chick 2nd edition.
Lingbeek, M. E., Jacobs, J. J. and van Lohuizen, M. (2002). The T-box repressors TBX2 and TBX3 specifically regulate the tumor suppressor gene p14ARF via a variant T-site in the initiator. *J Biol Chem* **277**, 26120-7.
Litingtung, Y., Dahn, R. D., Li, Y., Fallon, J. F. and Chiang, C. (2002). Shh and Gli3 are dispensable for limb skeleton formation but regulate digit number and identity. *Nature* **418**, 979-83.
Liu, C., Nakamura, E., Knezevic, V., Hunter, S., Thompson, K. and Mackem, S. (2003). A role for the mesenchymal T-box gene Brachyury in AER formation during limb development. *Development* **130**, 1327-37.
Logan, M., Martin, J. F., Nagy, A., Lobe, C., Olson, E. N. and Tabin, C. J. (2002). Expression of Cre recombinase in the Developing Mouse Limb Bud Driven by a Prx1 Enhancer. *Genesis* **33**, 77-80.
Logan, M., Simon, H. G. and Tabin, C. (1998). Differential regulation of T-box and homeobox transcription factors suggests roles in controlling chick limb-type identity. *Development* **125**, 2825-35.
Logan, M. and Tabin, C. (1998). Targeted gene misexpression in chick limb buds using avian replication-competent retroviruses. *Methods* **14**, 407-20.
Logan, M. and Tabin, C. J. (1999). Role of Pitx1 upstream of Tbx4 in specification of hindlimb identity. *Science* **283**, 1736-9.
Maden, M. (1982). Vitamin A and pattern formation in the regenerating limb. *Nature* **295**, 672-5.
Markel, H., Chandler, J. and Werr, W. (2002). Translational fusions with the engrailed repressor domain efficiently convert plant transcription factors into dominant-negative functions. *Nucleic Acids Res* **30**, 4709-19.
Marshall, H., Morrison, A., Studer, M., Popperl, H. and Krumlauf, R. (1996). Retinoids and Hox genes. *Faseb J* **10**, 969-78.
Martin, G. R. (1998). The roles of FGFs in the early development of vertebrate limbs. *Genes Dev* **12**, 1571-86.
Mercader, N., Leonardo, E., Azpiazu, N., Serrano, A., Morata, G., Martinez, C. and Torres, M. (1999). Conserved regulation of proximodistal limb axis development by Meis1/Hth. *Nature* **402**, 425-9.
Mercader, N., Leonardo, E., Piedra, M. E., Martinez, A. C., Ros, M. A. and Torres, M. (2000). Opposing RA and FGF signals control proximodistal vertebrate limb development through regulation of Meis genes. *Development* **127**, 3961-70.
Mic, F. A., Sirbu, I. O. and Duester, G. (2004). Retinoic acid synthesis controlled by Raldh2 is required early for limb bud initiation and then later as a proximodistal signal during apical ectodermal ridge formation. *J Biol Chem* **279**, 26698-706.

Min, H., Danilenko, D. M., Scully, S. A., Bolon, B., Ring, B. D., Tarpley, J. E., DeRose, M. and Simonet, W. S. (1998). Fgf-10 is required for both limb and lung development and exhibits striking functional similarity to Drosophila branchless. *Genes Dev* **12**, 3156-61.

Naiche, L. A. and Papaioannou, V. E. (2003). Loss of Tbx4 blocks hindlimb development and affects vascularization and fusion of the allantois. *Development* **130**, 2681-93.

Nelson, C. E., Morgan, B. A., Burke, A. C., Laufer, E., DiMambro, E., Murtaugh, L. C., Gonzales, E., Tessarollo, L., Parada, L. F. and Tabin, C. (1996). Analysis of Hox gene expression in the chick limb bud. *Development* **122**, 1449-66.

Ng, J. K., Kawakami, Y., Buscher, D., Raya, A., Itoh, T., Koth, C. M., Esteban, C. R., Rodriguez-Leon, J., Garrity, D. M., Fishman, M. C. et al. (2002). The limb identity gene Tbx5 promotes limb initiation by interacting with Wnt2b and Fgf10. *Development* **129**, 5161-5170.

Niederreither, K., Vermot, J., Schuhbaur, B., Chambon, P. and Dolle, P. (2002). Embryonic retinoic acid synthesis is required for forelimb growth and anteroposterior patterning in the mouse. *Development* **129**, 3563-74.

Niswander, L., Jeffrey, S., Martin, G. R. and Tickle, C. (1994). A positive feedback loop coordinates growth and patterning in the vertebrate limb. *Nature* **371**, 609-12.

Niswander, L., Tickle, C., Vogel, A., Booth, I. and Martin, G. R. (1993). FGF-4 replaces the apical ectodermal ridge and directs outgrowth and patterning of the limb. *Cell* **75**, 579-87.

Ohashi, Y., Brickman, J. M., Furman, E., Middleton, B. and Carey, M. (1994). Modulating the potency of an activator in a yeast in vitro transcription system. *Mol Cell Biol* **14**, 2731-9.

Ohuchi, H., Nakagawa, T., Yamamoto, A., Araga, A., Ohata, T., Ishimaru, Y., Yoshioka, H., Kuwana, T., Nohno, T., Yamasaki, M. et al. (1997). The mesenchymal factor, FGF10, initiates and maintains the outgrowth of the chick limb bud through interaction with FGF8, an apical ectodermal factor. *Development* **124**, 2235-44.

Ohuchi, H., Takeuchi, J., Yoshioka, H., Ishimaru, Y., Ogura, K., Takahashi, N., Ogura, T. and Noji, S. (1998). Correlation of wing-leg identity in ectopic FGF-induced chimeric limbs with the differential expression of chick Tbx5 and Tbx4. *Development* **125**, 51-60.

Packham, E. A. and Brook, J. D. (2003). T-box genes in human disorders. *Hum Mol Genet* **12 Spec No 1**, R37-44.

Persson, M., Stamataki, D., te Welscher, P., Andersson, E., Bose, J., Ruther, U., Ericson, J. and Briscoe, J. (2002). Dorsal-ventral patterning of the spinal cord requires Gli3 transcriptional repressor activity. *Genes Dev* **16**, 2865-78.

Pizette, S. and Niswander, L. (1999). BMPs negatively regulate structure and function of the limb apical ectodermal ridge. *Development* **126**, 883-94.

Prince, S., Carreira, S., Vance, K. W., Abrahams, A. and Goding, C. R. (2004). Tbx2 directly represses the expression of the p21(WAF1) cyclin-dependent kinase inhibitor. *Cancer Res* **64**, 1669-74.

Raible, F. and Brand, M. (2001). Tight transcriptional control of the ETS domain factors Erm and Pea3 by Fgf signaling during early zebrafish development. *Mech Dev* **107**, 105-17.

Rallis, C., Bruneau, B. G., Del Buono, J., Seidman, C. E., Seidman, J. G., Nissim, S., Tabin, C. J. and Logan, M. P. (2003). Tbx5 is required for forelimb bud formation and continued outgrowth. *Development* **130**, 2741-51.
Rancourt, D. E., Tsuzuki, T. and Capecchi, M. R. (1995). Genetic interaction between hoxb-5 and hoxb-6 is revealed by nonallelic noncomplementation. *Genes Dev* **9**, 108-22.
Retaux, S., Rogard, M., Bach, I., Failli, V. and Besson, M. J. (1999). Lhx9: a novel LIM-homeodomain gene expressed in the developing forebrain. *J Neurosci* **19**, 783-93.
Revest, J. M., Spencer-Dene, B., Kerr, K., De Moerlooze, L., Rosewell, I. and Dickson, C. (2001). Fibroblast growth factor receptor 2-IIIb acts upstream of Shh and Fgf4 and is required for limb bud maintenance but not for the induction of Fgf8, Fgf10, Msx1, or Bmp4. *Dev Biol* **231**, 47-62.
Riddle, R. D., Johnson, R. L., Laufer, E. and Tabin, C. (1993). Sonic hedgehog mediates the polarizing activity of the ZPA. *Cell* **75**, 1401-16.
Rodriguez-Esteban, C., Tsukui, T., Yonei, S., Magallon, J., Tamura, K. and Izpisua Belmonte, J. C. (1999). The T-box genes Tbx4 and Tbx5 regulate limb outgrowth and identity. *Nature* **398**, 814-8.
Ros, M. A., Lyons, G., Kosher, R. A., Upholt, W. B., Coelho, C. N. and Fallon, J. F. (1992). Apical ridge dependent and independent mesodermal domains of GHox-7 and GHox-8 expression in chick limb buds. *Development* **116**, 811-8.
Ruvinsky, I., Silver, L. M. and Gibson-Brown, J. J. (2000). Phylogenetic analysis of T-Box genes demonstrates the importance of amphioxus for understanding evolution of the vertebrate genome. *Genetics* **156**, 1249-57.
Sambrook, J., Fritsch, E.F., Maniatis, T. (1989). Molecular Cloning. A Laboratory manual. *Cold Spring Harbor Laboratory Press.*
Sanz-Ezquerro, J. J. and Tickle, C. (2000). Autoregulation of Shh expression and Shh induction of cell death suggest a mechanism for modulating polarising activity during chick limb development. *Development* **127**, 4811-23.
Sasaki, H., Hui, C., Nakafuku, M. and Kondoh, H. (1997). A binding site for Gli proteins is essential for HNF-3beta floor plate enhancer activity in transgenics and can respond to Shh in vitro. *Development* **124**, 1313-22.
Saunders, J. W. (1948). The proximo-distal sequence of origin of the parts of the chick wing and role of the ectoderm. *Journal of Experimental Zoology* **108**, 363-404.
Saunders, J. W., Cairns, J. M. and Gasseling, M. T. (1957). The role of the apical ridge of the ectoderm in the diffferentiation of the morphological structure and inductive specificity of limb parts in the chick. *Journal of Morphology* **101**, 57-88.
Saunders, J. W. and Gasseling, M. T. (1968). Ectodermal-mesenchymal interactions in the origin of limb symmetry. In *Epithelial-mesenchymal interactions*, (ed. R. Fleishmajer and R. A. Billingham), pp. 78-97: Baltimore, Williams and Wilking.
Saunders, J. W., Gasseling, M. T. and Cairns, J. M. (1959). The differentiation of the prospective thigh mesoderm grafted beneath the apical ectodermal ridge of the wing bud in the chick embryo. *Developmental Biology* **1**, 281-301.
Scholpp, S., Groth, C., Lohs, C., Lardelli, M. and Brand, M. (2004). Zebrafish fgfr1 is a member of the fgf8 synexpression group and is required for fgf8 signalling at the midbrain-hindbrain boundary. *Dev Genes Evol.*

Schulte-Merker, S. and Smith, J. C. (1995). Mesoderm formation in response to Brachyury requires FGF signalling. *Curr Biol* **5**, 62-7.
Schweitzer, R., Vogan, K. J. and Tabin, C. J. (2000). Similar expression and regulation of Gli2 and Gli3 in the chick limb bud. *Mech Dev* **98**, 171-4.
Searls, R. L. (1967). The role of cell migration in the development of the embryonic chick limb bud. *Journal of Experimental Zoology* **166**, 39-45.
Searls, R. L. and Janners, M. Y. (1969). The stabilisation of cartilage properties in the cartilage forming mesenchyme of the embryonic chick limb. *Journal of Experimental Zoology* **170**, 365-376.
Sekine, K., Ohuchi, H., Fujiwara, M., Yamasaki, M., Yoshizawa, T., Sato, T., Yagishita, N., Matsui, D., Koga, Y., Itoh, N. et al. (1999). Fgf10 is essential for limb and lung formation. *Nat Genet* **21**, 138-41.
Simon, H.-G., Kittappa, R., Khan, P. A., Tsilfidis, C., Liversage, R. A. and Oppenheimer, S. (1997). A novel family of T-box genes in urodele amphibian limb development and regeneration: candidate genes involved in vertebrate forelimb/hindlimb patterning. *Development* **124**, 1355-1366.
Smith, J. C., Price, B. M., Green, J. B., Weigel, D. and Herrmann, B. G. (1991). Expression of a Xenopus homolog of Brachyury (T) is an immediate-early response to mesoderm induction. *Cell* **67**, 79-87.
Stratford, T., Horton, C. and Maden, M. (1996). Retinoic acid is required for the initiation of outgrowth in the chick limb bud. *Curr Biol* **6**, 1124-33.
Stratford, T., Logan, C., Zile, M. and Maden, M. (1999). Abnormal anteroposterior and dorsoventral patterning of the limb bud in the absence of retinoids. *Mech Dev* **81**, 115-25.
Stratford, T. H., Kostakopoulou, K. and Maden, M. (1997). Hoxb-8 has a role in establishing early anterior-posterior polarity in chick forelimb but not hindlimb. *Development* **124**, 4225-34.
Summerbell, D. (1974). A quantitative analysis of the effect of excision of the AER from the chick limb-bud. *J Embryol Exp Morphol* **32**, 651-60.
Sun, X., Mariani, F. V. and Martin, G. R. (2002). Functions of FGF signalling from the apical ectodermal ridge in limb development. *Nature* **418**, 501-8.
Suzuki, T., Takeuchi, J., Koshiba-Takeuchi, K. and Ogura, T. (2004). Tbx Genes Specify Posterior Digit Identity through Shh and BMP Signaling. *Dev Cell* **6**, 43-53.
Szeto, D. P., Rodriguez-Esteban, C., Ryan, A. K., O'Connell, S. M., Liu, F., Kioussi, C., Gleiberman, A. S., Izpisua-Belmonte, J. C. and Rosenfeld, M. G. (1999). Role of the Bicoid-related homeodomain factor Pitx1 in specifying hindlimb morphogenesis and pituitary development. *Genes Dev* **13**, 484-94.
Tabin, C. J. (1991). Retinoids, homeoboxes, and growth factors: toward molecular models for limb development. *Cell* **66**, 199-217.
Takabatake, Y., Takabatake, T., Sasagawa, S. and Takeshima, K. (2002). Conserved expression control and shared activity between cognate T-box genes Tbx2 and Tbx3 in connection with Sonic hedgehog signaling during Xenopus eye development. *Dev Growth Differ* **44**, 257-71.
Takeuchi, J. K., Koshiba-Takeuchi, K., Matsumoto, K., Vogel-Hopker, A., Naitoh-Matsuo, M., Ogura, K., Takahashi, N., Yasuda, K. and Ogura, T. (1999). Tbx5 and Tbx4 genes determine the wing/leg identity of limb buds. *Nature* **398**, 810-4.
Takeuchi, J. K., Koshiba-Takeuchi, K., Suzuki, T., Kamimura, M., Ogura, K. and Ogura, T. (2003). Tbx5 and Tbx4 trigger limb initiation through activation of the Wnt/Fgf signaling cascade. *Development* **130**, 2729-39.

Tamura, K., Yokouchi, Y., Kuroiwa, A. and Ide, H. (1997). Retinoic acid changes the proximodistal developmental competence and affinity of distal cells in the developing chick limb bud. *Dev Biol* **188**, 224-34.
Tanaka, M. and Tickle, C. (2004). Tbx18 and boundary formation in chick somite and wing development. *Dev Biol* **268**, 470-80.
te Welscher, P., Fernandez-Teran, M., Ros, M. A. and Zeller, R. (2002a). Mutual genetic antagonism involving GLI3 and dHAND prepatterns the vertebrate limb bud mesenchyme prior to SHH signaling. *Genes Dev* **16**, 421-6.
te Welscher, P., Zuniga, A., Kuijper, S., Drenth, T., Goedemans, H. J., Meijlink, F. and Zeller, R. (2002b). Progression of vertebrate limb development through SHH-mediated counteraction of GLI3. *Science* **298**, 827-30.
Tickle, C. and Eichele, G. (1994). Vertebrate limb development. *Annu Rev Cell Biol* **10**, 121-52.
Tumpel, S., Sanz-Ezquerro, J. J., Isaac, A., Eblaghie, M. C., Dobson, J. and Tickle, C. (2002). Regulation of Tbx3 expression by anteroposterior signalling in vertebrate limb development. *Dev Biol* **250**, 251-62.
Vogel, A., Rodriguez, C. and Izpisua-Belmonte, J. C. (1996). Involvement of FGF-8 in initiation, outgrowth and patterning of the vertebrate limb. *Development* **122**, 1737-50.
Wang, B., Fallon, J. F. and Beachy, P. A. (2000). Hedgehog-regulated processing of Gli3 produces an anterior/posterior repressor gradient in the developing vertebrate limb. *Cell* **100**, 423-34.
Wilkinson, D. G., Bhatt, S. and Herrmann, B. G. (1990). Expression pattern of the mouse T gene and its role in mesoderm formation. *Nature* **343**, 657-9.
Williams, B. A. and Ordahl, C. P. (1994). Pax-3 expression in segmental mesoderm marks early stages in myogenic cell specification. *Development* **120**, 785-96.
Xu, X., Weinstein, M., Li, C., Naski, M., Cohen, R. I., Ornitz, D. M., Leder, P. and Deng, C. (1998). Fibroblast growth factor receptor 2 (FGFR2)-mediated reciprocal regulation loop between FGF8 and FGF10 is essential for limb induction. *Development* **125**, 753-65.
Yada, Y., Makino, S., Chigusa-Ishiwa, S. and Shiroishi, T. (2002). The mouse polydactylous mutation, luxate (lx), causes anterior shift of the anteroposterior border in the developing hindlimb bud. *Int J Dev Biol* **46**, 975-82.
Yamada, T., Pfaff, S. L., Edlund, T. and Jessell, T. M. (1993). Control of cell pattern in the neural tube: motor neuron induction by diffusible factors from notochord and floor plate. *Cell* **73**, 673-86.
Yonei-Tamura, S., Endo, T., Yajima, H., Ohuchi, H., Ide, H. and Tamura, K. (1999). FGF7 and FGF10 directly induce the apical ectodermal ridge in chick embryos. *Dev Biol* **211**, 133-43.
Yu, X., St Amand, T. R., Wang, S., Li, G., Zhang, Y., Hu, Y. P., Nguyen, L., Qiu, M. S. and Chen, Y. P. (2001). Differential expression and functional analysis of Pitx2 isoforms in regulation of heart looping in the chick. *Development* **128**, 1005-13.
Zaragoza, M. V., Lewis, L. E., Sun, G., Wang, E., Li, L., Said-Salman, I., Feucht, L. and Huang, T. (2004). Identification of the TBX5 transactivating domain and the nuclear localization signal. *Gene* **330**, 9-18.
Zuniga, A., Haramis, A. P., McMahon, A. P. and Zeller, R. (1999). Signal relay by BMP antagonism controls the SHH/FGF4 feedback loop in vertebrate limb buds. *Nature* **401**, 598-602.

Zuniga, A. and Zeller, R. (1999). Gli3 (Xt) and formin (ld) participate in the positioning of the polarising region and control of posterior limb-bud identity. *Development* **126**, 13-21.
Zwilling, E. (1956a). Ectoderm-Mesoderm Relationship in the development of the Chick Embryo Limb Bud. *Journal of Experimental Zoology* **128**, 423-441.
Zwilling, E. (1956b). Interaction Between Limb Bud Ectoderm and Mesoderm in the Chick Embryo I. Axis Establishment. *Journal of Experimental Zoology* **132**, 157-171.